OCCURRENCE AND DISTRIBUTION OF *DINOPHYSIS* SPP. IN BUDD INLET, WASHINGTON DURING A SEASONAL CYCLE FROM WINTER TO FALL OF 2019: POSSIBLE CAUSATIVE ENVIRONMENTAL FACTORS

by

Naomi Estrada-Packer

A Thesis
Submitted in partial fulfillment
of the requirements for the degree
Master of Environmental Studies
The Evergreen State College
December 2019

This Thesis for the Master of Environmental Studies Degree

by

Naomi Estrada-Packer

has been approved for

The Evergreen State College

by

_____

Gerardo Chin-Leo, Ph. D.
Member of the Faculty

_____

Date

ABSTRACT

Occurrence and Distribution of *Dinophysis* spp. in Budd inlet, Washington during a seasonal cycle from Winter to Fall of 2019: Possible Causative Environmental Factors

Naomi Estrada-Packer

Harmful algal blooms (HABs) are a major environmental problem. This study focused on *Dinophysis*, a HAB genus of marine dinoflagellates capable of producing phycotoxins responsible for diarrhetic shellfish poisoning (DSP) events. During a 10-month period (Jan-Oct 2019), I monitored phytoplankton species composition and biomass, and determined cell densities of various *Dinophysis* species (*D. norvegica, D. acuminata, D. fortii, D. rotundata, D. parva,* and *D. odios*a) at 2 stations with different oceanographic conditions in Budd Inlet, one at the head and other at the mouth of the estuary. A sampling method was developed to detect *Dinophysis* at low cell concentrations (> 2 cells/L). Samples were collected weekly (spring to summer) to monthly (fall and winter). To determine the environmental factors explaining *Dinophysis* abundance, water quality and physicochemical parameters were measured and data on meteorological conditions were examined. In addition, DSP toxin data from Washington Department of Health was obtained to determine if DSP toxin levels coincided with *Dinophysis* abundance. There were significant changes in phytoplankton species composition over space and time. Diatoms dominated in winter and dinoflagellates dominated in spring /summer. Dinoflagellates were more abundant at the head of the estuary and diatoms at the mouth. *Dinophysis* species were found in all but one sampling time with *D. norvegica* being the most common species. The largest *D. norvegica* abundance occurred at both stations during summer reaching densities of 23,857 cells/L at the estuary head and 3,590 cells/L at the mouth. While the cell densities at the head were greater than the mouth, blooms coincided over time suggesting widespread meteorological conditions may explain the timing of blooms with local differences in stratification and nutrients determining abundance. Chemical and physical parameters at both stations were significantly different ($p<0.05$). At the head of the estuary, river discharge, surface water temperature, nitrate and phosphate and nutrient ratios were strongly related to *Dinophysis* abundance suggesting that *Dinophysis* benefits from stratified conditions and proximity to the river nutrient source. DSP toxin levels were not significantly related to *Dinophysis* abundance. Toxicity of *Dinophysis* may be species-specific where individual species could be more toxic than others. The dominance of *D. norvegica*, a species with relatively low toxicity may explain this apparent discrepancy.

TABLE OF CONTENTS

LIST OF FIGURES

LIST OF TABLES

LIST OF APPENDICES

Acknowledgements

This has been a tremendous educational journey about growing as a person, student, and a scientist. I am honored to have learned and delved in deep into this particular subject involving our precious waters and the living organisms that need our attention and utmost care. If it were not for support of my advisor Gerardo Chin-Leo, Vera Trainer and Brian Bill from the SoundToxins team, Jerry Borchert from WDOH, Nick (my husband), my family, friends and ancestors, I would not come this far without you all. I thank you all from the depths of my soul for all of your guidance throughout this educational experience. All of you have inspired me to keep striving and moving forward no matter what obstacles lie ahead and continue to be a steward to our Earth and its waters.

Thank you all so much!

CHAPTER 1: INTRODUCTION

1.1: What are HABs?

Harmful Algal Blooms (HAB) are a global phenomenon impacting most marine ecosystems particularly in coastal and estuarine regions (Lelong et al., 2012). High-density blooms of phytoplankton—microscopic algae—produce biotoxins, also known as phycotoxins, affecting aquatic life and ecosystems along with human health (Anderson et al., 2012). There is a general scientific consensus that the number of toxic blooms, resulting economic losses of shellfish industries, disruption of subsistence practices, and the number of toxins and toxic species reported have all increased over the last few decades (2012). In Washington, HAB's have only been recently detected along the coast and within Puget Sound. The quality of marine waters has become a particularly important issue due to a large populace using aquatic resources involving shellfish industries and tribal subsistence. There are various state and government organizations extending great effort toward studying HABs. These agencies include: *SoundToxins—National Ocean and Atmospheric Administration (NOAA), Washington Department of Health (WDOH), Olympic Region Harmful Algal Blooms (ORHAB),* and *Puget Sound Marine Monitoring.*

1.2: Significance

HABs toxins are concentrated by bivalves (e.g. blue mussels and other shellfish), which filter feeders consume the toxic phytoplankton. Humans are affected by the toxins when they consume the contaminated shellfish. Exposure to toxins over the USDA action levels can cause health illnesses related to Diarrheic Shellfish Poisoning (DSP), Amnesic Shellfish Poisoning (ASP), Paralytic Shellfish Poisoning (PSP), and Neurotoxin Shellfish

Poisoning (NSP) (Grattan et al. 2016). Most HAB related illnesses have similar symptoms to gastrointestinal and neurological problems (Grattan et al., 2016). The impacts of HABs not only affect humans but can also affect wildlife that consume contaminated phytoplankton or shellfish causing similar yet more severe illness which can lead to death (Anderson, Cembella, & Hallegraeff, 2012).

1.3: Humans as Cause and Victims of HABs

HAB occurrence is associated with a complex set of physical, chemical, biological, hydrological, and meteorological conditions making it difficult to determine the causative factors. However, severe HAB events in coastal and estuarine areas have been related to anthropogenic activities (Lelong et al., 2012; Lehmann & Gobler, 2015). Extensive HAB research has been conducted over the past decades, and several anthropogenic mechanisms stimulating toxic bloom events have been identified. These include: 1) natural dispersal of species by currents and storms; 2) dispersal through human activities (such as ballast water discharge and shellfish translocation); 3) increased aquaculture operations in coastal waters; 4) increased anthropogenic eutrophication and climate change (Anderson et al., 2012; Lelong et al., 2012). HABs pose a major threat to human health. Therefore, it is essential to predict the occurrence of toxic blooms, their toxin production, and toxicity per cell in order to effectively continue to develop proactive management of coastal resources and minimize humans and public health risks (Anderson et al., 2012).

Anthropogenic inputs of excess nutrients of nitrogen, phosphorous, and ammonium have all been determined to alter the nutrient ratios leading to negatively affecting phytoplankton species composition and facilitating the onset and development

of toxic blooms (Davidson et al., 2016; Flynn, 2010; Pan, Bates, & Cembella, 1998). Due to the scarcity of particular nutrients (i.e. silica) and nutrient loading of nitrogen and phosphorous, phytoplankton have evolved to adapt to their surrounding waters. With these anthropogenic environmental pressures, as phytoplankton—both dinoflagellates and diatoms—evolved they have developed adaptations to outcompete other species for nutrients and defenses against other phytoplankton predators and grazers (Rossini, 2016). The production of toxins are an example of an adaptation technique to aid in survival of waters with low water quality and an imbalance of nutrient availability (2016). Toxins can aid in nutrient and prey acquisition by mixotrophic and autotrophic species of phytoplankton, and also deter predation from other phytoplankton, zooplankton, bivalves, and small fish (Smayda, 1997).

1.4: Concerns of *Dinophysis* in Washington State

Four HAB species have been reported in Puget Sound, Washington for more than a century, including *Dinophysis* spp., *Pseudo-nitzschia* spp., *Alexandrium catenella* and *Heterosigma akashiwo*, although *Dinophysis* bloom events have more recently been found (Trainer et al. 2013). The first shellfish closure due to high concentrations of Diarrheic shellfish toxins, including okadaic acid and dinophysistoxins, occurred in the Puget Sound in 2011 (Trainer et al. 2013). Due to the increasing frequency of blooms in the Puget Sound, especially Budd Inlet in South Sound near Olympia, concerns have been raised about issues regarding the state of water quality and health of marine organisms within the Puget Sound. Therefore, research scientists and state agencies are taking great measures to monitor *Dinophysis* blooms on a frequent basis.

1.5: Local Research Efforts

Due to the potential threats to human and marine organismal health, research organizations (those mentioned above) are routinely monitoring marine waters throughout Washington. *SoundToxins* is a citizen-science monitoring program, managed by Sea Grant—*NOAA* located in Puget Sound, WA. *SoundToxins* plays an integral role in educating local tribal harvesters, commercial shellfish and fish farmers, and other partnering state agencies about HABs and the importance of monitoring. *SoundToxins* provides a cost-effective, enhanced monitoring program, and emergency response to notify the possible onset and occurrences of HABs. The local community stakeholders assist in the decision-making process, thereby enabling the proper harvest the seafood by ultimately reducing the overall negative impacts to the economy sustained by fisheries in the Puget Sound, human health, and marine organismal health (SoundToxins, 2018).

WDOH also plays a primary role in minimizing risk and exposure to DSP toxins caused by *Dinophysis* spp. occurring throughout the Puget Sound. Sentinel mussels are continuously monitored by WDOH and sampled for DSP toxins at several sites within Puget Sound, including Budd Inlet. Collections of mussel tissue are sampled weekly to bi-weekly for DSP toxins, including okadaic acid, dinophysistoxin-1, and dinophysistoxin-2. The tissue samples are measured using a Liquid Chromatography-Mass Spectrometry (LC-MS) to analyze the concentrations of toxins to detect if the levels are above the regulatory limit for the public—each toxin has its own regulatory limit dependent on how fast or slow the toxin is metabolized by the human body. For DSP toxins, the regulatory limit for safe consumption is 16 micrograms per 100 grams (Trainer et al. 2013; FDA, 2011).

1.6: My Research Efforts and Contribution

Furthermore, to address the current need for information on the factors that explain the recurrence and growth of *Dinophysis* species in Budd Inlet, South Puget Sound, I decided to pursue a thesis project to understand the environmental conditions that contribute to *Dinophysis* blooms, production of Diarrheic Shellfish toxins (DST), and toxicity profiles and DST levels in mussel tissue. This thesis is contributing to the limited knowledge of *Dinophysis* blooms dynamics in relation to environmental conditions at two locations in Puget Sound with previous *Dinophysis* presence.

1.7: Research Objectives: Question-Hypothesis-Approach

My two research questions are:

1) What is the spatiotemporal distribution of *Dinophysis* between the estuary head (near Deschutes River) and the mouth (near south sound basin) over the seasonal cycle from winter to fall of 2019 in Budd Inlet?

2) What factors control the abundance of *Dinophysis* in Budd Inlet, South Puget Sound, Washington?

I hypothesize the estuary head is environmentally different than the mouth. The factors of primary activity (biomass), river discharge, stratification, surface water temperatures, and nutrients (ammonium, nitrate, phosphate) will be the main contributors to changing environmental conditions between the two stations. These differences may showcase the particular environmental variables influencing *Dinophysis* activity in Budd Inlet.

Several physicochemical factors control *Dinophysis* abundance during the seasonal period shifting from spring to summer. These factors include: the rise in surface

water temperatures, an increase in radiation, the limitation of nutrients of phosphorous, an excess of nitrogen, and an increase in ammonium levels. The Deschutes River discharge and anthropogenic nutrient inputs of nitrogen and phosphorous from local wastewater treatments plants and land runoff can greatly influence the composition of nutrients over the seasonal cycle. Due to the nutrient loading of nitrogen, phosphorous becomes the limiting factor of dinoflagellates growth during the summer months, especially when concerning *Dinophysis*. The alterations of the Redfield ratios of DSI:DIN and DIN:DIP can shift to support the cellular growth of diatoms during winter to spring and dinoflagellates from summer to fall. Nutrient ratios are critical to cellular growth and nutrient uptake, while water quality parameters of low salinity and high surface water temperatures can also be significant factors positively influencing total *Dinophysis* abundance.

To answer this question, this study will investigate phytoplankton species composition and the dynamics between *Dinophysis* abundance, environmental conditions, and toxin profiles (found in mussel tissue) over a 10-month monitoring period (winter to fall) at two locations within Budd Inlet, Puget Sound—one station at the estuary head (North Point Landing (NPL)) and the second station at the estuary mouth (Boston Harbor Marina (BHM)). These sites were chosen because Budd Inlet has been known to have the highest concentrations of DSP levels recorded in Washington State. In 2016, the DSP toxin levels were recorded at 250 μg/100g of DSP toxins in blue mussel tissue (unpublished data, WDOH, Jerry Borchert).

To date, *Dinophysis* species found in the Puget Sound include*: D. acuminata, D. fortii, D.* norvegica, *D. acuta,* and *D. caudata* (Trainer et al., 2013). However, their

relative toxicities differ per cell for each species; *D. fortii* and *D. acuminata* are two species that have been known to cause an increase in the levels of okadaic acid and dinophysistoxins (Trainer et al. 2013). Therefore, this study will identify *Dinophysis* to the species level. This will further provide baseline data on the interactions between *Dinophysis* presence and particular environmental parameters that potentially influence intensity, frequency, and toxicity of blooms in the Puget Sound.

Environmental parameters such as air temperature, rainfall, radiation, and wind patterns will be recorded to understand the seasonality of blooms in relation to associated environmental parameters. Biologically important water quality parameters such as surface water temperatures, salinity (stratification), dissolved oxygen, biomass (chlorophyll-a), and nutrient concentrations of ammonium, phosphorus, nitrogen, and silica will be measured, along with calculation of nutrient ratios between DIN:DSI:DIP. The nutrient ratios were computed to determine the changes in nutrient composition. Variations of these ratios from the Redfield ratios can provide clues on when specific nutrients are limiting for growth.

I will be analyzing the environmental data to understand if there are qualitative and statistically significant relationships between *Dinophysis* abundance and all other physicochemical, water quality parameter, and DSP toxin levels. Data analysis will be conducted using time series, regression analysis, and independent t-test analysis to identify potential environmental mechanisms influencing the spatiotemporal distribution of *Dinophysis* species in Budd Inlet, and further understand *Dinophysis* dynamics to detect future threats of DSP events in estuarine ecosystems.

CHAPTER 2: LITERATURE REVIEW

2.1: Overview of Biology & Ecology of the genus *Dinophysis*

The majority of harmful algal blooms (HABs) are caused by toxin-producing dinoflagellates that can be phototrophic, heterotrophic, and mixotrophic, even though historically HAB species have been thought to be strictly phototrophs (Anderson et al., 2012). The genus, *Dinophysis* ("*Dino*" meaning "terrible" and "*physis*" mean "nature"), is characterized as an armored, mixotrophic, toxin producing dinoflagellate. *Dinophysis* is a cosmopolitan genus of dinoflagellates comprised of over 120 taxonomically identified species (Reguera et al. 2012, 2014; Simoes et al. 2015). Certain species of the *Dinophysis* genus have been recently discovered to produce intoxicating phycotoxins known to have adverse effects on humans and wildlife. To date, only 12 species of *Dinophysis* have been identified to synthesize harmful, lipophilic toxins called okadaic acid (OA) and its congeners of Dinophysistoxin-1 (DTX-1) and Dinophysistoxin-2 (DTX-2), collectively known as Diarrhetic Shellfish Poisoning Toxins (DSTs) (Reguera et al., 2014; FAO, 2004) (Figure 1).

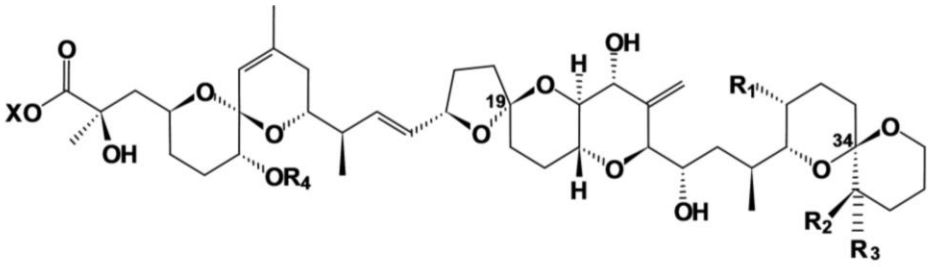

Name	R1	R2	R3	R4	C-19*	C-34*
Okadaic acid (OA)	CH_3	H	H	H	S	S
Dinophysistoxin-1 DTX1	CH_3	CH_3	H	H	S	R
Dinophysistoxin-2 DTX2	H	H	CH_3	H	S	R

* Relative stereochemistry. OA, X = H; Methyl okadaate, X = CH_3; OA diol esters, X = C_4 to C_{10} unsatured diols

Figure 1: Chemical structures of okadaic acid and its congeners of dinophysistoxin-1 and dinophysistoxin-2 (DTX-1 and DTX-2) (Reguera et al., 2014).

The toxic species of *Dinophysis*, include: *D. fortii, D. acuminata, D. norvegica, D. acuta, D. parva, D. caudata, D. infundbulium, D. miles, D. sacculus, D.ovum, D. tripos, D. rotundata, and D. mitra* (Reguera et al., 2014). Only seven (*D. acuminata, D. acuta, D. fortii, D. ovum, D. caudata, D. miles,* and *D. sacculus*) of these species have been associated with DSP outbreaks worldwide (Reguera et al., 2012).

Dinophysis (*Dinophysaceae*) has been identified as the primary organism to induce harmful algal outbreaks known as Diarrhetic Shellfish Poisoning (DSP) events (Anderson et al., 2012; Reguera et al., 2012). Although OA, DTX-1, and DTX-2 are the main contributors to DSP events, *Dinophysis* species can also co-produce pectenotoxins (PTXs), known to be strictly regulated by the European Union due to its reported intraperitoneal hepatotoxic effects on mice (Terao et al., 1986; Reguera et al., 2012). However, PTXs have not been known to cause issues in other regions of the world, except for Europe where their toxicity has been up

for debate (Reguera & Blanco, 2019). These okadates (OA, DTXs, and PTXs) are secondary metabolites which are highly stable polyether compounds. Okadates produced by toxic species of *Dinophysis* have recently presented increasingly adverse effects on human health, a condition known as DSP.

Several studies have demonstrated DSTs are biological active compounds that can promote the onset of various health disorders (Trainer et al., 2013; Reguera et al., 2014). When DSTs are ingested by humans, various symptoms of gastrointestinal illness can occur, such as nausea, diarrhea, vomiting, headache, fever, and severe abdominal pain, with the onset of symptoms occurring within 30 minutes and reducing within a few days (FDA, 2011; Trainer et al. 2013). OA and dinophysistoxins (DTX-1 and DTX-2) can inhibit protein phosphatases in mammalian cells by its ability to bind to the receptor site (Cohen et al., 1990). When consumption of high toxin levels happens, gastrointestinal symptoms occur due to OA and DTXs triggering increase of phosphorylated proteins, theeby resulting in hyperphosphorylation of the ion channels in the cells (Cohen et al., 1990; Cordier et al., 2000; FDA, 2011; Uberhart et al., 2013). Although gastrointestinal illnesses are most characteristic symptoms of intoxification, OA and its analogues have been identified to emit tumor-promoting, mutagenic, and immosuppressive effects, as shown in studies investigating toxicity on mice (Fujiki & Suganuma, 1999; FAO, 2004. Furthermore, other studies have reported that chronic exposure to DSTs, specifically OA and DTX-1, promotes gastrointestinal cancers in humans (Van Egmond et al., 1993; Draisci et al., 1996; Cordier et al., 2000; Manerio et al., 2008).

2.2: Diarrhetic Shellfish Poisoning

Emergence of DSP occurrences associated with *Dinophysis spp.* have increased in frequency and duration on a global scale, progressively posing various consequences to marine ecosystems, public health, and economic losses to local shellfish industries (Anderson et al., 2012; Reguera et al., 2012). Due to the public health consequences, DSTs have been globally recognized and regulated for the majority of coastal waters with recurring DSP events, however, the United States does not regulate monitoring for DSTs nationwide. DSTs have been routinely monitored in Europe and has a regulatory limit of 160 micrograms per kilograms of DSTs (EC, 2004). Although the United States does regularly monitor for DSTs, the U.S. Food and Drug Administration (FDA) established a standard that all commercial shellfish products are "unsafe" when containing more than 160 micrograms per kilograms of DSTs equivalents (includes the combination of OA, DTX-1, DTX-2 and esterified constituents of OA, DTX-1 and DTX-2). Contaminated shellfish products that do not meet the regulatory threshold are highly recommended to be removed immediately and to not be sold on the public market (Miles et al., 2004; FDA, 2011; Reguera et al., 2012).

Once the DSTs are produced by *Dinophysis* and toxins can accumulate intracellularly. The toxins are transferred up the food chain via grazing whereby the toxin are consumed by secondary consumers, such as shellfish and other planktivorous fish, that can highly concentrate the toxins over a period of time. Once the bioaccumulation occurs, the affected secondary consumers are ingested by higher trophic levels (e.g. marine mammals and humans), causing illnesses

recognized as Diarrhetic Shellfish Poisoning (DSP). Most cases of DSP in humans are caused by the consumption of toxin-laden and contaminated shellfish. On small scale outbreaks, mussels are usually the culprit; however, other marine organisms, such as Brown Crabs, have been connected to large scale outbreaks of DSP (Reguera et al., 2014; Torgensen set al., 2005).

2.2.1: History and Global Distribution of DSP Events

The first clinical report to be associated with gastrointestinal symptoms occurred in the Netherlands in 1961 after the consumption of commercially harvested mussels, yet there was no causative agent found correlated with this event (Korringa & Roskam, 1961). The second reported outbreak occurred along the Chilean coast in 1970 where 100 people suffered major gastrointestinal illnesses, yet it did not receive international public recognition until 1991 (Lembeye et al., 1993). More severe outbreaks were reported in Northern Japan during 1976 and 1977, where DSP was officially and publicly known to have a causative agent of *Dinophysis* species.

Before *Dinophysis* finally was recognized as responsible for DSP events, *Prorocentrum* species were associated with the major outbreaks occurring during the 1960s and 1970s because of their high cell abundance relative to other dinoflagellate densities recorded. *Dinophysis acuminata* was recorded with *Prorocentrum*; however, the investigators did not correlate the low cellular counts with the DSP event. There have been various misdiagnoses reported in primary literature correlating *Prorocentrum*, primarily the benthic species *P. lima*, as the

causative agent for producing of OA and DTXs which has made the issue even that much more complex (Kat, 1979).

DSP was not fully documented until the late 1970s, when several outbreaks occurred inducing severe gastrointestinal disorders after the consumption of mussels (*Mytilus edulis*) and scallops (*Patinopecten yessoensis*) in Northeastern Japan (Reguera et al., 2014). Yasumoto was the first to isolate two fat-souble toxins and tested the toxins on mice to investigate the toxicity effects (Yasumoto et al., 1978; Yasumoto et al., 1979). *Dinophysis fortii* was the causative agent for the outbreaks in Japan (Yasumoto et al., 1980). OA was first isolated and reported in the sponge *Halichondria okadai*, then later described to be the bioactive component attributed to cause DSP (Tachibana et al., 1981; Murata et al., 1982).

After the new discovery of DSTs, Europe started to experience major DSP outbreaks during the early 1980s. Spain was the first country to report a major DSP outbreak. In 1981, more than 5,000 people in northeastern Spain were affected by the consumption of contaminated Mediterranean mussels (*Mytilus galloprovincialis*), with *Dinophysis acuminata* being the suspected culprit (Campos et al., 1982). Another outbreak occurred in France during the summer (June to July) of 1983: over 3300 consumers of contaminated mussels (*Mytilus edulis*) were affected, *D. acuminata* was associated with the outbreak (Krogh et al., 1985; Underdahl et al., 1985). The following year in 1984, more than 300 mussel consumers were affected from Sweden and Norway, where *D. acuta* and *D. norvegica* were attributed to the DSP event.

DSP cases with the causative agent of toxic *Dinophysis* spp. have become a widespread phenomenon (Reguera et al., 2014). Over the past two decades, DSP events have been reported to be an increasing threat to the coastal waters of Spain, Norway, Northern Japan, Germany, Mexico, Argentina, Brazil, Greece, Italy, and Africa (Caroppo et al., 2001; Koike et al., 2001; Klopper et al., 2003; Koukaras & Nikolaidis 2004; Pizarro et al, 2009; Naustvoll et al., 2012; Harred & Campbell 2014; Reguera et al., 2014; Fabro et al., 2016; Danji-Rapkova et al., 2018; Fernandez et al., 2019). More recently, however, DSP events have posed a public health concern in the United States with toxin levels above the action limit, and several cases of gastrointestinal disorders occurred in coastal regions where they were once considered to be "DSP-free" (Reguera et al., 2014). The western (Washington), eastern (New York), and southern coastal regions (Texas) have been affected by increasing levels of DSTs (Swanson et al., 2010; Hattenrath-Lehmann et al., 2013; Trainer et al., 2013).

2.2.2: DSP Events in the Puget Sound

The first reported clinical case of DSP in the United States occurred in Sequim, Washington during early summer (June) of 2011. Three people became ill after ingesting recreationally harvested shellfish (Trainer et al., 2013). Later that summer, during July and August, there was another outbreak in the Pacific Northwest, located in in the city of Vancouver, British Columbia, Canada, wherein 62 consumers of Pacific coast mussels reported gastrointestinal symptoms associated with DSP (Eberhart et al., 2013). *Dinophysis* has been reported throughout the Washington State coastal waters for several decades, yet

the events occurring in 2011 presented the initial cases of DSP to be a public health hazard due to illness causally associated with high levels of DSTs.

Dinophysis has been a recurring problem along the west coast of the United States. More recently, however, the Pacific Northwest has experienced an increasing prevalence of *Dinophysis* blooms and increasing levels of DSTs. The first shellfish closure occurred in the summer of 2012 at Ruby Beach located on the Pacific coast of Washington State (Trainer et al. 2013). California mussels, manila clams, varnish clams, and Pacific Oyster were all found with toxin levels to be considerably above the regulatory action limit of 160 micrograms per 100 grams of mussel tissue (Trainer et al 2013 & Eberhart et al., 2013).

Since the first shellfish closure, *Dinophysis* has become an increasing environmental threat to Washington coastal waters and has primarily gained prevalence in the region of Puget Sound. Budd Inlet—located at the southern end of the Puget Sound—is a "hotspot" for *Dinophysis* blooms, and reported DST levels above the action level of 160 micrograms per kilograms of mussel tissue have been historically reported (J. Borchert, personal communications, April 1, 2019). In 2013, WDOH reported the highest levels of DST toxins (250 mg/100g in blue mussel tissue) in Budd Inlet, Washington. Two sites, Boston Harbor Marina and North Point Landing, have been continuously sampled for DSTs by WDOH since 2013 and sampled for harmful algal species off and on by SoundToxins since the blooms started (J. Borchert & Vera Trainer, personal Communication, March 15 & April 1, 2019).

2.3: Trophic Dynamics and Diarrhetic Shellfish Toxins in Puget Sound

Due to the rarity in most marine and coastal environments, *Dinophysis* spp. constitute a small percentage of the phytoplankton contributing to the base of the food chain. However, toxic *Dinophysis* spp. can induce health problems in humans when high levels of DSP toxins are synthesized intracellularly. Bioaccumulation of the toxins can occur when they are transferred up the food chain via passive filter-feeders and, to a lesser extent, by crabs (predators of lower trophic levels); zooplankton, annelids, and other invertebrates can also uptake and transmit OA and DTXs to other predators (e.g. gastropods, crustaceans, and echinoderms) (Prego-Faraldo et al., 2013). However, bivalve filter-feeders are the main consumers of the toxic cells located within the water-column. When they feed continuously on toxic cells, the toxins can be highly concentrated within the tissues (i.e. mussel tissue). The consumption of highly concentrated mollusks, such as blue mussels, can act as the most common vector organism to transfer to higher trophic levels, including human and to a lesser extent marine mammal (less common), where the toxins can induce DSP episodes (Figure 2).

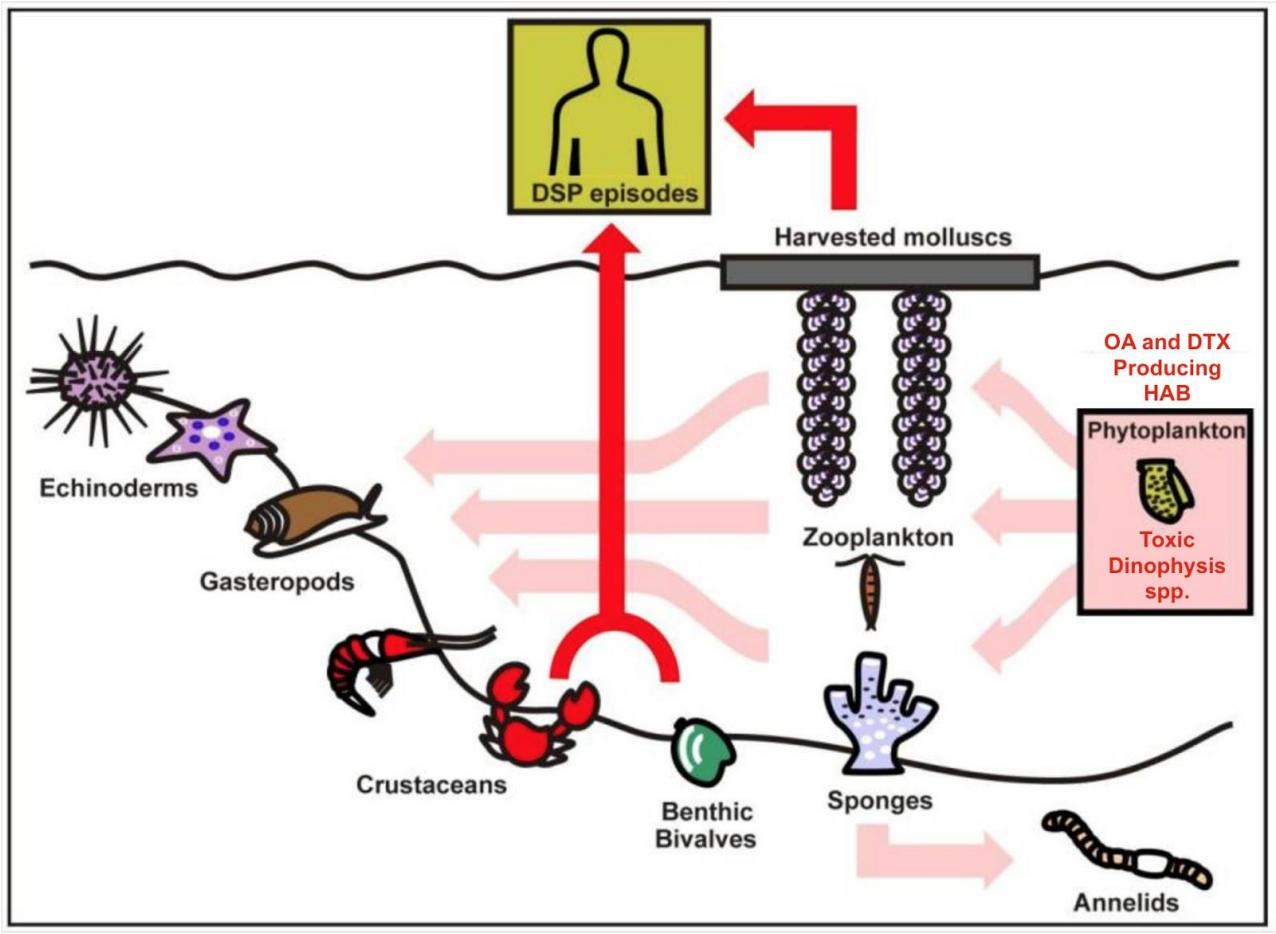

Figure 2 (adapted from Prego-Faraldo et al., 2013): The transfer of OA and DTXs through the food chain.

Most of the dissolved okadates can be readily accumulated in the tissues of various shellfish species due to its highly lipophilic properties. The metabolic processes of shellfish can, thereby, biotransform OA, DTX-1, and DTX-2 into several different derivatives and fatty acid esters (FAO, 2004; Reguera et al., 2014; Nielsen et al., 2016). Little is known about the retention and depuration rates of okadates in bivalves. The metabolism of the toxins by shellfish is specific and can take hours up to days; however, maturity and size of the mussels has not been shown to have an effect on the uptake rate of the toxins (Fux et al., 2009; Neilsen et al., 2016). For example, Nielsen et al. (2016) demonstrated *Mytilus*

edulis has a depuration rate of about 4 days after toxin accumulation with a half-life of 5-6 days and showed more than 66% net retention of toxins of OA and DTX relative to the total amount of toxins ingested. They further observed that medium-sized blue mussels reached the regulatory threshold by toxin exudation of 75 cells per liter in laboratory conditions.

Since the major DSP outbreak in 2011 in Washington state, there have been several DSP outbreaks attributed to high concentrations of okadates. Passive samplers, such as sentinel blue mussels, are currently used by WDOH for monitoring and evaluating DSP toxins for early warning of DSP outbreaks and *Dinophysis* blooms at several sites within inland estuarine waters of Puget Sound and the outer coastal regions. Liquid-mass chromatography mass spectrometer (LC-MS/MS) allows each toxin to be fully characterized and identified to gather information on the toxin profile of the shellfish tissue contents. Most DSP cases in Puget Sound have been attributed to contaminated blue mussels (*M. edulis)* and Pacific coast mussels (*M. californianus*) primarily concentrated with DTX-1 and sometimes co-occurring with low levels of DTX-3 or OA (Trainer et al., 2013; J. Borchert, personal communications, April 1, 2019). During the study between 2011-2012, DSP toxin profiles were very similar in oysters, clams, and mussels in Puget Sound; mussels had the highest toxin content while clams and oysters had more than 50% less toxins (Trainer et al., 2013).

2.4: Ecophysiology of *Dinophysis* in Estuarine-Coastal Ecosystems

Over the years, *Dinophysis* has been determined to be a complex HAB genus due to it recently being characterized as an obligate mixotrophic dinoflagellate. It werent until 2006 that Park et al. (2006) was able to successfully culture *Dinophysis* in the laboratory. Culturing was a challenge for researchers due to the capability of *Dinophysis* species to functionally utilize two modes of nutrition to maintain growth and survival: phototrophy (the use of light to uptake inorganic nutrients) and phagotrophy (sequestration of particulate food or prey) (Hattenrath-Lehmann et al., 2013; Reguera et al., 2013).

Dinophysis is one of the few toxic dinoflagellates that heavily rely on ingesting and utilizing the chloroplasts of its prey, the marine ciliate *Myrionecta rubra* whereby *Dinophysis* spp. project their peduncle (or a feeding tube) to suck up the cytoplasm (Park et al., 2007; Wisecaver and Hackett, 2010; Kim et al., 2012). This form of phagotrophy has also been characterized as "acquired phototrophy," where cells of *Dinophysis* are able to effectively use the chloroplasts from phototrophic prey for their growth (Hansen, 1991; Hansson et al., 2013). Other studies noticed *Dinophysis* does not strictly rely on its prey for growth in nutrient-replete conditions; various species have illustrated they require a continuous food uptake as well as increased photosynthetic activity for optimal growth and cannot survive in totally dark conditions even with extra prey available (Nielsen et al., 2013). If one of the modes of nutrition is limited (e.g. prey source of *M. rubrum* or light availability), growth is minimal, photosynthetic autotrophic activity is reduced, and *Dinophysis* can transition into starvation mode

allowing survival up to several months as long as there is minimal light (Kim et al., 2008; Riisgard and Hansen, 2009; Nielsen et al., 2012).

The combination of both nutritional modes enables *Dinophysis* to use and augment various sources of nutrients, supplement with photosynthesis when nutrients are in limited supply, and employ more than one trophic level (Sanders et al., 1990; Cloern & Dufford, 2005). Thus, mixotrophy provides a competitive advantage compared to genera categorized solely as phototrophs or heterotrophs (Bockstahler & Coats, 1993).

2.4.1: Eutrophication and Toxic Dinophysis

A primary factor for growth and survival of all phytoplankton is the bioavailability of inorganic and organic nutrients. During the turn of the century, increasing anthropogenic activities, such as land use changes, industrialization, energy demands, human population growth, animal farming, aquaculture, and agriculture production have transformed the majority of estuarine-coastal ecosystems by inducing a global problem of nutrient pollution (Cloern, 2001; Howarth et al., 2002). Furthermore, coastal development has caused nutrient loading from sewage, agriculture waste, fertilizers, and inputs from the atmosphere have significantly elevated the supply of nitrogen and phosphorus to coastal and estuarine waters (Glibert & Burkholder, 2011; Larsson et al., 2017). Human-induced nutrient loading promotes eutrophic conditions that can lead to intense eutrophication which has been generally known to alter nutrient ratios necessary for growth of phytoplankton and facilitating the onset of blooms (Jickells, 1998; Cloern, 2001).

During the last two decades, HABs have been increasing linked to eutrophic conditions and nutrient loading of nitrogen and phosphorous (Smayda, 1997; Anderson et al., 2002; Trainer et al., 2003; Glibert et al., 2005; Hattenrath-Lehmann et al., 2015). It has been generally known that the availability of dissolved inorganic nitrogen in the form of ammonium (NH_4^+), nitrate (NO_3^-), nitrite (NO_2^-) is the primary limiting nutrient to restricting the growth of phytoplankton Ryther & Dunstan, 1971; Howarth & Marino, 2006). However, studies have illustrated phosphorus (PO_3^-) can also be the limit nutrient in particular aquatic environments, such as the Baltic Sea, eastern Mediterranean, and Pearl River Estuary in China (Andersson et al., 1996; Yin et al., 2001; Krom et al., 2004; Xu et al., 2008).

Most current estuarine-coastal waters have been observed to deviate from the normal Redfield ratios of 16:1of nitrogen to phosphorus (Redfield, 1934; 1965; Harris, 1986; Larsson et al., 2017). This molar ratio is intended to clarify which of the two nutrients are limiting for these phytoplankton communities (Davidson et al., 2012). When the ratio is less than 16:1 nitrogen limitation is inferred; on the other hand, ratios greater than 16:1 indicate there is a limitation of phosphorous. The potential consequences of altering the ratio of nutrients and the form of nutrients increasing the growth and occurrence of harmful algal species are based on the nutrient ratio hypotheses in natural systems, thereby suggesting a strong relationship between nutrient resource availability and the stoichiometry of phytoplankters (Tilman, 1977; Officer & Ryther, 1980).

Overall, anthropogenic nutrient inputs have been strongly linked to facilitating changes in the community structure and seasonality of phytoplankton in estuarine-coastal ecosystems (Cloern, 2001; Larsson et al., 2017). Historically, coastal increases of nitrogen and phosphorus in relation to the concentrations of silicate—the critical inorganic nutrient for diatom frustule formation—has prompted the shift in phytoplankton community structure from diatom to dinoflagellate assemblages (Berg et al., 1997; 2003, Cloern, 2001; Gobler et al., 2002; Glibert et al., 2001, 2004, 2005). The majority of eutrophic estuarine waters are comprised of mixotrophic dinoflagellates (Glibert et al., 2005; Glibert & Burkholder, 2011). There is supporting evidence suggesting levels of toxicity in shellfish have increased due to toxic dinoflagellates assemblages constituting the majority of the total phytoplankton populations in estuaries and coastal waters, especially during the seasonal period from spring to autumn (Glibert et al., 2005; Glibert & Burkholder, 2011; Davidson et al., 2012). The current nutrient loading has been conducive to the selection of harmful species over non-toxic phytoplankton (Hallengraeff, 1993; Anderson et al., 2002; Heisler et al., 2008; Conley et al., 2009).

2.4.2: Theory of Ecological Role of DSTs

When nutrient composition deviates from normal Redfield ratios, it can cause "stress" conditions to phytoplankton. Evolution of harmful algal species has been proposed to be an adaptation to endure these nutrient-stressed conditions characterized as nutrient-rich or nutrient over-enriched (Glibert & Burkholder, 2011; Davidson et al., 2012). Furthermore, studies have shown that HAB species

have the functional capacity to combat nutrient stress by creating toxins intracellularly to manage the physiologic responses to altering ambient nutrient concentration in the water-column. They also have the capacity to form intense blooms by excreting toxic metabolites intracellularly, consequently facilitating their dominance in the phytoplankton community (Davidson et al., 2012). The ability of toxic *Dinophysis* and other harmful algal species to produce toxins might suggest their evolutionary selection to exhibit fundamental adaptive responses to nutrient limitations and high frequency changes to the bioavailability of nutrients over the past century (Graneli et al., 2008; Davidson et al., 2012).

Since *Dinophysis* is mixotrophic in nature, the DSP toxins potentially allow the cells to physiologically control their nutritional intake of inorganic nutrients and prey compared to that of other non-HAB phytoplankton. The synthesis of okadates (OA and DTXs) have shown to play ecological roles between the relationship of the availability of prey source, nutrients, and light emittance (Nielsen et al., 2013; Smith et al., 2018). Yet, the ecological role of DSTs are widely unknown and currently intense topics in HAB research. There are several potential evolutionary functions of these toxins that provide biological advantages for *Dinophysis* in marine waters: including allelopathy, grazer defense, food capture, and antibacterial deterrent (Nagai et al., 1990; Carlsson et al., 1995; Gross, 2003, Graneli & Hansen, 2006).

Dinophysis polyether toxins--both OA and DTXs--have been found to also negatively affect prey, competitors, and grazers. DSP toxins act as a "stress surveillance system" where they can serve as an early-warning protective

mechanism communicating to other viable cells about stressors in the ambient environment, such as low concentrations of inorganic nutrients or prey (Vardi et al., 2006). When nutrients are minimal, the toxins released from "wounded" or stressed *Dinophysis* cells could further minimize cellular death of nearby healthy cells and aid in competing for those limited nutrient resources.

According to several studies, toxins exuded from *Dinophysis* have been observed to exhibit allelopathic properties concerning the predator-prey relationship between toxic *Dinophysis* spp. and *M. rubra*, resulting in elevated DSP toxins from *D. fortii* blooms which induced changes in growth, behaviors, and mobilization of *M. rubra* (Nagai et al., 2008; Nishitani e al., 2008; Nielsen et al., 2013). Once exposed, *M. rubra* was found to form into clumps, and individuals no longer possessed the ability to move in a normal rapid orientation; rather, they hardly moved and *Dinophysis* was able to capture its prey with ease (Nagai et al., 2008).

Graneli and Hansen (2006 suggest polyethers have a "hemolytic" properties where interactions of the chemical constituents can lyse the cell membranes of other competing and grazing phytoplankton. For example, *Dinophysis fortii* has also demonstrated they can use these polyether lipids as a defense mechanism to deter against other mixotrophic dinoflagellate grazer that predate on *Dinophysis.* According to Neilsen et al. (2008), it takes approximately 1 µmol/L of total concentrations of freely dissolved OA to inhibit 10% of the growth of competitors (Nielsen et al., 2013).

In addition, OA and DTXs have been shown to function as a bacterial grazer. Bacteria tend to assimilate most of the new forms of dissolved organic nitrogen (DON) and phosphorous (DOM) in estuarine waters. *Dinophysis* targets bacteria in order to release the recycled and limiting nutrients (Glibert & Burkholder, 2011).

All these factors suggest the toxins are not intended for any specific organism, rather they merely negatively affect any organism seen as a competitor or a threat to survival and growth. To date, these theories of DSTs have not been fully investigated to prove whether or not polyether toxins exhibit allelochemical effects to other marine plankton in ambient seawaters.

2.5: Ecophysiological Response of *Dinophysis* to Environmental Conditions

Toxic *Dinophysis* species are distributed throughout temperate, tropical, subtropical, and boreal waters, yet each species and strain of each species has demonstrated variances in toxin quotas (the intracellular synthesis of DSTs intracellularly) in different coastal and estuarine environments. There is mounting evidence from laboratory and field studies demonstrating populations of *Dinophysis* species have shown strong contrasting levels of toxin production of both OA and DTXs among the same species (Nagai et al., 2011; Trainer et al., 2013; Hattenrath et al., 2015; Reguera & Blanco, 2019). Variability in strains and species is due to the ability of members to produce more than one group of okadates. For example, *D. acuminata*--the most studied species of the *Dinophysis* genus--has been found along the majority of the North American coastline. *D. acuminata* found on the east coast (New York, Massachusetts and Maryland) has

been known to produce both OA and DTX-1. The southern coastal (Texas) strains have only been known to excrete OA, while on the west coast (Washington state and British Columbia in Canada), DTX-1 is primarily an isomer produced, although OA and DTX-2 can also be present but rarely seen (Hackett et al., 2009; Fux et al., 2011; Tong et al, 2011; Trainer et al., 2013; Hattenrath-Lehmann et al., 2015; Tong et al., 2015a). These variances in toxin profiles suggest the responses to environmental conditions are species-specific.

The advantage of the toxins means species of *Dinophysis*, including each strain of species, can create their own "microenvironment" with DSP toxins produced, whereby resulting in advantageous functional capability to compete against their competitors (Glibert & Burkholder, 2011). By modulating their intracellular environment, they can change the physical-chemical relationships by altering the elemental composition of nitrogen and phosphorous. Thus, the availability of the nutrients is dependent on the rates of adsorption and desorption of these dissolved inorganic nutrients which can potentially interfere with the physiology of the cell. Toxins allow *Dinophysis* to strategically mobilize and recycle the nutrients to continue photosynthesizing, especially at high rates of photosynthesis during blooms (Glibert & Burkholder, 2001).

Toxic species of *Dinophysis* are rare in natural waters usually with concentrations of 1-100 cells/L, although *Dinophysis* populations can occur greater than 1,000 cells/L and form large blooms (Trainer et al., 2013). Studies have shown toxic *Dinophysis* species can produce these toxins at both low cell abundances and during bloom events (Reguera et al., 2012; Reguera et al., 2014;

Simoes et al. 2015). Toxin production leading to DSP events has been attributed to various environmental dynamics encompassing physical, chemical, and biological conditions. Several studies suggest toxin production and bloom formation of each *Dinophysis* species is influenced by its ambient environmental and hydrological conditions (Escalera et al., 2006; Jephson & Carlsson et al., 2009; Seeyae et al., 2009; Gonzalez-Gil et al., 2010; Vanucci et al., 2010; Diaz et al., 2013; Alvest-de-Souza et al., 2014; Valamis & Katikou, 2014; Velo-Suarez et al., 2014; Hattenrath-Lehmann et al., 2015; Hattenrath-Lehmann & Gobler, 2015; Tong et al., 2015b; Moita et al., 2016; Accroni et al., 2018; Ajani et al., 2018; Basti et al., 2018; Danchecnko et al., 2019).

2.5.1: Response to Nutrients and Eutrophic Conditions

Although nitrogen and phosphorous can be found globally, these nutrients are not distributed equally across marine waters (Seizinger et al., 2005; Bouwman et al., 2009). There is evidence suggesting a connection between decreasing inorganic nitrogen to phosphorus ratios and increasing total cellular abundance of *Dinophysis* (Hattenrath-Lehmann & Gobler, 2015). Excess nitrogen and limitations of phosphate have both shown strong relationships to high *Dinophysis* abundances.

According to Anjani et al. (2016) both dissolved forms of phosphorus and nitrogen—nitrite and nitrate—were linked to increasing abundance of *D. caudata* in two different sites. Several studies further emphasize the fact that *Dinophysis* species have necessary physiological requirements of both nutrients and thus growth can be elevated by both as well (Singh et al., 2014; Hattenrath-Lehmann

et al., 2015; Anjani et al., 2016). As a result, several studies mention *Dinophysis* growth by nutrients can be either stimulated directly to the individual or indirectly to the prey due to its mixotrophic characteristics. However, it has been noted that the immediate input of nutrients might have a lagging effect on the growth on Dinophysis (Vale et al., 2003).

Another study has supporting evidence illustrating that both inorganic (nitrate and ammonium) and organic (glutamine and sewage effluent) forms of nitrogen can stimulate the growth rates of *Dinophysis* species, yet ammonium and nitrate displayed the greatest effects on increasing density of *Dinophysis* (Hattenrath-Lehmann et al., 2015). Another study displayed a similar link of *Dinophysis* communities to ammonium enrichment (Seeyave et al., 2009).

Moreover, the San Francisco estuary inhabits another DSP producer, the toxic dinoflagellate *Prorocentrum minimum.* Laboratory and field conclusions displayed differing results, where in the laboratory maximum growth rates were yielded from low nutrient ratios and field studies of blooms showed increasing nutrient ratios of nitrogen-phosphorous (Glibert et al., 2012). On an alternate note, there have been a few field studies that did not find any links between nutrient concentrations and densities of *Dinophysis* (Delmas et al., 1992; Giacobbe et al., 1995; Koukaras & Nikolaides, 2004).

Furthermore, nutrient loading has been highly correlated to production of intracellular toxins and excretion of DSP toxins into the ambient seawaters (Hattenrath-Lehmann et al., 2015). After a nutrient loading episode ensues, *Dinophysis* cells can reach maximum growth in the exponential growth phase

until nutrients become limiting. Then, in starvation "mode" during the beginning to middle of the stationary phase, not only do growth rates decline but toxins are rapidly excreted relative to the other growth phases (log, exponential, and decline) (Nielsen et al., 2013; Basti et al., 2018; Smith et al., 2018). There is growing evidence that the changes in nutrient regime have negatively impacted *Dinophysis* physiology to induce toxin synthesis and increase the toxicity of OA and DTXs from *several Dinophysis* populations, including *D. acuminata*, *D. cuadata,* and *D. fortii* (Nielsen et al., 2013; Hattenrath-Lehmann & Gobler, 2015). To extend the argument, other harmful dinoflagellates such as *Alexandrium tamarense,* a saxitoxin producer, was able to increase toxin production three to four times more in phosphorous limited environments (Graneli & Flynn, 2006).

2.5.2: Response to Hydrological Conditions and Other Environmental Parameters

Most of the existing laboratory research demonstrate the difficulties in understanding the effects of more than one environmental condition because it is challenging to reproduce the dynamic relationships between *Dinophysis* and its ambient natural environment. Field research has supported the notion that environmental and hydrological variability of the coastal and estuarine systems can negatively impact the biological physiology of harmful algal species, including *Dinophysis*. These variabilities can have synergistic effects which directly or indirectly influence the onset of toxin production and formation of blooms (Wells et al., 2015).

Most HABs have been attributed to be affected by climate change inducing pressures of altering the intensity of light, warming of surface water temperatures, increased thermal stratification, alteration of salinity, ocean acidification (decreasing pH), and stormwater runoff nutrient input in estuaries and coastal regions (Fu et al., 2012; Vlamis & Katikou, 2014; Wells et al., 2015). *Dinophysis* has exhibited various levels of physiological plasticity allowing them to respond well to environmental stress, where species can grow in a vast range of light intensity, salinity, and temperature conditions (Tong et al., 2015).

Temperature of the surface seawater is a critical factor found to regulate the growth and physiology of toxin producing species of *Dinophysis*. For example, Basti et al. (2018) explain that *Dinophysis acuminata* isolate from Japan exhibited high plasticity in various surface water temperatures from 8 to 32 °C, with the highest growth rates from 20 to 26 °C and highest total toxin production rates at 20 to 23 °C. Field studies have consistently observed *Dinophysis* within the 0 to 5 m depth in shallow brackish waters and mainly aggregated within the first meter which is known to be the most stratified and warmer conditions (Gonzalez-Gil et al., 2010; Reguera et al., 2014)

Dinophysis has been monitored in various stratified systems and, according to Reguera et al. (2012), *Dinophysis* species are found to thrive well in highly stratified conditions. Due to their morphology, they are able to use their flagella to migrate in a vertical motion where their pattern of behavior is related to the intensity of thermal stratification. *Dinophysis* have been observed in thin

layers in near or above the pycnocline (Jephson & Carlsson, 2009). Furthermore, another mixotrophic, DSP producer *Prorocentrum minimum*, are found to thrive well to short term salinity stress (Skarlato et al., 2018).

In addition, river runoff is a significant source of introduced dissolved oxygen into estuarine zones. Eutrophic conditions could also decrease the oxygen levels further (Anjani et al., 2016). *Dinophysis* success has been correlated with low dissolved oxygen levels near river plumes and in eutrophic environments (Trainer et al., 2013; Hattenrath-Lehmann et al., 2015).

According to Hattenrath-Lehmann et al. (2015), dramatic changes in wind direction and patterns can influence the transportation of nutrients. During that long-term study, the onset of *Dinophysis* blooms occurred two months after the maximal wind differences were noticed. Low velocity winds from the south and north have been associated with maximum counts of several *Dinophysis* species in the Greek coastal waters (Vlamis & Katikou, 2014). Hydrological forcing (advection) and intense upwelling with associated winds have also been known to potentially induce growth of population, aid in transporting the bloom, or spreading out the bloom (Anjani et al., 2016; Moita et al., 2016). However, Gonzalez-Gil et al. (2010) recognized the dominance of *Dinophysis* during the relaxation period of the upwelling-downwelling cycle.

Also, precipitation patterns have also been known to influence the densities of *Dinophysis* and concentrations of toxins. According to Vale et al. (2003), maximum DSP levels correlated with the lowest rainfall periods from

June to September. While May and October presented relatively moderate levels of DSPs; during the winter months DSP levels were very low.

2.6: Toxic *Dinophysis* in Budd Inlet

Budd Inlet is an estuary that has been known to exhibit very poor water quality due to its historically known anthropogenic influences. Site A (head of estuary) has been imposed upon the most from land use changes of dredging, sewage treatment plants, and dam placement at the mouth of Deschutes River. Capitol Lake is known for high nutrient loads as well as increasing percent of dissolved oxygen, where levels of nitrogen are on average 0.5 mg/L during spring to summer months (Roberts et al., 2015; McCarthy et al., 2018). However, Site B (mouth of estuary) has not reported to have extensive impact by human activities relative to the extent of Site A.

Several *Dinophysis* species, including *D. acuminata, D. fortii*, *D. norvegica*, and *D. rotundata* have been found within the Puget Sound and have been associated with the occurrence of *Dinophysis* blooms (Trainer et al., 2013). To date, Trainer et al. (2013) and WDOH are the sole investigators of both abundance and toxin analyses of *Dinophysis* spp. in Puget Sound. *D. acuminata* constitute the majority of the species present in the study, while D. norvegica, *D. rotundata*, and *D. fortii* constitute a significantly smaller portion of *Dinophysis* species found within central and northern Puget Sound (Trainer et al., 2013).

2.7: Conclusion

Despite our heightened understanding of physicochemical factors stimulating blooms, not all blooms are a direct result of anthropogenic influence

and multiple factors could be at play. This generates many challenges to predict these dynamic toxic outbreaks and blooms. Although DSP outbreaks and toxin-producing species of *Dinophysis* have been recognized in Washington state for almost a decade, there is limited knowledge and understanding of the drivers initiating the formation of *Dinophysis* blooms and DSP outbreaks. This presents various problematic issues with the management and strategies used to predict *Dinophysis* abundance, blooms, and toxicity locally in the Puget Sound and globally where toxic *Dinophysis* species are presenting a nuisance and posing a threat to public health and local shellfish industries. Since DSP events pose a threat to human health, a knowledge gap is presented regarding the environmental mechanisms influencing the onset, development, and succession of *Dinophysis* blooms and DSP outbreaks (Trainer et al., 2013; Hattenrath-Lehnman et al., 2015; Ajani et al., 2016).

This study will document the pattern of selected water quality parameters from winter to summer, in addition to the environmental conditions that may determine *Dinophysis* species, blooms, DSP levels in mussel tissue, and composition of phytoplankton assemblages at two sites in Budd Inlet (south puget sound).

CHAPTER 3: MATERIALS AND METHODS

3.1: Study Area and Monitoring Stations

Puget Sound is characterized by high biological productivity of diverse flora and fauna. Southern Puget Sound is an important area for shellfish cultivation generating over 13 million pounds yearly of commercial and recreational harvest (Rau, 2015). In addition, they are increasing commercial and recreational harvest rates of clams and oysters.

Since 2015, Budd Inlet has been identified as a hotspot for Diarrhetic Shellfish Poising (DSP) toxins by the Washington Department of Health (WDOH). WDOH has placed sentinel mussels for continuous sampling of diarrheic shellfish toxins (DTX-1, DTX-2, and okadaic acid) throughout the year at two locations—at the northern and southern ends of the inlet. Sentinel mussels have been placed to monitor the DST toxins because Budd Inlet has been known to have the highest recorded DSP toxin levels of 250 mg/100g in the U.S. and second highest worldwide (J. Borchert, personal communications, April 1, 2019).

Regular phytoplankton monitoring was conducted at two stations within Budd Inlet **(**47.0966° N, 122.9094° W; Fig. 3**)** located inland, at the southernmost end of the Puget Sound in Washington state. Station 1 was located at north end (North Point Landing, 47.0585 W, -122.905119 N) at the estuary head closest to the Deschutes River and station 2 was at the southern end at mouth of the estuary closest to the south basin of Puget Sound (Boston Harbor Marina, 47.1400 N, -122.9053 W). These stations were selected because they represent different environmental conditions for phytoplankton species diversity and growth. Budd Inlet has been reported to have more dynamic

circulation relative to other bodies of water in Puget Sound (LOTT Waste Management Partnership, 1998). This increase in mixing is caused by the flow of the Deschutes River, the second largest river in the Puget Sound and large tidal amplitudes. Station 1 at the head of the estuary is closest to the river input which, in theory, provides more nutrients from the river drainage and density stratification due to high fluctuations in salinity. Station 2 at the mouth is more representative of marine conditions where the salinity is relatively uniform with depth representing low density stratification.

Figure 3: Two monitoring stations within Budd Inlet, South Puget Sound, WA.

Although the placement of the Deschutes River dam has restricted the flow and movement of water entering Budd Inlet, this human-induced restriction along with other anthropogenic activities of dredging and nutrient-loading from local wastewater

treatment plants and runoff into the river has the potential to provoke environmental consequences to the biota within the local estuarine ecosystem (Ahmed et al., 2019).

The stations were located at the same area of placement as sentinel mussels for DSP sampling by WDOH. In addition, there is a history of phytoplankton sampling within Budd Inlet by The Evergreen State College collaborating with SoundToxins in previous years providing evidence of overall dinoflagellate dominant community at the estuary head while the mouth was primary a diatom dominant community (G. Chin-Leo, personal communications, June 15, 2018).

3.2: Research Design: Field Sample Collection and Lab Processing

The study period was from January through October of 2019, which encompassed the seasonal cycle from winter to fall. At both stations, the frequency of phytoplankton and water sampling was monthly during winter and fall seasons and weekly during the spring and summer seasons. Samples were collected to determine cell abundance and species composition using two different methods.

To determine abundance, the method included quantitatively concentrating surface waters. *Dinophysis*, the target species and sometimes dominant species were counted. Due to the low abundance of *Dinophysis* spp., in winter, a large amount of water was concentrated (~15-120 L) using a 20 μm mesh phytoplankton net used as a sieve. The concentrated phytoplankton were condensed further by using a 20 μm mesh sieve with the final concentration ~200-400 mL. Thus, the concentration factor could be as high as 600 times the normal cell density. The water volume collected for concentration was adjusted depending on the concentration of cells in natural waters. During blooms, for example, 15 L were sufficient to produce a dense sample for counts.

The sample for species composition was completed via a vertical tow near or during high tide; three tows were completed each time to collect enough water for concentration. The vertical tow allowed for collection of plankton throughout the water column. This was important because some species migrate vertically or accumulate and density interfaces. The concentrated phytoplankton was preserved with 2.5% Glutaraldehyde for storage and possible subsequent Scanning Electron Microscope analysis.

Biological, physicochemical, and water quality parameters were also measured. Surface seawater samples were collected for phytoplankton biomass (chlorophyll-a) and nutrient (ammonium, nitrate, silicate, and phosphate) analysis. Measurements of temperature, salinity, and dissolved oxygen where obtained in situ with a multi-parameter sensor YSI-2030. Light transparency was measured with the Secchi disk. Coastal Salinity Index (CSI) was also computed by subtracting the bottom salinity by the surface salinity. This was used to estimate changes in density stratification.

3.3: *Dinophysis* Abundance, DSTs, and Environmental Analyses

3.3.1: Dinophysis Abundance and Species Composition

Concentrated phytoplankton samples (~200 mL) were examined with a gridded Sedgewick Rafter counting chamber and observed on an Olympus BX63 microscope. Three rows, at a minimum, were chosen randomly and enumerated for the majority of the concentrated samples so there would be at least ~10 cells per row. The mean counts per mL were then multiplied by the number of rows on the slide. *Dinophysis* cells was also identified to the species level.

For phytoplankton species composition, relative abundance observations were determined for each genus present. One drop of the species composition sample was

placed on the microscope slide, and the relative abundance was calculated by determining the percent of species of one genus relative to the total population. The classifications are as follow: absent (no cells were found), rare (1 cell was found), common (2 cells were found), and abundant (3 or more cells were found). *Dinophysis* species and most of the common phytoplankton were confirmed via light microscopy and scanning electron methods.

Diarrhetic Shellfish Poisoning (DSP) data was obtained from the WDOH Marine Biotoxin Monitoring Program. Their sampling procedure is as follows: blue mussels (*Mytilus edulis*) were collected bi-weekly on an annual basis at the estuary head and in summer (May-Sept) at the estuary mouth. Sentinel mussels at these sites were initiated in 2015 and since then have been monitored continuously. WDOH monitors and analyses the mussel tissue for DSP toxin profile of Okadaic acid, DTX-1, and DTX-2 using the method of liquid chromatography-mass spectrometer (LC-MS).

3.3.2: Measurements of Environmental Parameters

Seawater samples were collected, frozen, and processed at the laboratory for quantification of chlorophyll-a and inorganic nutrient concentrations. Triplicate chlorophyll-a samples were filtered onto a glass fiber filter (Whatman GF/F) and stored frozen below 0 °C. For processing, filters were extracted for 24 hours in 90% high grade acetone, and filtrate from the chlorophyll-a samples were used for nutrient analysis and stored in -10 °F freezer. The chlorophyll-a was measured with an10-AU Fluorometer (Parsons et al., 1984).

Nutrient filtrates were analyzed for nitrogen, silicate, phosphate, and ammonium using the standard methods. Nitrogen (nitrate and nitrite), phosphate, and silicate were

quantified using standard microplate reader colorimetric methods, and the samples were read by the Molecular Devices VersaMax (Ringuet et al., 2011). Ammonium samples were analyzed with the orthophthaldialdehyde (OPA) method and read on Turner designs 10-AU (Trilogy) fluorometer (Holmes et al. 1999).

Other physical and meteorological data were obtained. Wind speed/direction, air temperature, and average precipitation were results reported in Budd Inlet, Olympia by the NOAA National Weather Service (archived). Deschutes River flow discharge was also obtained from the U.S. Geological Survey. Solar radiation data was obtained from the Scientific Computing Weather Station of The Evergreen State College. DSP concentrations at both of the sample locations were provided by the Washington Department of Health to determine if toxicity was related to abundance.

3.4: Statistical Analyses

To understand if the environmental parameters measured are related to *Dinophysis* abundance, statistical analyses were performed via a simple linear regression, where the abundance is the response variable while the environmental parameter is the independent variable. Log transformations to the *Dinophysis* abundance data were executed to meet the assumptions of normality to run the test. The best way to deal with heteroscedastic and skewed results is by using a log transformation of the data (Hattenrath-Lehmann et al., 2013).

In order to run regression, the data has to meet the assumption of linearity. To meet this assumption, I performed sensitivity testing of the data at both the head and mouth. The log transformation was used to reduce the skew of dependent and independent variables because they are not necessarily linear in nature. I also ran the tests

without the transformation and compared the results and found that the regression analysis showed different significant outcomes related to abundance at the head of the estuary, but not at the mouth. This may mean that the non-transformed data from the estuary head was more skewed than the data obtained from the estuary mouth since the larger density blooms occurred. Independent t-tests were run to determine if the differences in biological, meteorological, and water quality parameters between the estuary head and mouth.

In addition to the statistical analysis, qualitative analyses of *Dinophysis* densities and environmental parameters were also performed. Time series graphs were analyzed to assist in the evaluation of possible delays in environmental conditions, especially since the statistical relationships potentially do not fully represent the lag time between the response of *Dinophysis* to the environmental factors.

CHAPTER 4: RESULTS

4.1: Phytoplankton Species Composition

Phytoplankton species composition varied over the study period. For simplicity, I will refer to the mouth of the estuary as BHM (Station 1) and NPL (Station 2) as the head. NPL exhibited high species richness of species, and a total of 75 species were observed with diatoms dominating throughout the majority of the year, with the exception of summer months when dinoflagellates dominated. NPL had lower species richness with a total of 63 species. Both stations had a total 23 species of dinoflagellates, and the remaining were diatom species. About 34.8% of the species observed were dinoflagellates and 65.2% were diatoms. The estuary head also exhibited a similar pattern: 32.9% of the species were dinoflagellates and 67.1% were diatoms. Although species richness was similar at both stations, overall there was a greater relative abundance of diatoms at BHM while more dinoflagellates were present at NPL. About 4% of the species were commonly found throughout the study, being detected greater than 20 times at the estuary head, and 3% of common species were found at the estuary mouth.

Diatoms dominated winter to late spring (January to early June) and dinoflagellates dominated summer to fall (early June to October). There was a difference in species composition between sites. NPL's most abundant species was *Ceratium fusus* and most common was *Chaetoceros debilis.* The most abundant species was *C. debilis* and most common species was *Skeletonema costatum* at BHM. Several diatoms and dinoflagellates were present but were considered rare because they were observed infrequently at very low concentrations. Also, there were several HAB species found

throughout the study including: *Pseudo-nitzschia* spp., *Alexandrium* spp., *Dinophysis* spp., *Heterocapsa triquetra,* and *Protoceratrium reticulatum. Dinophysis* spp. and *Pseudo-nitzschia* spp. were the two dominant HAB species, often co-occuring throughout the seasonal cycle at both stations. Other harmful but non-toxic algae, *Ceratium fusus* and *Akashiwo sanguinea,* were found to co-occur with *Alexandrium* spp. (see Appendix A).

4.2: Spatiotemporal Differences

There were significant differences ($p < 0.05$, $n = 55$) between both stations in the following parameters averaged over the study period, including: dissolved oxygen, ammonium concentrations, silicate concentrations, transparency (Secchi depth), surface water temperature at 1m depth, and coastal salinity index (Table 1). Nutrient ratios, nitrate concentrations, phosphate concentrations, and salinity at 1m depth were not found to be statistically significant.

Biomass levels were not significantly different between both sites (Table 1). Biomass of phytoplankton as estimated from chlorophyll-a varied from 0.78 mg of seawater/L seawater to 58.2 mg of seawater/L with maximal values on 9/7/19 at NPL (Fig. 4). Chlorophyll-a ranged from 1.55 to 14.78 mg of seawater/L with highest concentrations occurring on 7/2/19 at BHM (Fig. 5).

Table 1: Differences in environmental parameters between the estuary head and estuary mouth (significant p-values are boldfaced).

Mean Differences between estuary head (NPL) and mouth (BHM)	
Parameters	**P-value**
Density	0.06
Chlorophyll-a (biomass)	0.47
Dissolved Oxygen (mg/L)	**0.01**
DIN:DIP	0.08
DSI:DIN	0.72
DSI:DIP	0.18
Ammonium (NH4+)	**2.0 e-6**
Nitrate (NO3-)	0.31
Silicate (SiO4-)	**5.0 e-4**
Phosphate (PO4-)	0.16
Seechi Depth	**1.6 e-9**
Surface Water Temperature (1m depth)	**1.5 e-39**
Salinity (1m depth)	0.75
Coastal Salinity Index	**0.04**

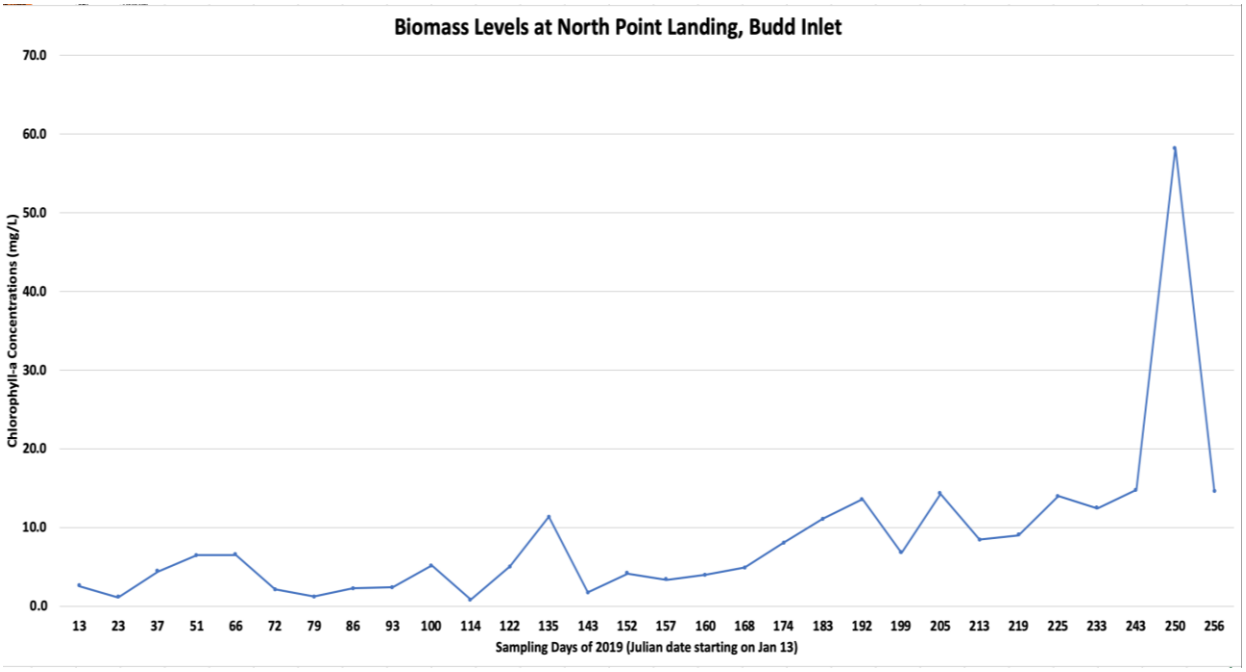

Figure 4: Time series of biomass (chlorophyll-a) levels throughout the annual seasonal cycle at the estuary head (NPL) in Budd Inlet.

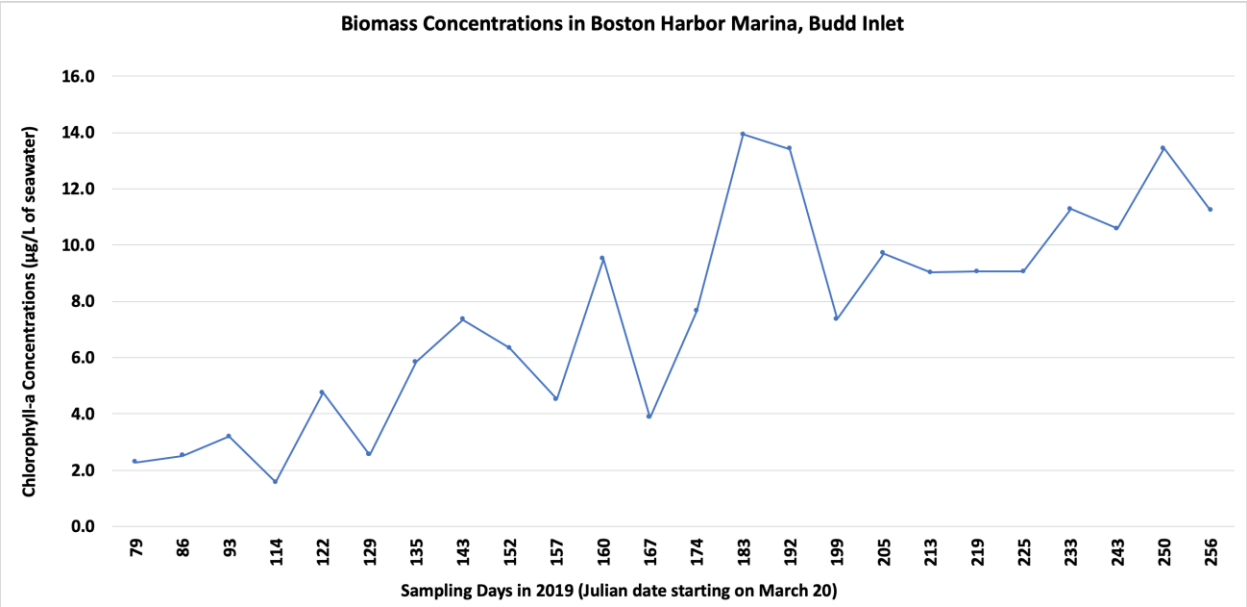

Figure 5: Time series of biomass (chlorophyll-a) levels throughout the annual seasonal cycle at the mouth of the estuary (BHM) in Budd Inlet.

Biomass was significantly related to nitrate (NO_3^-) at both stations (estuary head: $p = 0.0004, r^2 = 0.36$; estuary mouth: $p = 0.002, r^2 = 0.37$) and phosphate (PO_4^-) ($p = 0.002, r^2 = 0.30$) at the estuary head. To determine how changes in nutrient composition might affect species composition, I computed the ratios of total nitrogen to phosphorous and silica to nitrogen and determined if changes in these ratios were related to biomass. Using simple linear regression, two nutrient ratios were correlated to chlorophyll-a concentrations. Nutrient ratios of DIN:DIP are a significant factor at both stations (NPL: $p = 4.15 \times 10^{-5}$; $r^2 = 0.46$; BHM: $p = 0.002, r^2 = 0.37$) (Table 2). In addition, the ratios of DSI:DIN were found to be significant at both stations (NPL: $p = 6.1 \times 10^{-5}, r^2 = 0.44$; BHM: $p = 8 \times 10^{-3}, r^2 = 0.29$) (Table 2).

Table 2: Regression analysis between biomass and environmental parameters at the estuary head (NPL) and mouth (BHM) in Budd Inlet (significant p-values are boldfaced).

Environmental Parameters	Statistics	Estuary Head (NPL)	Estuary Mouth (BHM)
DIN:DIP	R-squared	0.46	0.44
	P-value	**4.1 e-5**	**5.2 e-4**
DSI:DIP	R-squared	0.12	0.00
	P-value	0.07	0.89
DSI:DIN	R-squared	0.44	0.29
	P-value	**6.1 e-5**	**8.4 e-3**
Ammonium (NH_4^+)	R-squared	0.08	0.13
	P-value	0.12	0.25
Nitrate (NO_3^-)	R-squared	0.36	0.38
	P-value	**4.5 e-4**	**1.8 e-3**
Phosphate (PO_4^-)	R-squared	0.30	0.00
	P-value	**1.8 e-3**	1.00
Silicate (SiO_4^-)	R-squared	0.05	0.00
	P-value	0.21	0.87
Salinity (1m)	R-squared	0.00	0.04
	P-value	0.73	0.32
DO (mg/L)	R-squared	0.00	0.32
	P-value	0.81	**3.6 e-3**
Surface Water Temperature (1m depth)	R-squared	0.34	0.70
	P-value	**7.2 e-4**	**3.6 e-7**
Air Temperature (℉)	R-squared	0.12	0.34
	P-value	0.06	**2.8 e-3**

4.3: *Dinophysis* Species Diversity and Abundance

Dinophysis species were present throughout the study at both stations. *Dinophysis* was not detected once in 34 weeks of sampling at the head of the estuary station. At the estuary mouth, *Dinophysis* was observed in all the 31 weeks monitored. *Dinophysis* was found to be both abundant and dominant during the peak densities in summer months at both sites. During the blooms, *Dinophysis* was co-occurring with other diatoms, primarily *Thalassiosira* spp. The relative abundance of *Dinophysis* was largely considered rare and occasionally common during all other months during the spring,

summer, and fall. *Dinophysis* typically co-occurred with another HAB diatom genus, *Pseudo-nitzschia.*

D. norvegica was the most abundant *Dinophysis* species at both sites, reaching densities of 23,857 cells/L at the estuary head and 3,590 cells/L at the estuary mouth on 6/6/19. Other species observed during the study included: *D. acuminata, D. fortii*, *D. rotundata*, *D. odiosa*, *and D. parva.* Their abundances were much lower with the largest densities of 1,933 cells/L of *D. fortii* (9/13/19), 542 cells/L of D. acuminata (10/2/19), 71 cells/L of *D. odiosa* (8/7/19), 30 cells/L of *D. rotundata* (8/31/19), and 50 cells of *D. parva* (8/13/19) at the station near the head of the estuary. At the estuary mouth, abundances of *Dinophysis* were considerably lower reaching densities of 115 cells/L for *D. acuminata* (6/6/19), 67 cells/L of *D. fortii* (6/6/19), 84 cells/L of *D. rotundata* (7/2/19), 318 cells/L of *D. odiosa* (7/18/19), and 1 cell/L of *D. parva* (9/7/19). For most of the year, *D. norvegica*, *D. acuminata*, and *D. fortii* co-occurred at both sites.

4.4: Spatiotemporal Distribution of *Dinophysis* Species

Maximal densities of *Dinophysis* illustrated a similar correspondence at both of the sites during the summer months (Fig. 6). Variations of abundance were considerably noticeable at both sites from June to August. The major difference is that the concentrations vary more widely at the head of the estuary showing the highest values of *Dinophysis* abundance. Generally speaking, *Dinophysis* densities greater than 1,000 cells/L are considered blooms (Macknenzie, 2019). The majority of the *Dinophysis* blooms occurred during the summer months at both sites but were also seen during the fall months at the estuary head.

There were at total of 13 bloom events at NPL and 6 events at estuary head (BHM) (Fig. 6). There were distinct peaks in *Dinophysis* abundance in the summer months from early June to late July at both stations. A total of four dense blooms occurred at the estuary head on 6/6/19, 6/23/19, 7/11/19, and 7/24/19 (Fig. 3). At the estuary mouth there were three peaks occurring on 6/6/19, 6/23/19, and 7/18/19. Maximal values occurred at both locations on two occasions during the early summer (6/6/19 and 6/23/19). *Dinophysis* abundance ranged from 1 cell/L to 33,600 cells/L with highest abundance on 6/27/19 at the head of the estuary. Also at the NPL station near the estuary mouth, *Dinophysis* densities ranged from 1 cell/L to 3,705 cells/L with the highest density occurring on 6/6/19. *Dinophysis* was the dominant species during the peak blooms. The relative total of the entire *Dinophysis* species was considered abundant during these summer months starting in June to August at both sites, although other diatoms co-occurred but were relatively rare in abundance.

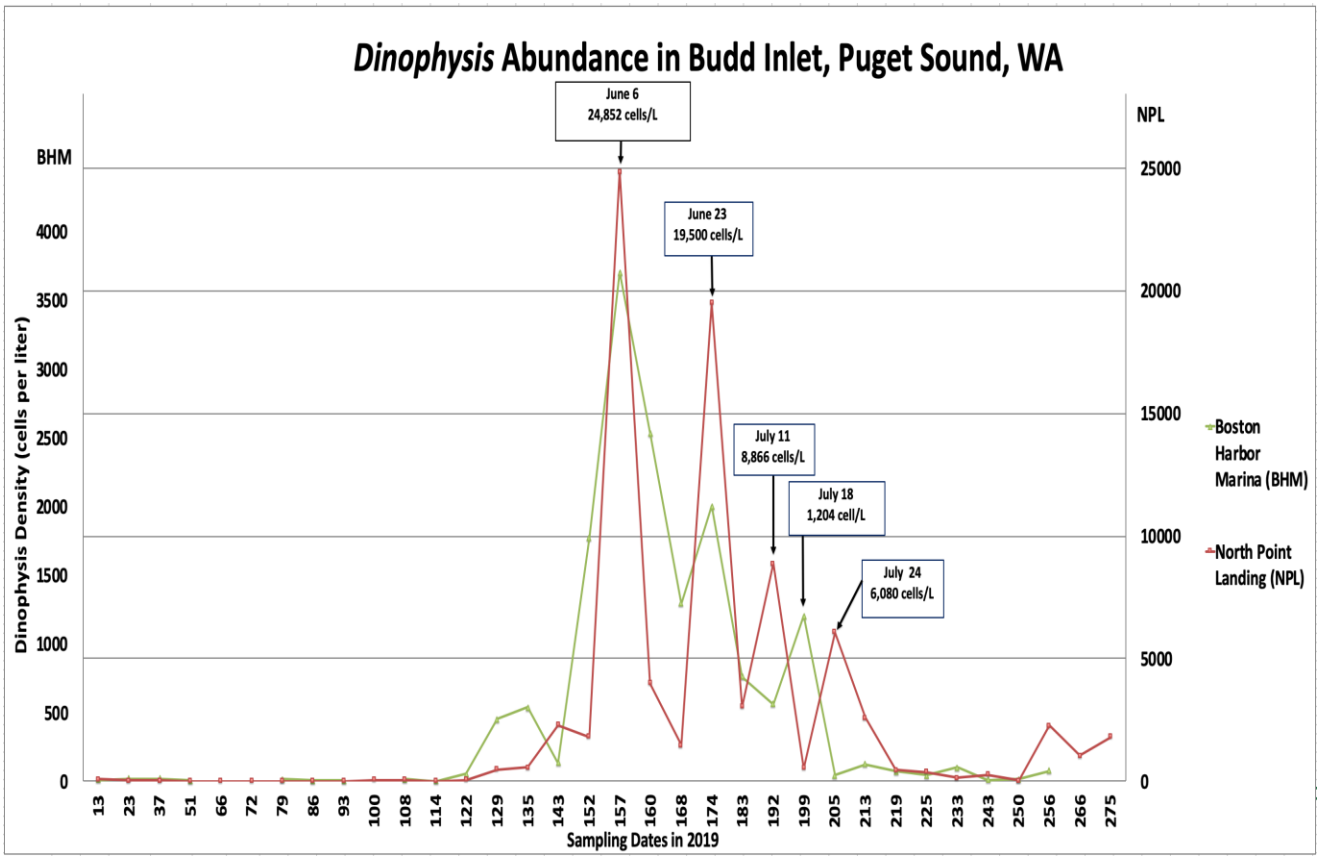

Figure 6: *Dinophysis* abundance over the seasonal cycle from winter to fall of 2019 at the estuary head (NPL) and mouth (BHM) in Budd Inlet, WA.

4.5: Influence of Environmental Conditions on the Distribution of *Dinophysis*

Regression and qualitative analyses were evaluated to determine whether there is a relationship between biomass and *Dinophysis* densities. At the estuary head, *Dinophysis* abundance was significantly related to biomass, but not at the mouth ($p = 0.02, r^2 = 0.17$) (Table 3). The biomass (chlorophyll-a concentrations) demonstrated two different patterns in relation to the *Dinophysis* blooms. NPL biomass levels ranged from 2.6 to 11.3 mg/L of seawater during the summer bloom period (May to July). As the densities of the blooms decreased, the chlorophyll-a concentrations increased, showing a positive

relationship. BHM had a variable biomass from 3.9 to 13.9 mg/L of seawater during the same duration, not demonstrating any particular pattern related to abundance.

The estuary head biomass was relatively low in the winter and spring. During the summer, biomass increased as the *Dinophysis* bloom abundances decreased. There was a considerable increase in chlorophyll-a concentrations during the late summer and early fall. On the other hand, the estuary mouth presented an overall increase in biomass throughout the four seasons. At NPL, the biomass decreased to 1.7 mg/L of seawater during the biggest *Dinophysis* bloom on 6/6/19.

Table 3: Independent means t-test statistical analysis of *Dinophysis* abundance related to biomass (chlorophyll-a) (significant p-values are boldfaced).

Dinophysis Density vs. Biomass (Chlorophyll-a)			
Parameters	**Statistics**	**Estuary Head (NPL)**	**Estuary Mouth (BHM)**
Chlorophyll-a	R-squared	0.17	0.11
	P-value	**0.02**	0.11

Linear regression was used to test if nutrients explained the timing and magnitude of blooms. In addition to the importance of elemental composition for the stimulation of *Dinophysis* blooms, it is also important to understand the composition of nutrient ratios. Nutrient composition not just magnitude can affect phytoplankton growth. Investigating these nutrient ratios characterizes their role in shaping phytoplankton assemblages, specifically focusing on the dinoflagellate community with a dominance of HAB species (i.e. *Dinophysis* spp.).

The Redfield-Belinksi ratio of 106:15:16:1 represents the total dissolved inorganic nutrient composition of carbon to nitrogen to silica to phosphate (DIC:DSI:DIN:DIP) available for phytoplankton utilization via the biogeochemical cycling of nutrients (Choudhury & Bhadbury, 2015). I wanted to analyze the relationship

between abundance and nutrient composition, therefore, I choose to analyze the composition by evaluating the ratios. I computed the following nutrient ratios of DIN:DIP, DSI:DIN, and DSI:DIP to examine if there are deviations from the standard nutrient ratios to influence dinoflagellate assemblages, specifically focusing on *Dinophysis* abundances.

For the total dissolved inorganic nitrogen, I included both ammonium and nitrate concentrations but have omitted the analysis of nitrite because of the lack of equipment to quantify the concentrations, which is usually a very small fraction of the total inorganic in nature. Specifically, we are looking at deviation from nutrient ratios which is looking at ratios at which cells are made.

I tested the relationship of abundance with nutrients, but the regressions don't capture that possible delay between nutrient changes to which the phytoplankton respond. To examine the possible connection between the changes in one or the other that, I analyzed how the nutrients varied around the time of the blooms via time series data to see the correspondence of changes in the various parameters.

Dinophysis abundance at the head of the estuary was negatively related to nitrate ($p = 0.01, r^2 = 0.19$) and positively related to phosphate ($p = 0.0006, r^2 = 0.33$) concentrations. *Dinophysis* abundance was not significantly related to ammonium and silicate. At the mouth of the estuary, all four nutrients measured were not significantly related to *Dinophysis* abundance (Table 4).

Table 4: Simple linear regression analysis of *Dinophysis* abundance related to nutrients (nitrate, ammonium, silicate, and phosphorous) at the estuary mouth (NPL) and head (BHM) in Budd Inlet (significant p-values are boldfaced).

Dinophysis Density vs. Nutrients			
Parameters	**Statistics**	**Estuary Head (NPL)**	**Estuary Mouth (BHM)**
Ammonium (NH4+)	R-squared	0.06	0.01
	P-value	0.19	0.66
Nitrate (NO3-)	R-squared	0.19	0.11
	P-value	**0.01**	0.13
Phosphate (PO4-)	R-squared	0.33	0.06
	P-value	**6.0 e-4**	0.26
Silicate (SiO4-)	R-squared	0.01	0.03
	P-value	0.63	0.44

The phosphate concentrations at the estuary head ranged from 0.8 to 4.6 μM and 1.1 to 5.7 μM at the estuary mouth (Fig. 7; Fig. 8) and levels were low throughout the winter and considerably higher throughout the summer and fall. The time series shows that the peak concentrations of phosphate overlap with the *Dinophysis* blooms in the summer from June to the end of August (Fig. 9). The time series graphs for the estuary head shows that during the peak blooms from June to September, the phosphate concentrations were greater than in winter. Also, the estuary mouth shows phosphate concentrations were low in the first half of the spring season, while the second half shows a pulse of phosphate reaching maximal value of 5.7 μM on 5/15/19 (Fig. 10). Shortly after the surge, there was a sharp decline of phosphate to 1.1 μM. A bloom of *Dinophysis* followed two weeks after the steep decline in phosphate. During the peak blooms, phosphate concentrations remained low until the blooms declined. After the blooms ceased, the phosphate levels increased.

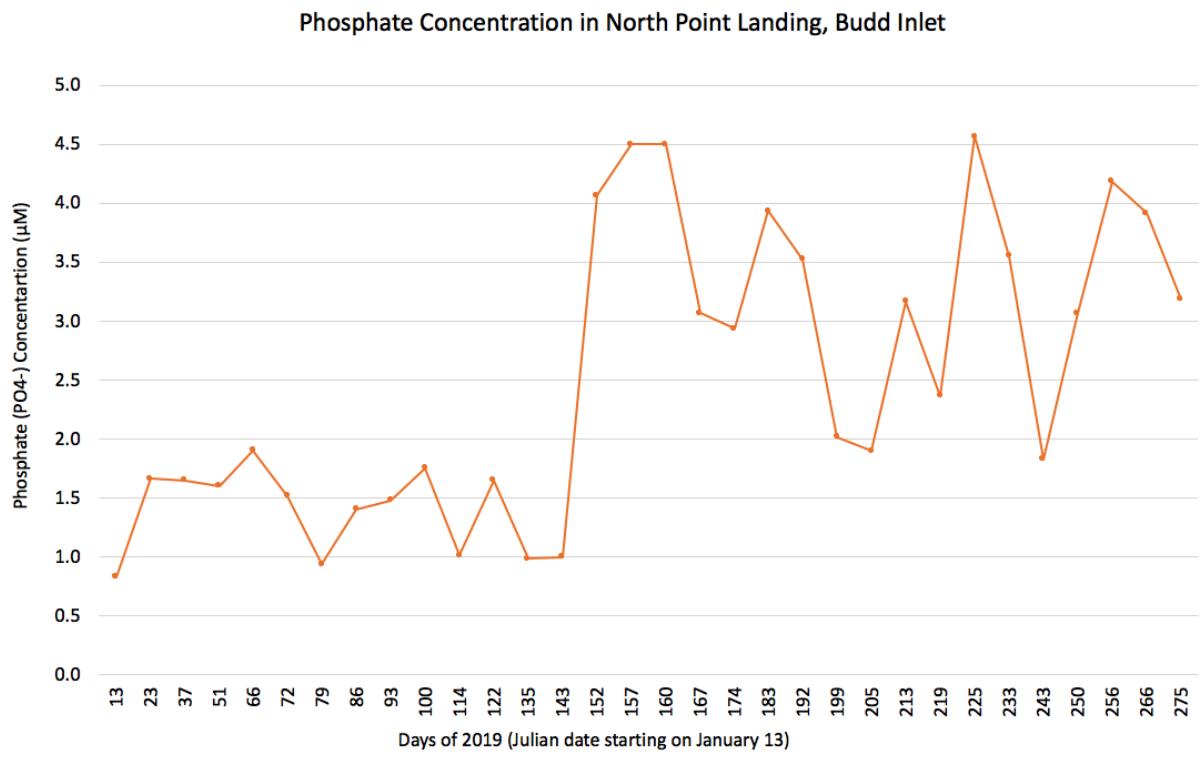

Figure 7: Time series of phosphate levels over the seasonal cycle of winter to fall of 2019 at the estuary head (BHM) in Budd Inlet.

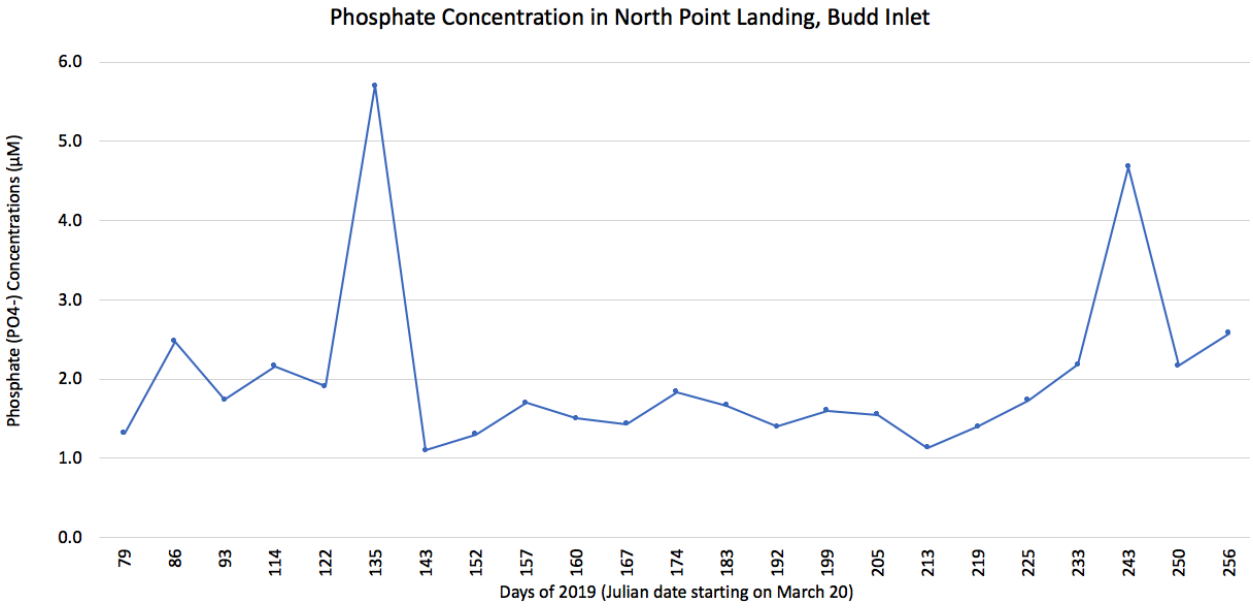

Figure 8: Time series of phosphate levels over the seasonal cycle of spring to fall of 2019 at the estuary mouth (NPL) in Budd Inlet.

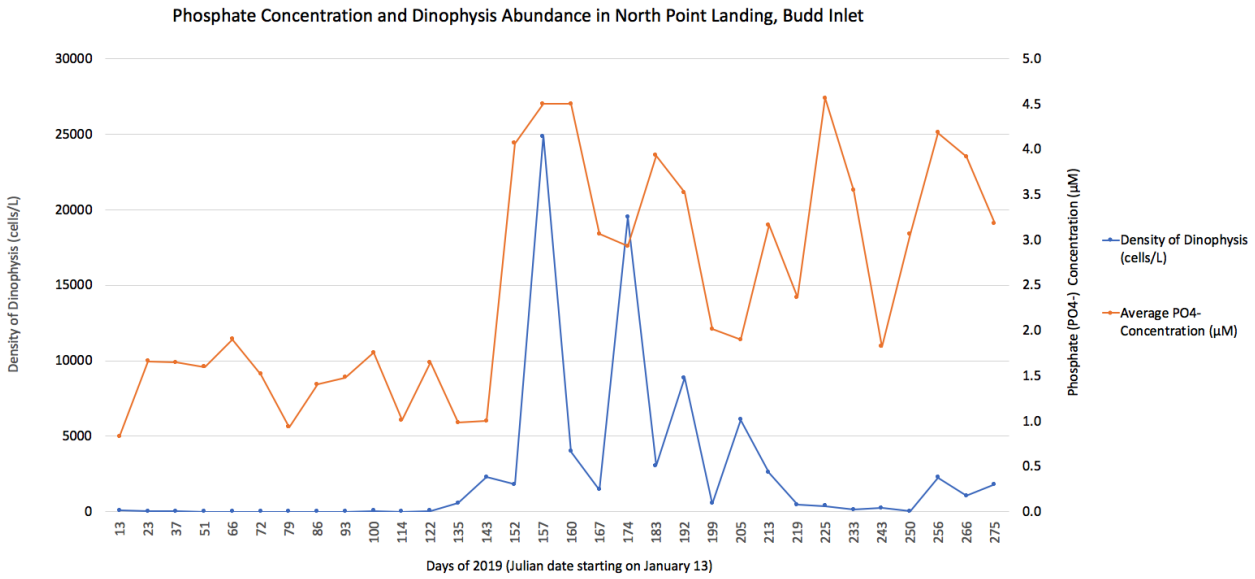

Figure 9: Time series of *Dinophysis* abundance versus phosphate levels at the estuary head (NPL) in Budd Inlet.

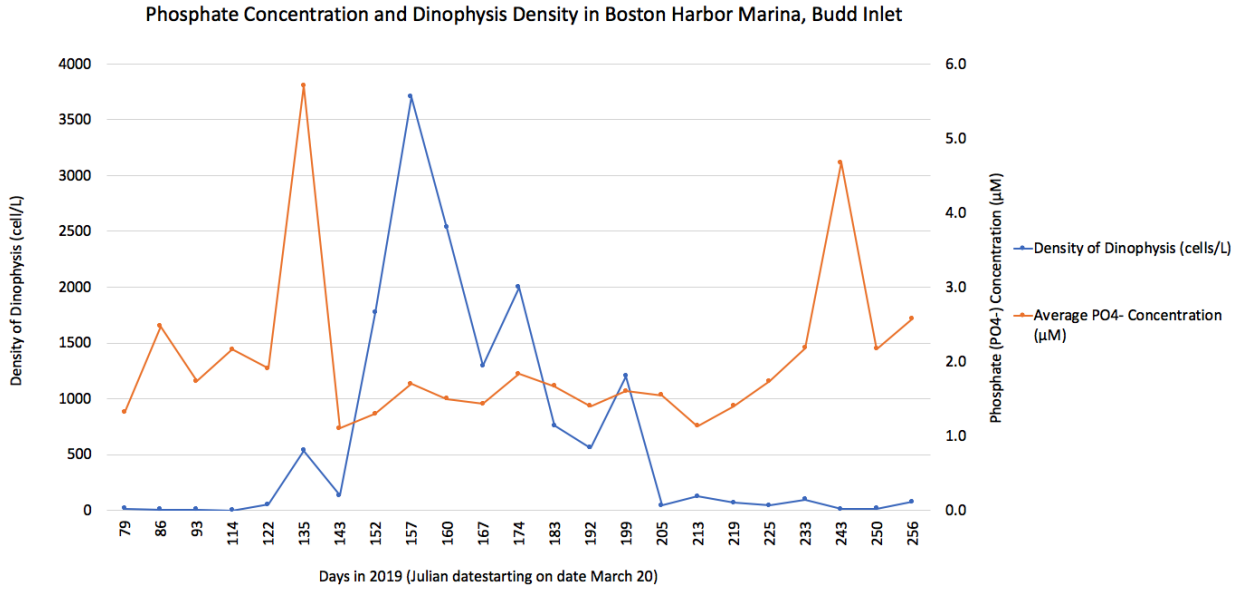

Figure 10: Time series of *Dinophysis* abundance versus phosphate levels at the estuary mouth (BHM) in Budd Inlet.

At the estuary head, nitrate concentrations were noticeably higher in the winter and spring (Fig. 11). In summer, nitrate levels were low and increased in the fall. Before the blooms occurred, nitrate levels were very high. During the bloom, the nitrate concentrations decreased while *Dinophysis* abundances increased (Fig. 12). Also, the mouth of the estuary shows a similar trend during the spring, summer bloom season, and fall (Fig. 13). The peak of *Dinophysis* abundances occurred a few weeks after the elevated levels of nitrate were present (Fig 14).

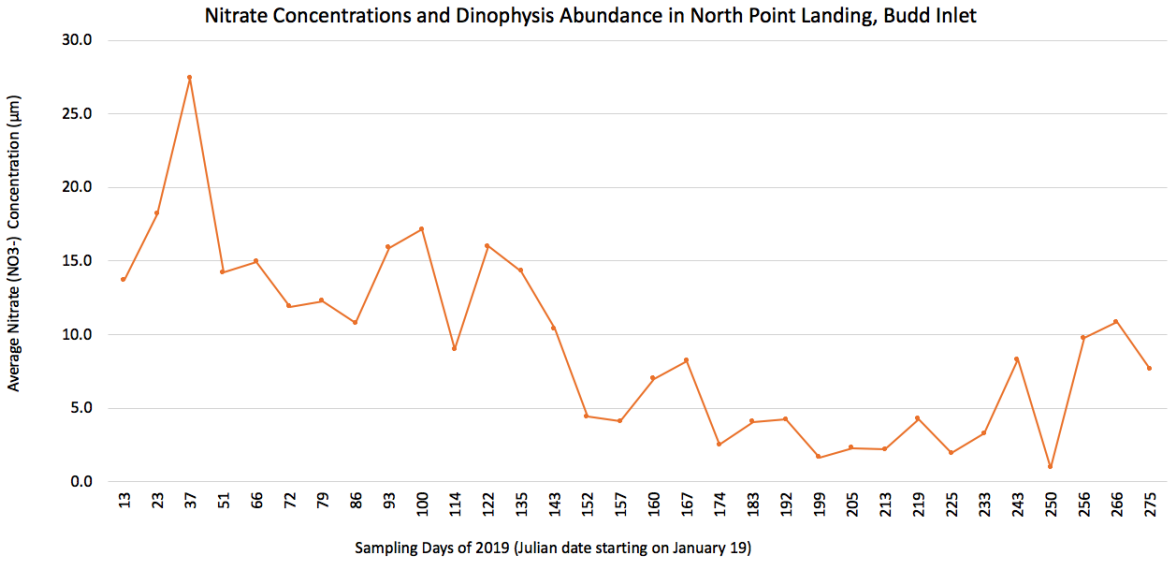

Figure 11: Time series of phosphate levels over the seasonal cycle of spring to fall of 2019 at the estuary head (NPL) in Budd Inlet.

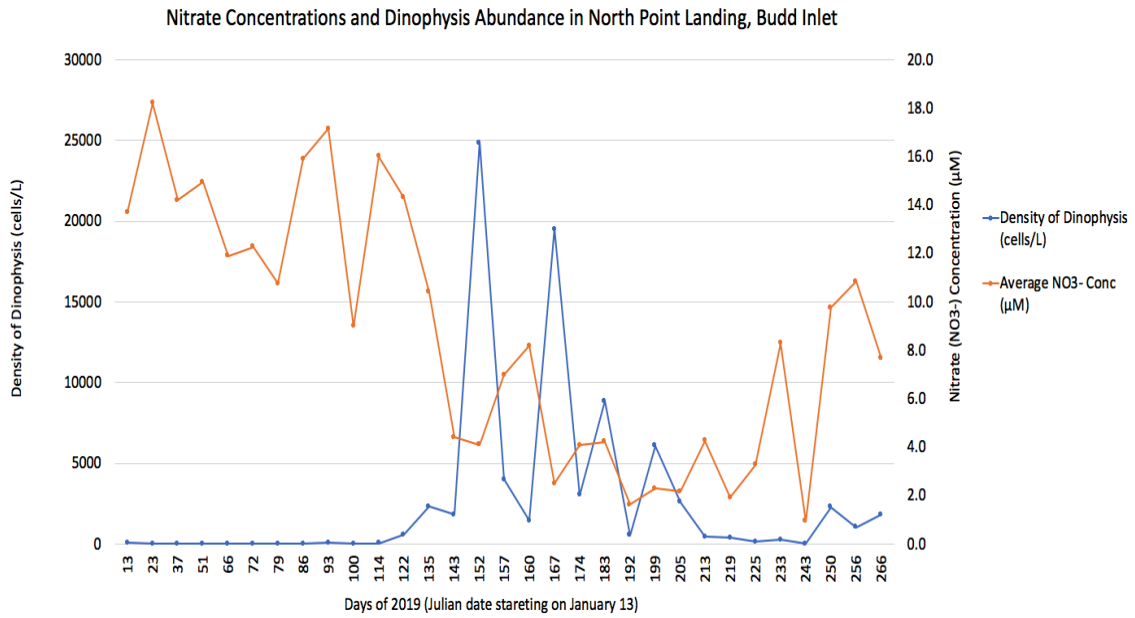

Figure 12: Time series of *Dinophysis* abundance versus nitrate levels at the estuary head (NPL) in Budd Inlet.

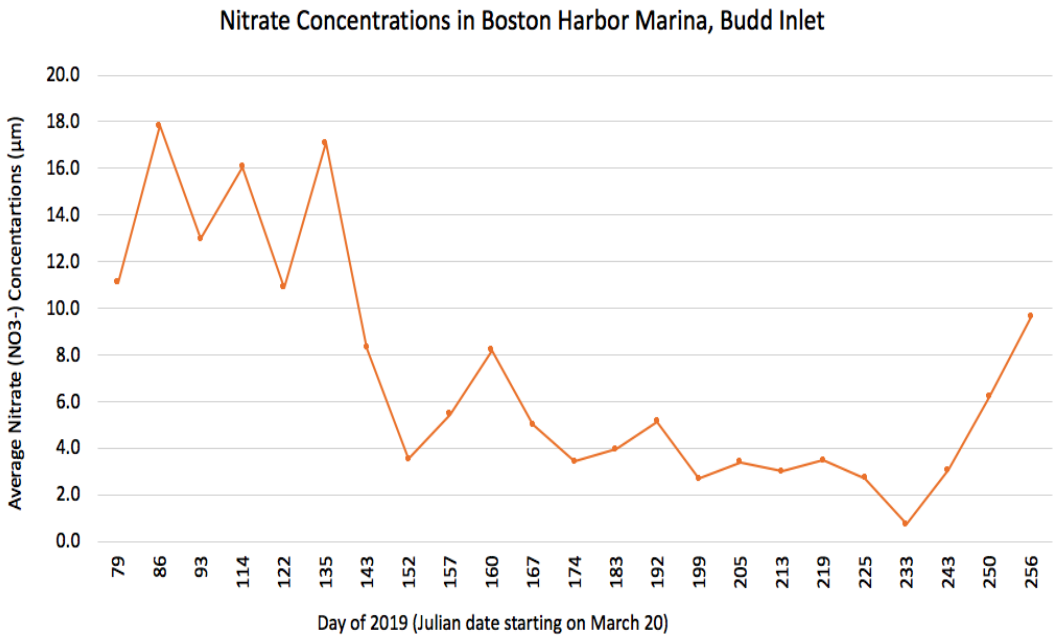

Figure 13: Time series of phosphate levels over the seasonal cycle of spring to fall of 2019 at the estuary head (NPL) in Budd Inlet.

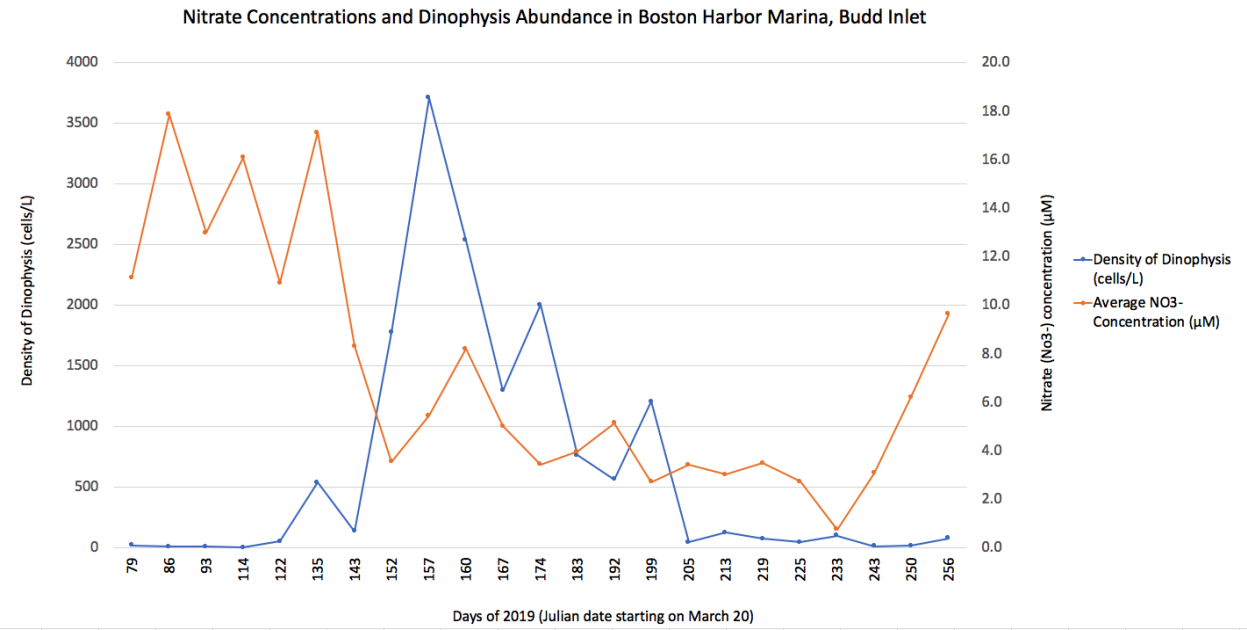

Figure 14: Time series of *Dinophysis* abundance versus nitrate levels at the estuary mouth (BHM) in Budd Inlet.

In addition, *Dinophysis* abundance at NPL was significantly related to nutrient ratios of dissolved inorganic nitrogen to dissolved inorganic phosphate (DIN:DIP) $(p = 0.014, r^2 = 0.19)$and dissolved silica to dissolved inorganic phosphate (DSI:DIP) $(p = 0.01, r^2 = 0.19)$ (Table 5). On the other hand, the estuary mouth was not significantly related to any of the nutrient ratios. The DIN ratios only consist of ammonium and nitrate concentrations due to lack of equipment at this time to determine nitrite levels. However, it is known that nitrite is a small fraction of the total concentrations thus should have minor influence in the ratio.

Table 5: Simple linear regression analysis of *Dinophysis* abundance related to nutrients ratios at the estuary mouth (NPL) and head (BHM) in Budd Inlet.

Dinophysis Density vs. Redifeld Ratios			
Parameters	**Statistics**	**Estuary Head (NPL)**	**Estuary Mouth (BHM)**
DIN:DIP	R-squared	0.19	0.04
	P-value	**0.01**	0.39
DSI:DIP	R-squared	0.19	0.00
	P-value	**0.02**	0.79
DSI:DIN	R-squared	0.05	0.05
	P-value	0.21	0.31

The nutrient ratio of DSI:DIP ranged from 0.4 to 21.4 with maximal values occurring during the winter to spring at the estuary head (Fig. 15; Fig 16). The ratios decreased in early June to August, the same periods when the peak blooms occurred (Fig. 17). Similar occurrences appeared at the mouth of the estuary: when *Dinophysis* densities were low, DSI:DIP ratios were high (Fig. 18). However, when cell densities were high, the ratios decreased. A large inversion peak occurred at the same time the largest bloom occurred on 6/6/19. Overall, the nutrients ratios were higher and more variable at the head of the estuary compared to the mouth.

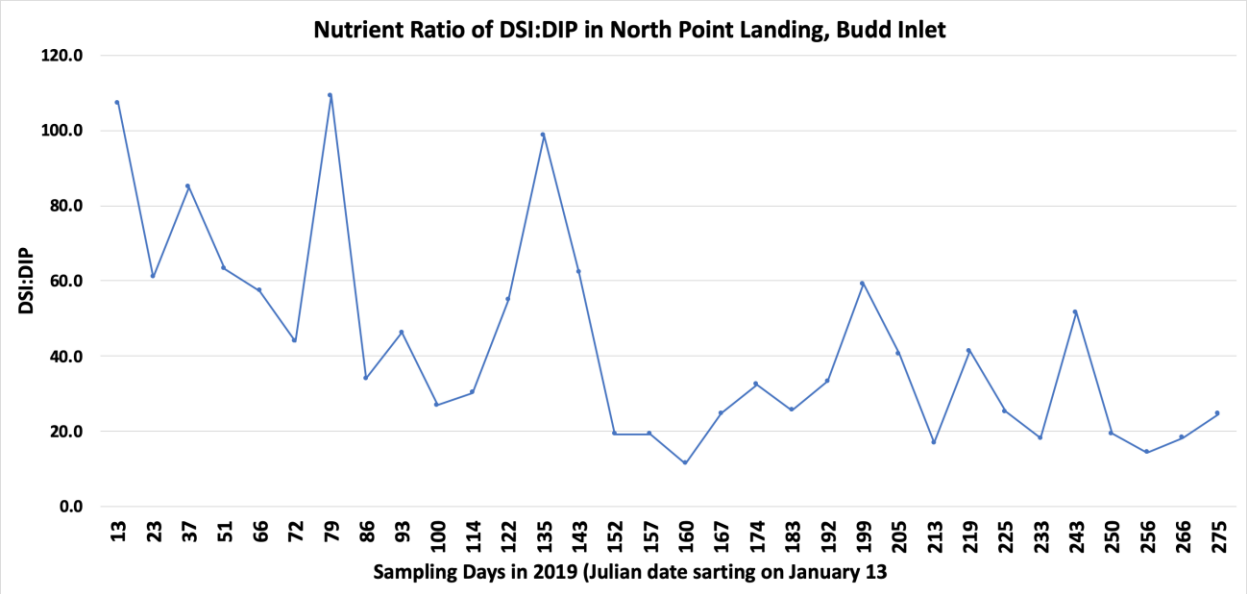

Figure 15: Time series of nutrient ratios of dissolved silica to dissolved inorganic phosphate (DSI:DIP) over the seasonal cycle of spring to fall of 2019 at the estuary head (NPL) in Budd Inlet.

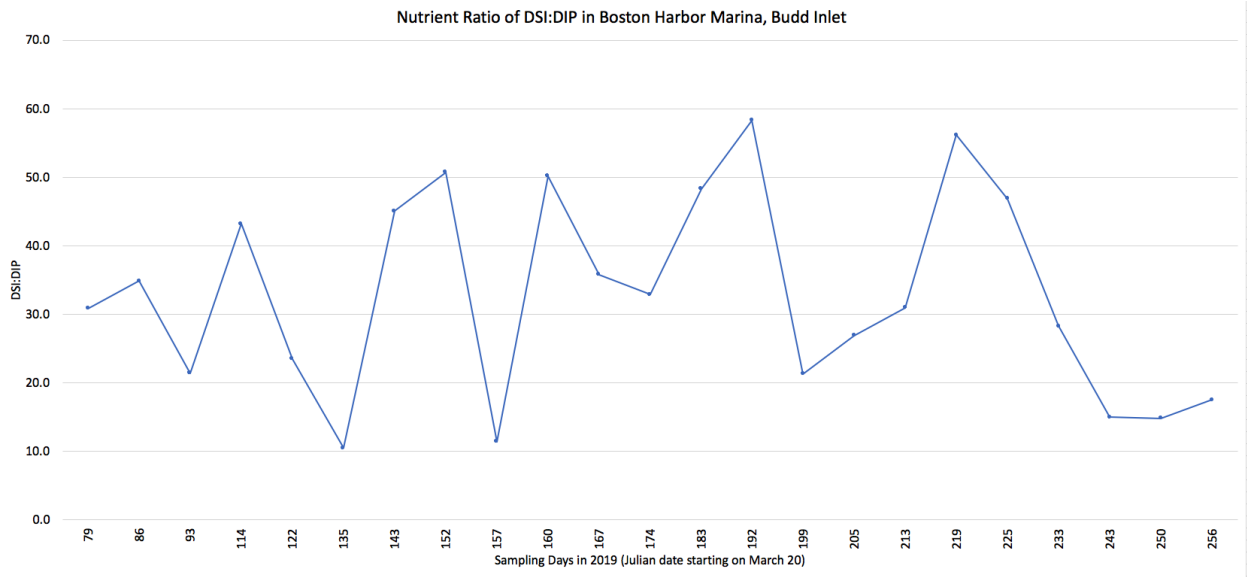

Figure 16: Time series of nutrient ratios of dissolved silica to dissolved inorganic phosphate (DSI:DIP) over the seasonal cycle of spring to fall of 2019 at the estuary mouth (BHM) in Budd Inlet.

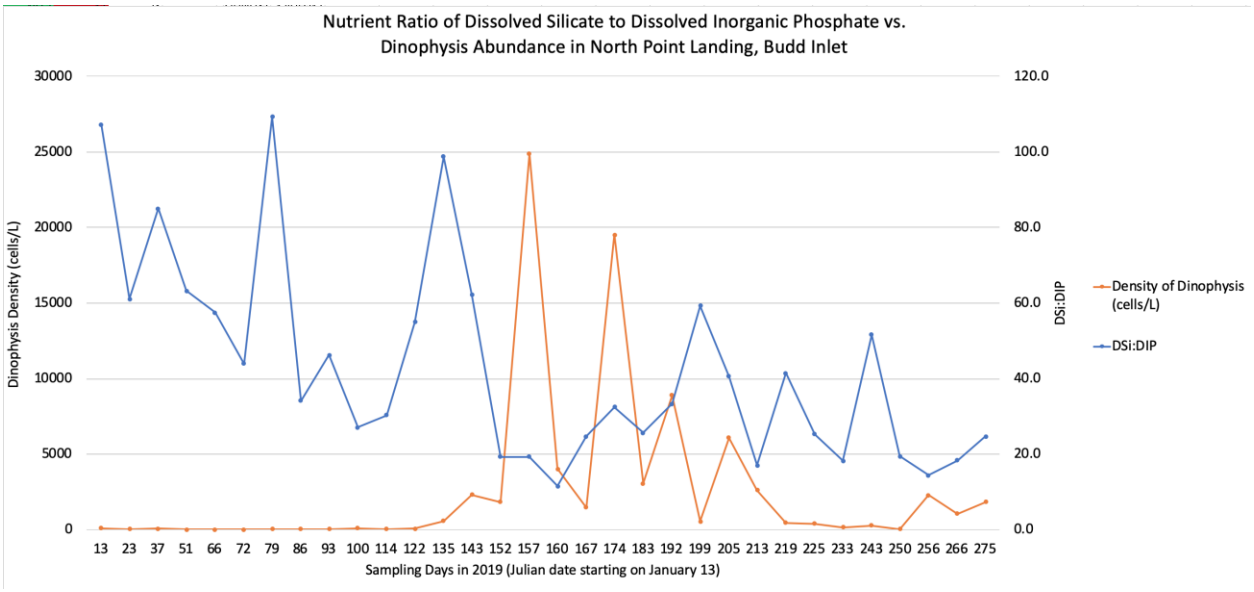

Figure 17: Time series of *Dinophysis* abundance versus nutrient ratios of dissolved silica to dissolved inorganic phosphate (DSI:DIP) at the estuary head (NPL) in Budd Inlet.

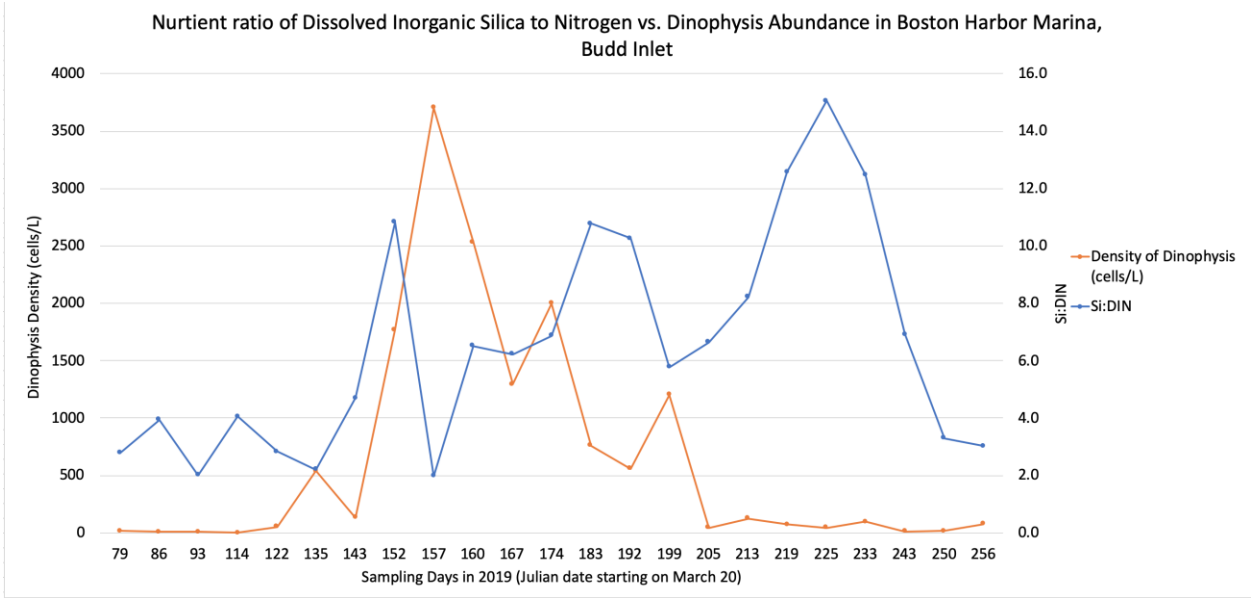

Figure 18: Time series of *Dinophysis* abundance versus nutrient ratios of dissolved silica to dissolved inorganic phosphate (DSI:DIP) at the estuary mouth (BHM) in Budd Inlet.

Nutrient ratios of DIN:DIP ranged from 0.4 to 21.6 at the estuary head (Fig. 19). Ratios were elevated during the winter to the end of spring. When the summer season ensued, a sharp decline in DIN:DIP occurred on 6/1/19 and very low ratios of DIN:DIP remained low thru the fall. Shortly after this decline of phosphate levels, the first bloom followed on 6/6/19 (Fig. 20). In contrast, the mouth of the estuary showed a gradual decline in the DIN:DIP ratios over spring to end of the summer (Fig. 21). Ratios decreased when the blooms were present.

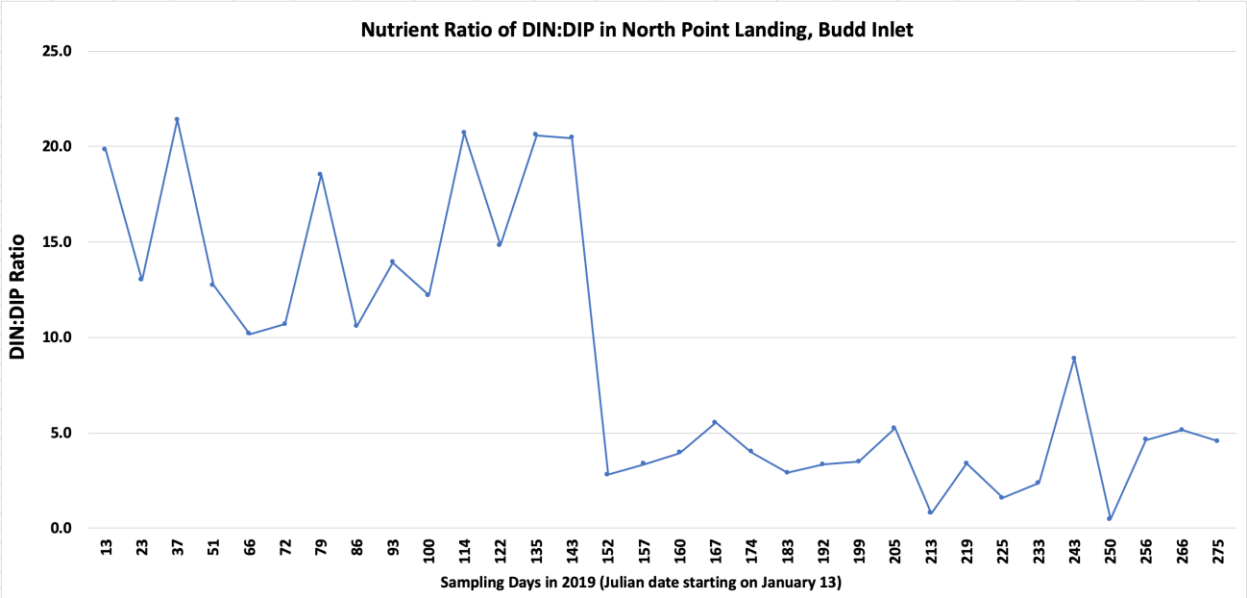

Figure 19: Time series of nutrient ratios of dissolved inorganic nitrogen to dissolved inorganic phosphate (DIN:DIP) over the seasonal cycle of spring to fall of 2019 at the estuary head (NPL) in Budd Inlet.

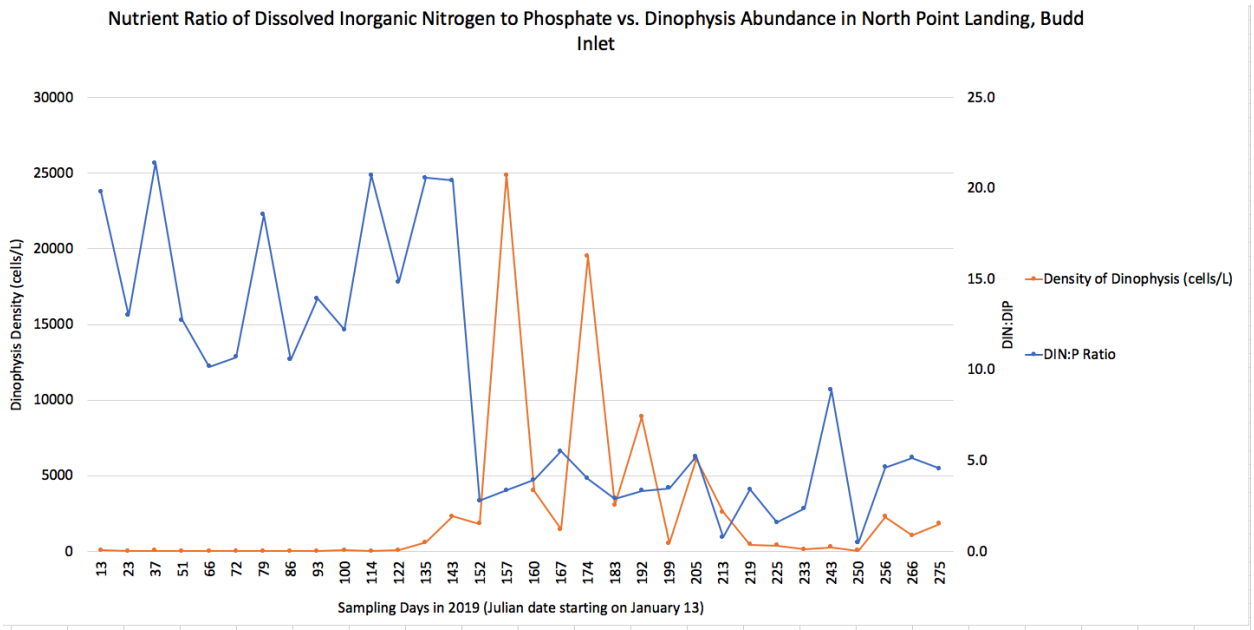

Figure 20: Time series of *Dinophysis* abundance versus nutrient ratios of dissolved inorganic nitrogen to dissolved inorganic phosphate (DIN:DIP) at the estuary head (NPL) in Budd Inlet.

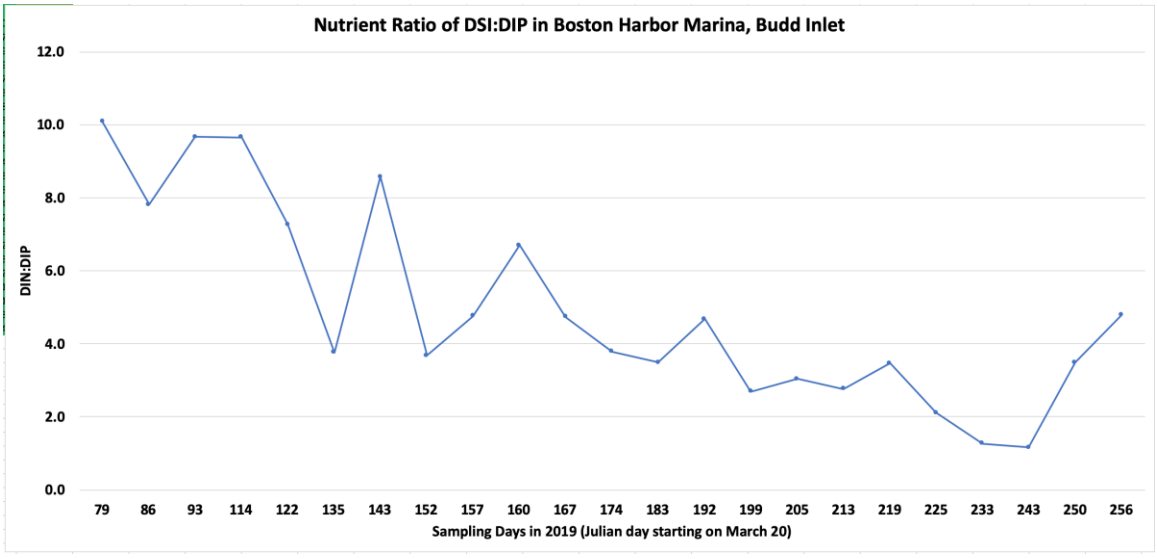

Figure 21: Time series of nutrient ratios of dissolved inorganic nitrogen to dissolved inorganic phosphate (DIN:DIP) over the seasonal cycle of spring to fall of 2019 at the estuary mouth (BHM) in Budd Inlet.

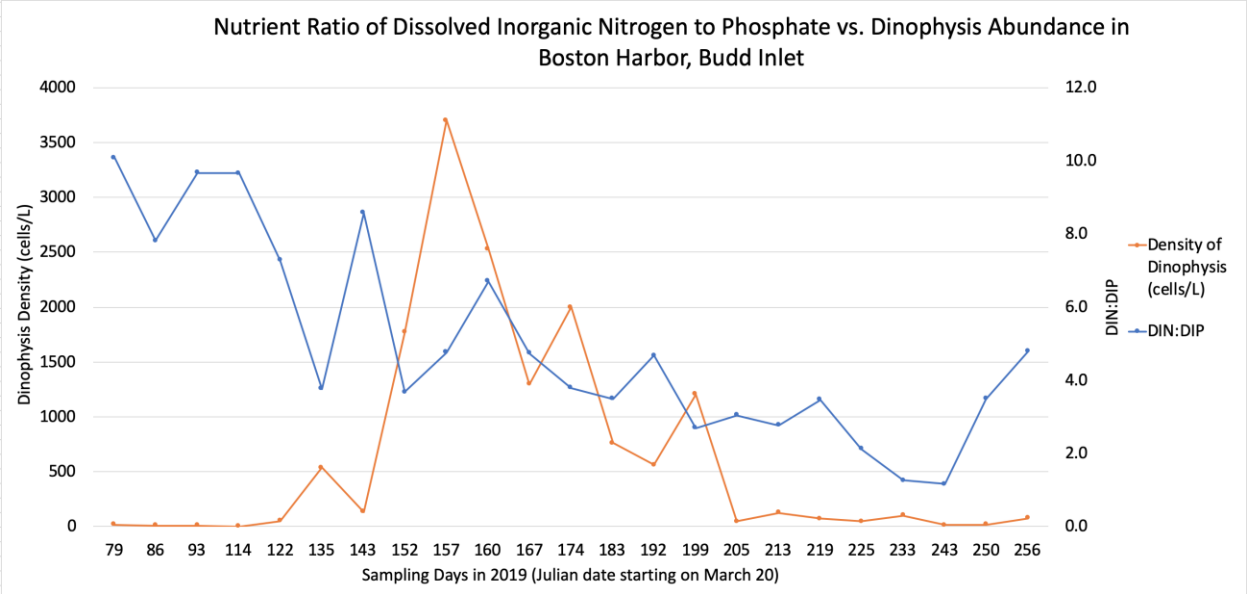

Figure 22: Time series of *Dinophysis* abundance versus nutrient ratios of dissolved inorganic nitrogen to dissolved inorganic phosphate (DIN:DIP) at the estuary mouth (BHM) in Budd Inlet.

Although the relationship between ammonium and *Dinophysis* abundance was not statistically significant, both stations exhibited elevated levels of ammonium during the spring before the *Dinophysis* blooms. Ammonium levels were substantially greater at the head of the estuary relative to the mouth, reaching maximal levels of 12.0 μM (Fig. 23). The estuary head time series showed moderate levels of ammonium in winter, then increased throughout spring until beginning of summer (6/6/19). As summer progressed, ammonium concentrations declined from 11.0 μM to 0.3 μM from 6/6/19 to 8/1/19. This decline in ammonium concentrations during the summer months corresponded with the high-density blooms of *Dinophysis* at both stations between 6/6/19 to 7/24/19 (Fig. 24). The levels decrease in accordance with decreasing bloom activity until 8/1/19. In comparison, ammonium concentrations were significantly lower at the estuary mouth (Fig. 25). Spring showed a similar trend with highest levels of ammonium concentrations

ranging from 1.1 µM to 4.4 µM during 3/17/19 to 5/23/19. Levels of ammonium decreased after the first bloom on 6/1/19. The lowest ammonium concentrations occurred on 8/1/19 directly after the last bloom of the summer season (Fig. 26).

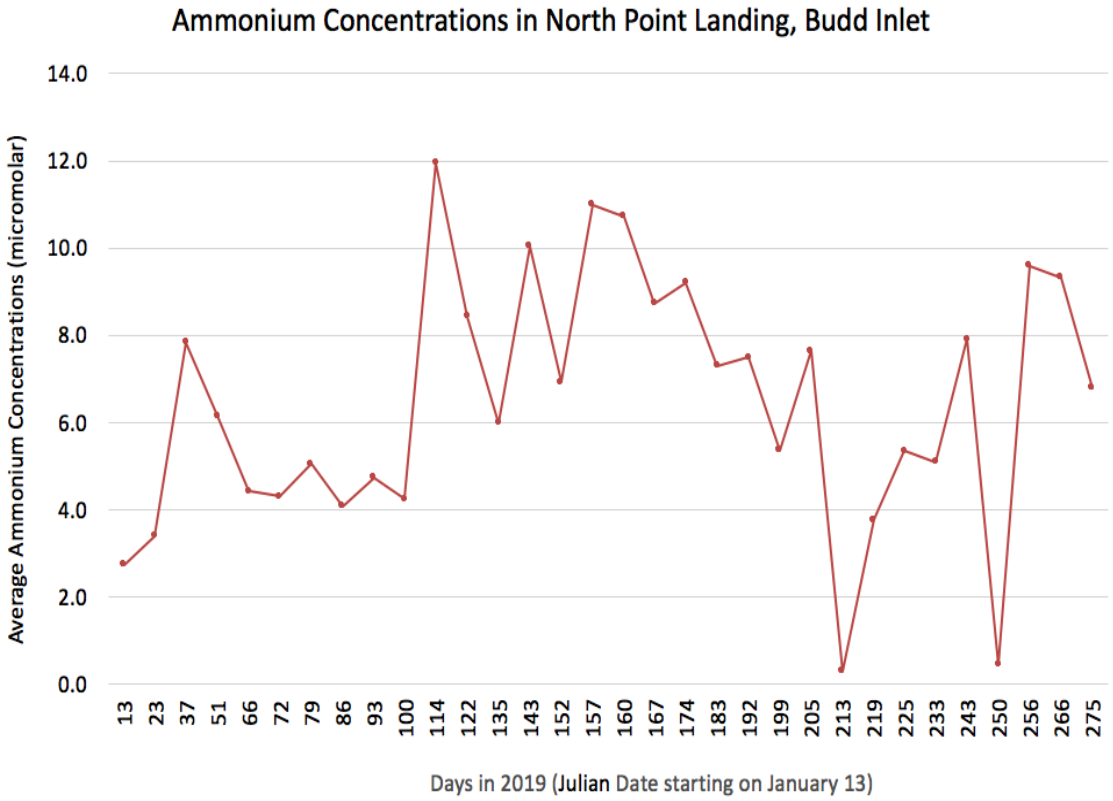

Figure 23: Time series of ammonium levels over the seasonal cycle of spring to fall of 2019 at the estuary head (BNPL) in Budd Inlet.

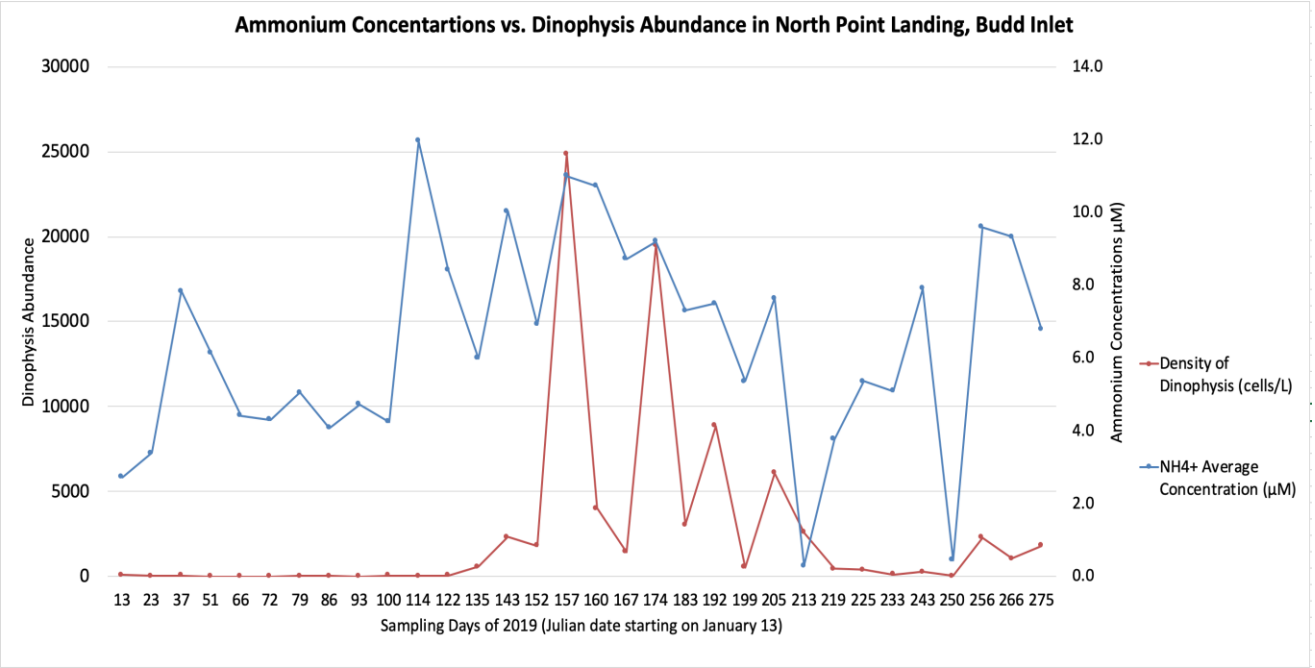

Figure 24: Time series of *Dinophysis* abundance versus ammonium levels at the estuary head (NPL) in Budd Inlet.

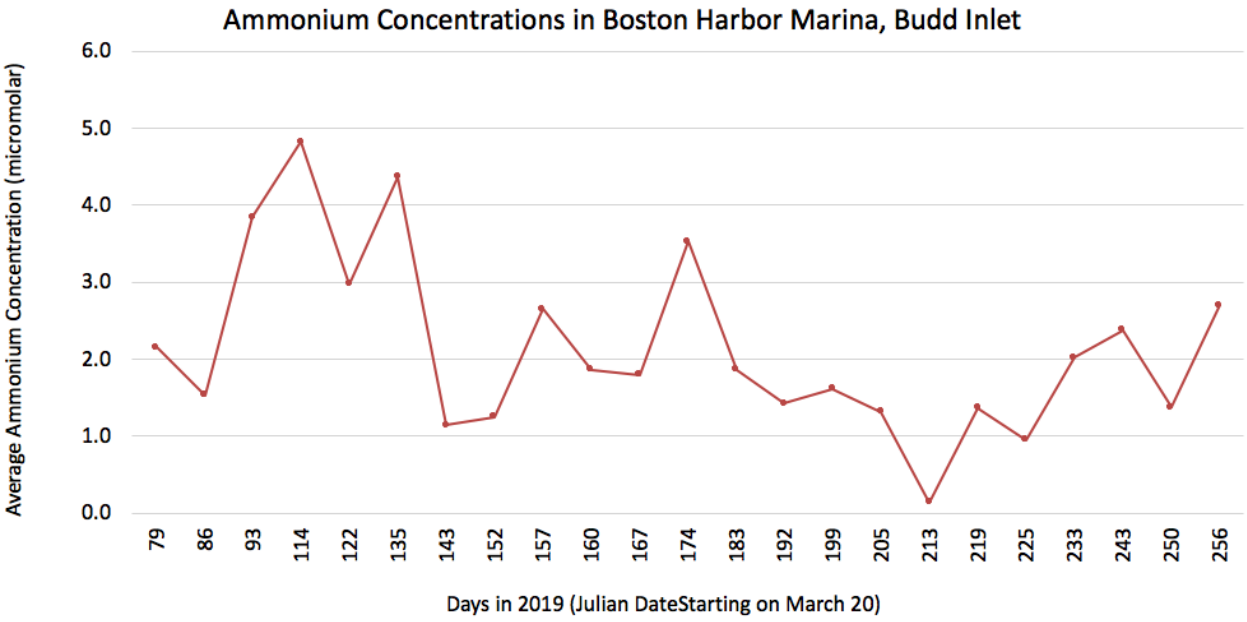

Figure 25: Time series of ammonium levels over the seasonal cycle of spring to fall of 2019 at the estuary mouth (BHM) in Budd Inlet.

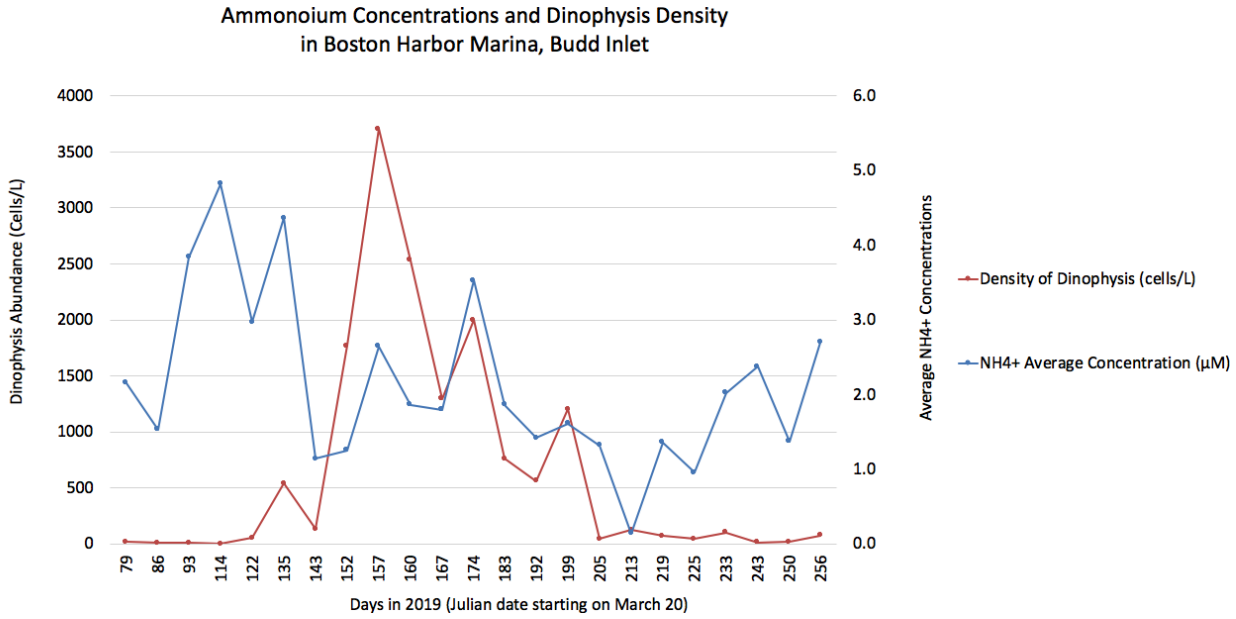

Figure 26: Time series of *Dinophysis* abundance versus ammonium levels at the estuary mouth (BHM) in Budd Inlet.

Each of the water quality and meteorological factors were measured and analyzed in order to examine the how environmental conditions might influence *Dinophysis* densities. Analyses of simple linear regressions and time series were performed. There were statistically significant correlations ($p < 0.05$) between *Dinophysis* abundance and changes in environmental conditions. At the head of the estuary, *Dinophysis* abundance was significantly related to dissolved oxygen ($r^2 = 0.19$), surface water temperature at 1m depth ($r^2 = 0.44$), air temperature ($r^2 = 0.32$), river discharge ($r^2 = 0.51$), and solar radiance ($r^2 = 0.17$) (Table 6; Table 7). River discharge and surface water temperature were the largest contributors to *Dinophysis* abundance at NPL. In comparison, the station at the estuary mouth was significantly ($p < 0.05$) related to salinity ($r^2 = 0.28$), surface water temperature (1m depth) ($r^2 = 0.18$), air

temperature ($r^2 = 0.27$), river discharge ($r^2 = 0.31$), wind speed ($r^2 = 0.15$), and solar radiance $r^2 = 0.19$) (Table 6; Table 7). River discharge and salinity were the most significant factors at BHM.

Table 6: Simple linear regression analysis of *Dinophysis* abundance related to meteorological conditions at the estuary mouth (NPL) and head (BHM) in Budd Inlet.

Dinophysis Density vs. Meterological Conditions			
Parameters	**Statistics**	**Estuary Head (NPL)**	**Estuary Mouth (BHM)**
Air Temperature (℉)	R-squared	0.32	0.27
	P-value	**6.0 e-4**	**4.0 e-3**
Rainfall (m)	R-squared	0.04	0.06
	P-value	0.25	0.19
River Discharge (m^3/s)	R-squared	0.51	0.32
	P-value	**7.1 e-6**	**1.0 e-3**
Wind Speed (m^2/s)	R-squared	0.03	0.15
	P-value	0.37	**0.04**
Solar Irradiance (W/m^2)	R-squared	0.17	0.19
	P-value	**0.02**	**0.02**

Table 7: Simple linear regression analysis of *Dinophysis* abundance related to water quality parameters at the estuary mouth (NPL) and head (BHM) in Budd Inlet (significant p-values boldfaced).

Dinophysis Density vs. Water Quality Conditions			
Parameters	**Statistics**	**Estuary Head (NPL)**	**Estuary Mouth (BHM)**
Salinity (1m depth)	R-squared	0.00	0.28
	P-value	0.85	**4.0 e-3**
Coastal Salinity Index	R-squared	0.08	0.11
	P-value	0.40	0.39
DO (mg/L)	R-squared	0.12	0.00
	P-value	**0.05**	0.79
Seechi Depth (m)	R-squared	0.00	0.01
	P-value	0.99	0.51
Surface Water Temperature (1m)	R-squared	0.44	0.18
	P-value	**3.0 e-5**	**0.02**

Dissolved oxygen was qualitatively analyzed via time series plots to understand if the levels decreased during the *Dinophysis* blooms periods. Levels of dissolved oxygen were highly variable throughout the seasonal cycle at the estuary head ranging from 3.60 to 10.2 mg/L (Fig. 27). High levels occurred during the winter, spring, and fall. In the summer, when *Dinophysis* reached peak densities, dissolved oxygen levels greatly decreased (Fig. 28). The second peak bloom shows dissolved oxygen made very sharp declines, reaching low of 3.60 mg/L on 7/2/19. Dissolved oxygen levels at the estuary mouth were relatively stable in contrast to the head, staying within the range of 6.25 to 9.99 mg/L (Fig. 29). The dissolved oxygen levels did show slight decline from 9.99 to 7.33 in when high *Dinophysis* abundances were present (Fig. 30).

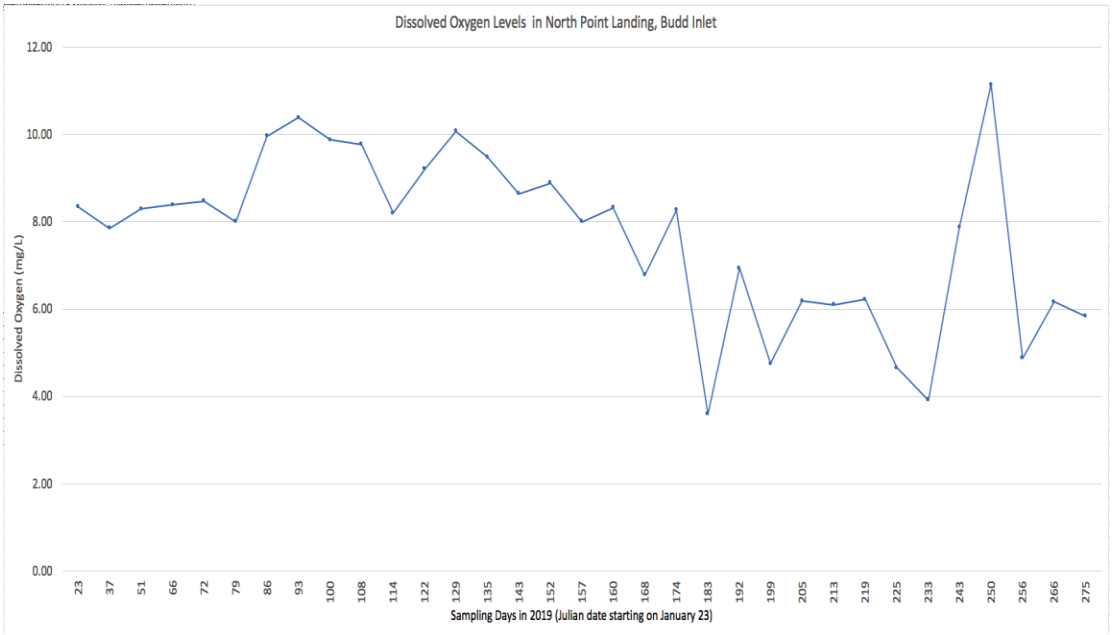

Figure 27: Time series of dissolved oxygen levels over the seasonal cycle of spring to fall of 2019 at the estuary mouth (BHM) in Budd Inlet.

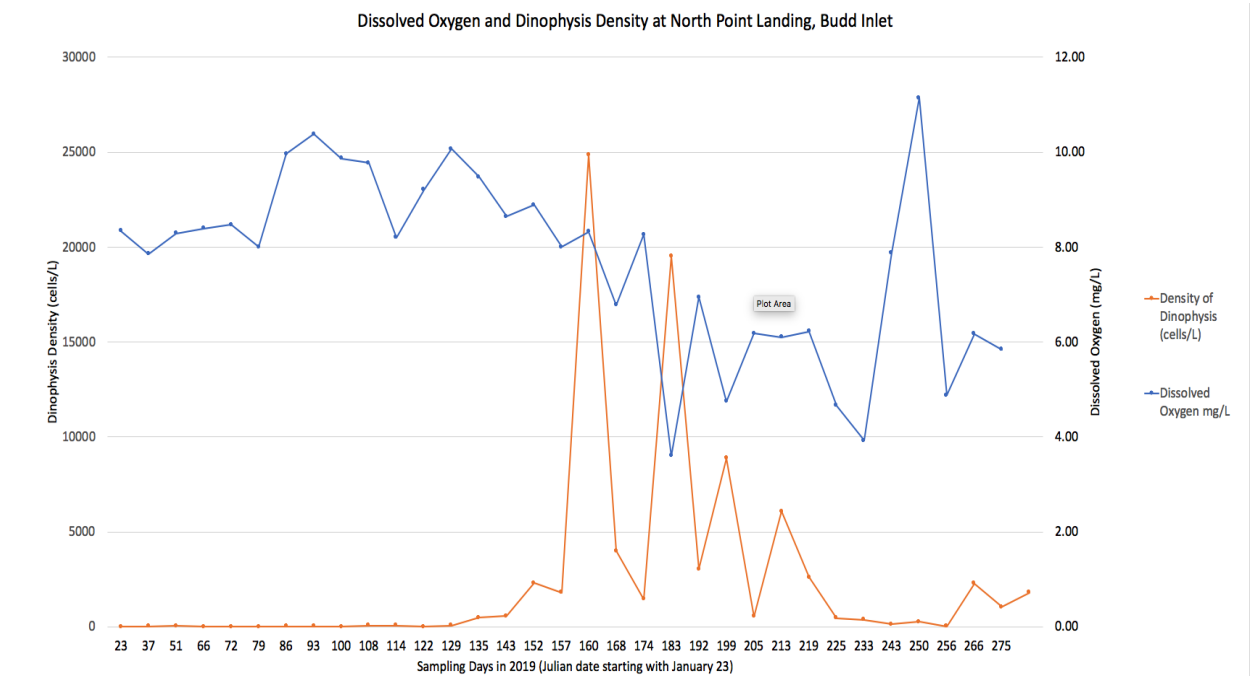

Figure 28: Time series of *Dinophysis* abundance versus dissolved oxygen levels at the estuary head (NPL) in Budd Inlet.

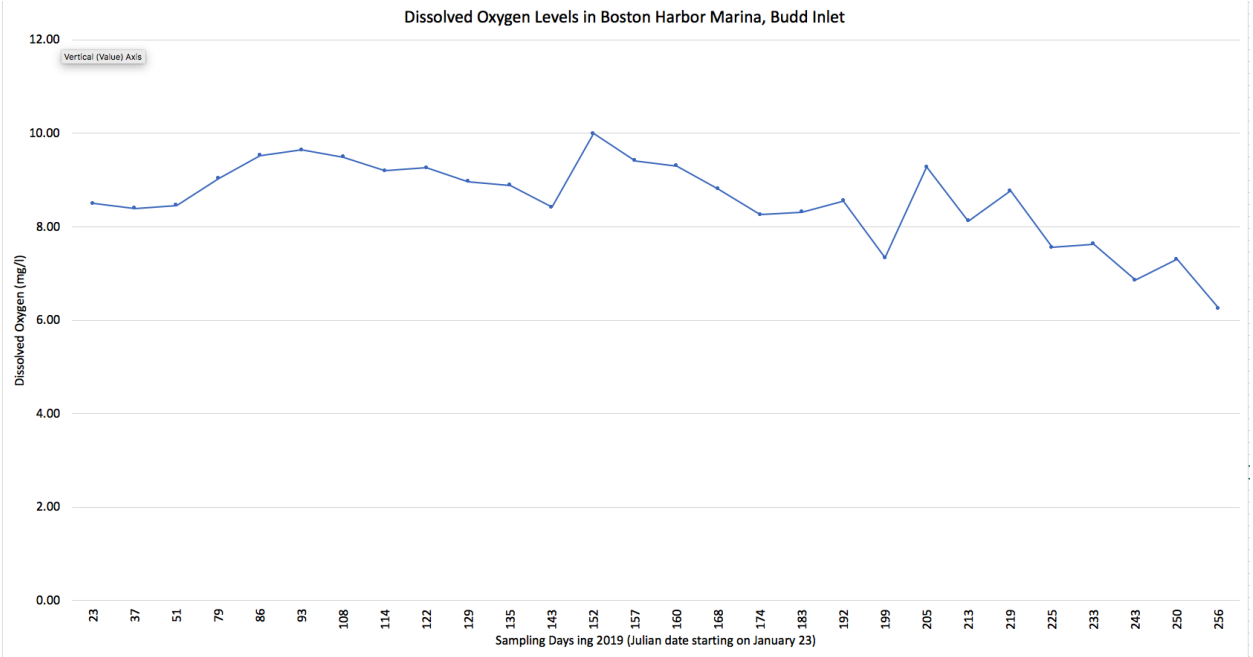

Figure 29: Time series of dissolved oxygen levels over the seasonal cycle of spring to fall of 2019 at the estuary mouth (BHM) in Budd Inlet.

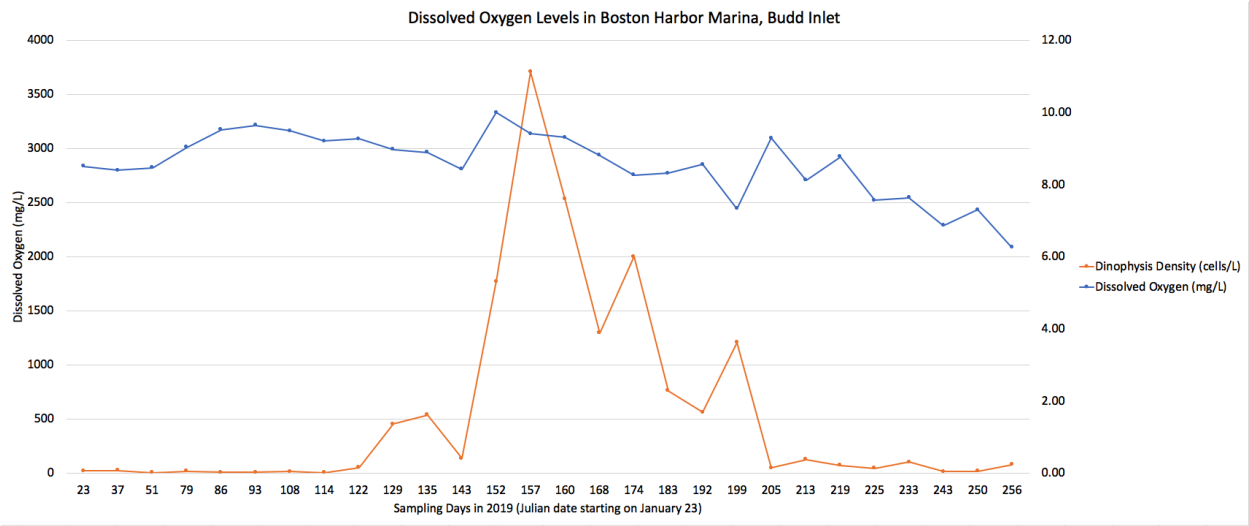

Figure 30: Time series of *Dinophysis* abundance versus dissolved oxygen levels at the estuary mouth (BHM) in Budd Inlet.

Surface water and air temperatures were evaluated to determine whether warm waters prevent mixing, allowing algae to growth densely. With lack of mixing, cells can become concentrated locally in the waters. Air and surface water temperatures (1m depth) followed the same trend of gradually increasing in temperature from the period of winter to summer then a decline in fall at the head of the estuary (Fig. 31). The mouth of the estuary showed similar appearances in temperatures from winter to spring, however the surface water temperatures remained fairly stable in the fall (Fig. 32). *Dinophysis* abundances coincide with the rising surface water temperatures at both stations (Fig. 33). During the winter to spring, surface water temperature increased from 7.7°C to 13.6°C between 3/7/19 and 6/1/19. The first two blooms occurred during surface water temperatures of 13.3°C to 13.6°C. Second set of blooms happened when temperatures increased ranging from 14.7°C to 15°C. On the other hand, a similar pattern was

displayed at the mouth of the estuary. In a similar trend, the first peak bloom at the estuary mouth coincided after the primary increase in surface water temperatures from winter (2/20/19) to early June (6/1/19) ranging from 8°C to 14.2°C (Fig. 34). The other two peak blooms corresponded with higher temperatures: second peak bloom at 13.6°C and third peak blooms at 14.9°C.

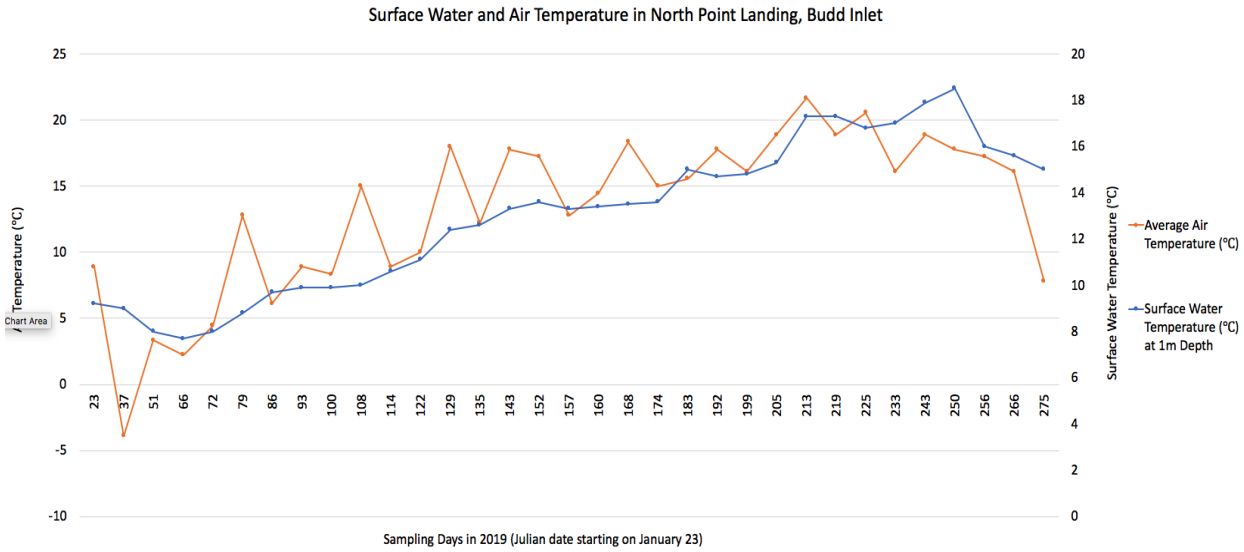

Figure 31: Time series of air and surface water temperatures over the seasonal cycle of spring to fall of 2019 at the estuary head (NPL) in Budd Inlet.

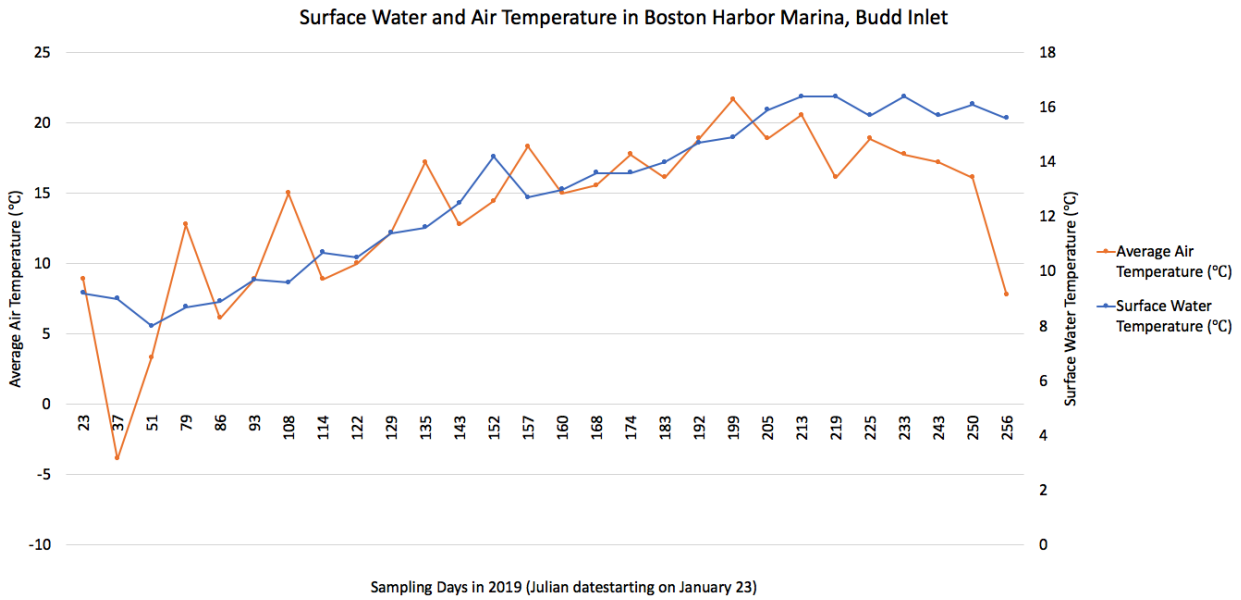

Figure 32: Time series of air and surface water temperatures (1m depth) over the seasonal cycle of spring to fall of 2019 at the estuary mouth (BHM) in Budd Inlet.

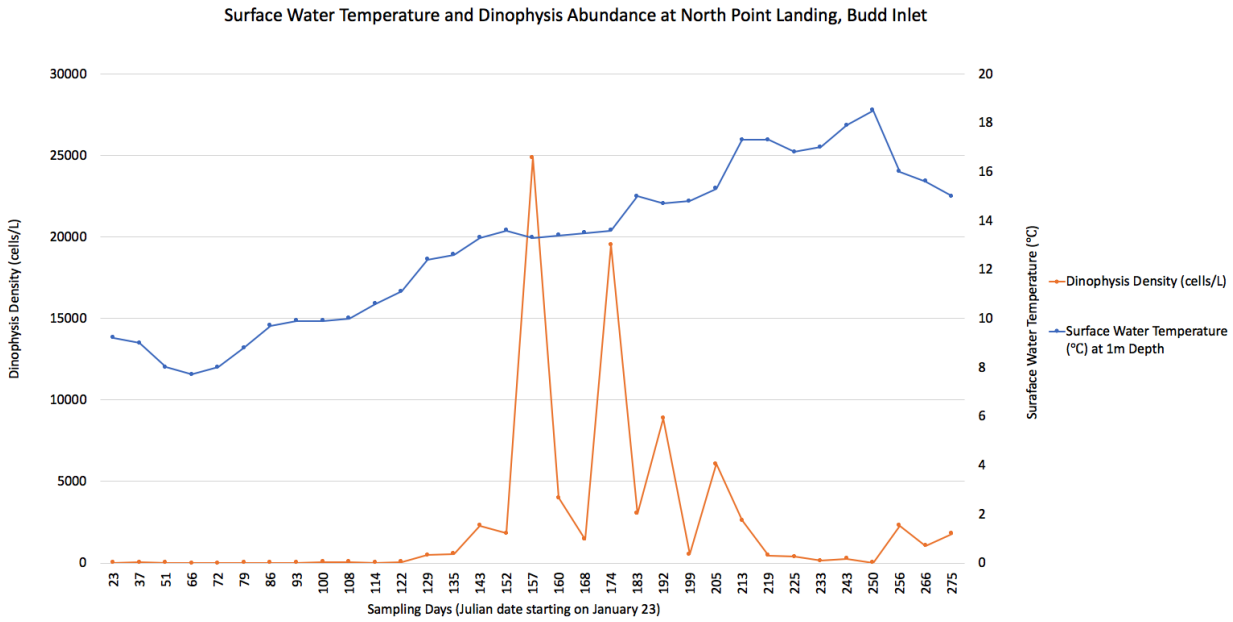

Figure 33: Time series of *Dinophysis* abundance versus surface water temperatures (1m depth) at the estuary head (NPL) in Budd Inlet.

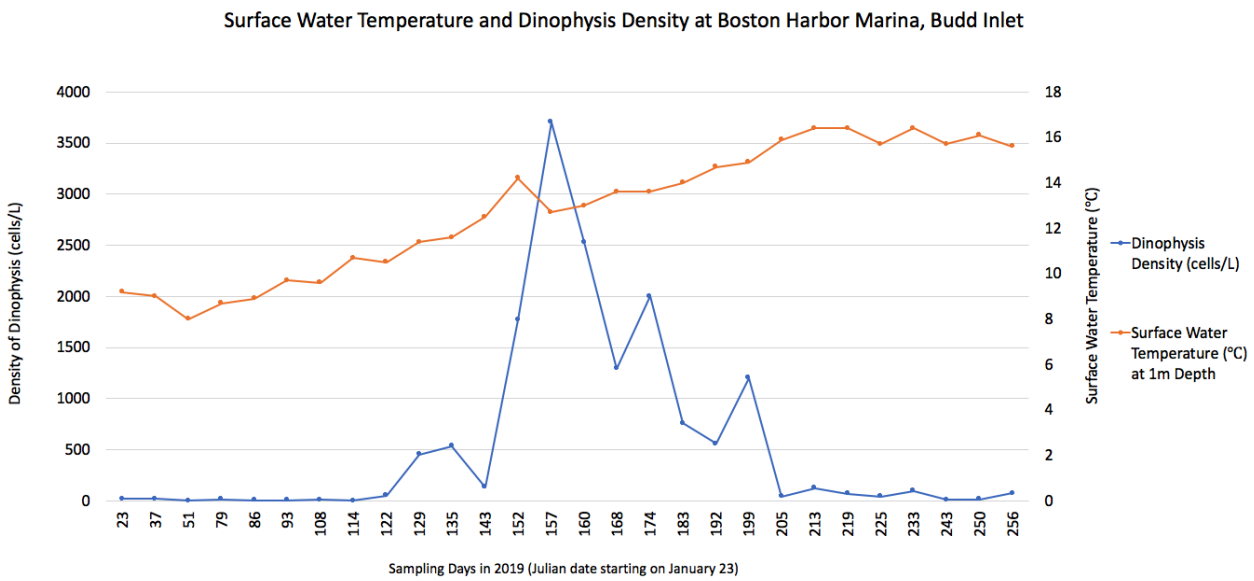

Figure 34: Time series of *Dinophysis* abundance versus surface water temperatures (1m depth) at the estuary mouth (BHM) in Budd Inlet.

River discharge plays a major role in the biogeochemical cycling of estuaries which are critical in the circulation of the waters and provide nutrient loading of inorganic compounds that are essential for instating blooms and shaping phytoplankton community structure. In addition to the statistical analysis, time series represented the form and magnitude of the Deschutes River discharge relative to *Dinophysis* abundance. The placement of the river adjacent to NPL relative to BHM might be a major factor explaining the larger density blooms at NPL.

River discharge presented high levels in the winter to mid-spring (1/13/19 to 4/18/19) ranging from 273 ft^3/sec to 662.7 ft^3/sec (Fig. 31). After 4/18/19, there was a major decline in river outputs during the summer and fall (Fig. 35). *Dinophysis* abundances at both stations coincide with low levels of river discharge from June to end of August (Fig. 36; Fig 37).

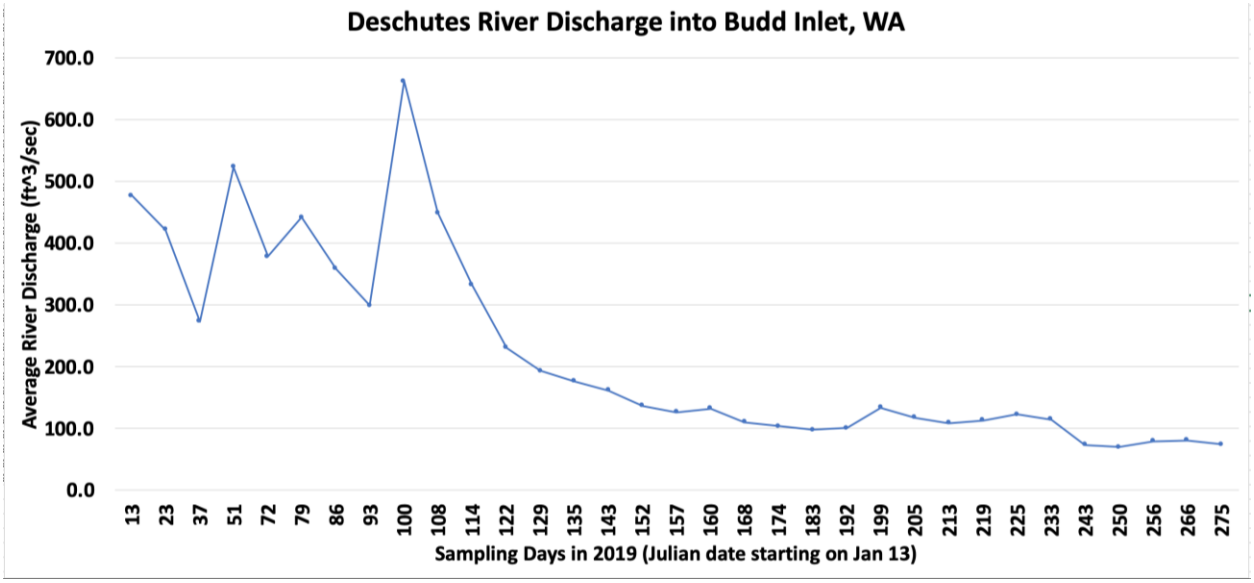

Figure 35: Time series of the Deschutes River discharge into Budd Inlet during the seasonal cycle of winter to fall of 2019.

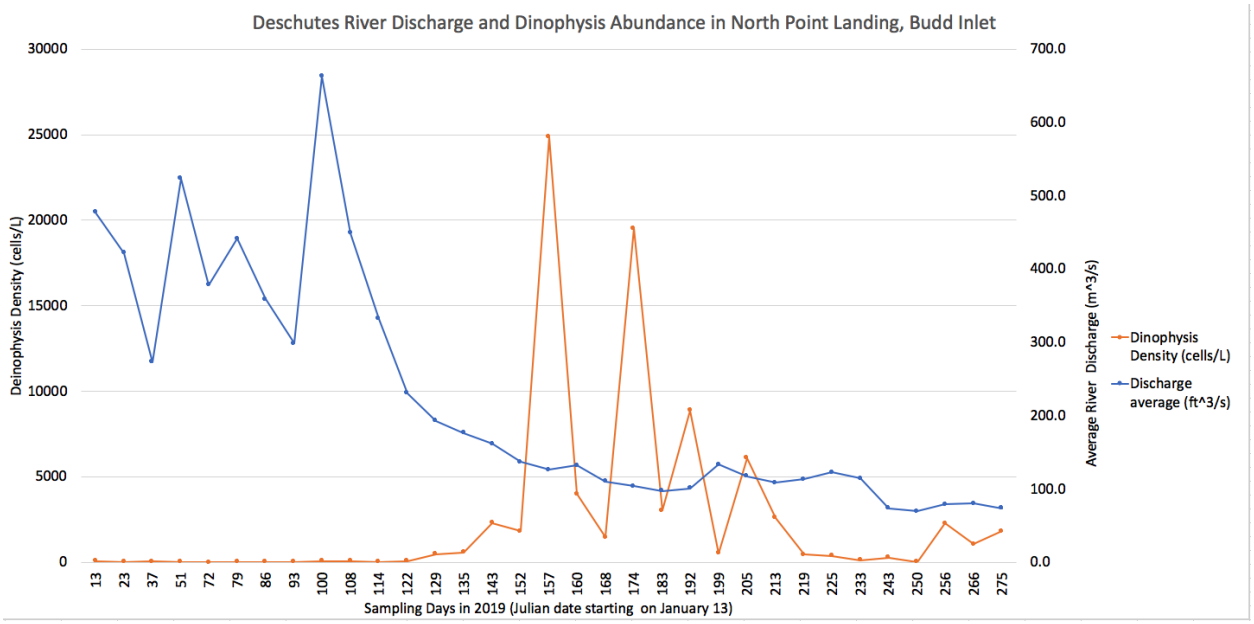

Figure 36: Time series of *Dinophysis* abundance versus river discharge at the estuary head (NPL) in Budd Inlet.

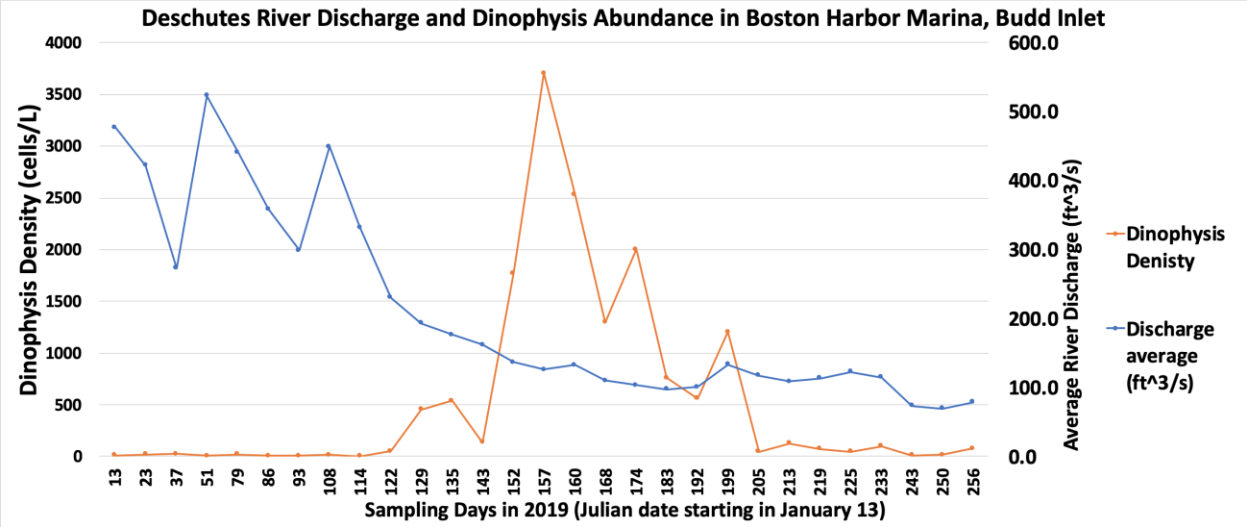

Figure 37: Time series of *Dinophysis* abundance versus river discharge at the estuary mouth (BHM) in Budd Inlet.

Wind can influence the phytoplankton activity by concentrating or diluting the dispersal of phytoplankton; therefore, time series of wind speed with direction were evaluated to determine if there is a relationship to *Dinophysis* abundance. Wind speed and direction in Budd Inlet varied considerably throughout the study period (Fig. 38). Shifts in wind direction from north to south, along with increases in wind speed overlap with two major peaks densities of *Dinophysis* at both stations (Fig. 39; Fig 40).

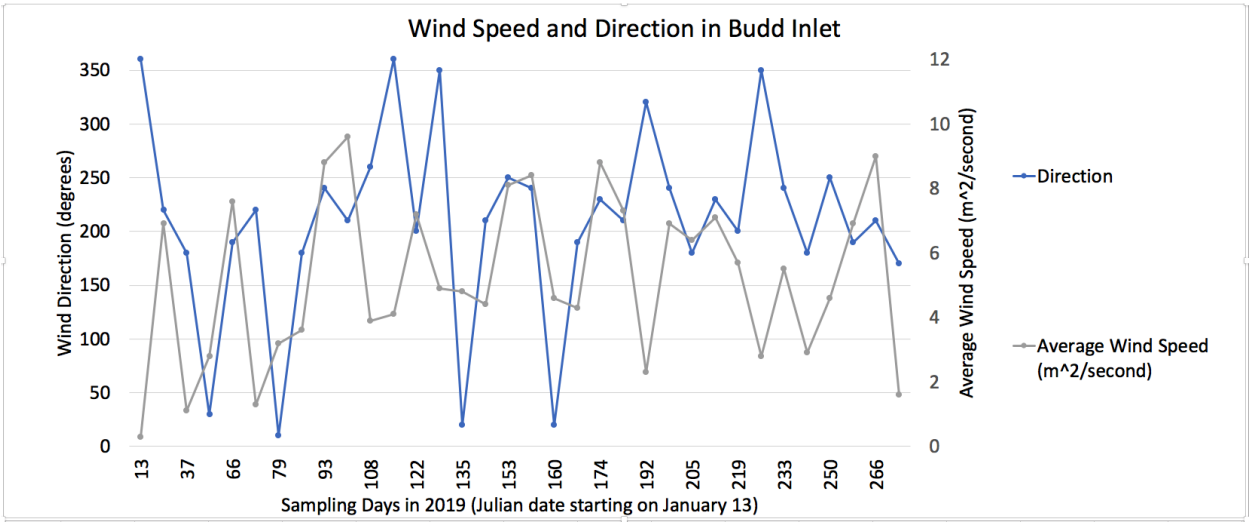

Figure 38: Time series of the wind speed and direction in Budd Inlet during the seasonal cycle of winter to fall of 2019.

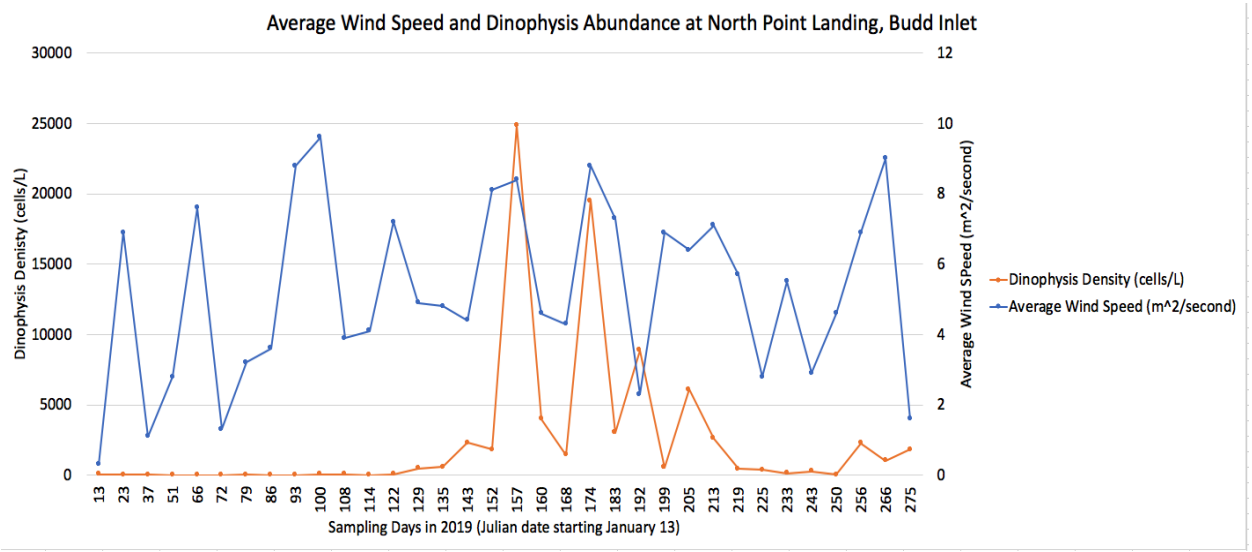

Figure 39: Time series of *Dinophysis* abundance versus wind speed at the estuary head (NPL) in Budd Inlet.

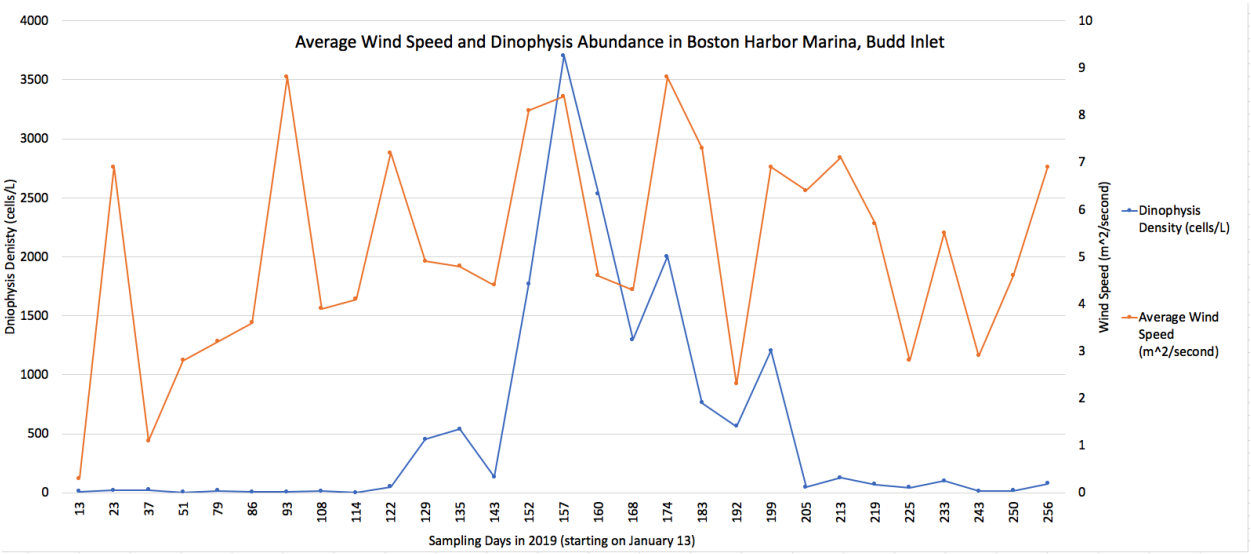

Figure 40: Time series of *Dinophysis* abundance versus wind speed at the estuary mouth (BHM) in Budd Inlet.

Solar radiation is one of the main factors for phytoplankton growth. Phytoplankton are able to absorb light, in turn promoting warmer conditions in the surface water as well as prompt algal blooms. Solar radiation was variable but gradually increased during the winter to spring. Highest levels of solar radiation appeared during 5/23/19 to 6/23/19 ranging from 257.6 to 289.0 W/m^2 and between 7/18/19 to 8/13/19 ranging from 208.3 W/m^2 to 290.4 W/m^2 (Fig. 41). At the estuary head, the peak of solar radiation corresponded during the two primary *Dinophysis* blooms events during May to June corresponds; however, the other bloom events show correspondence with the second phase in elevated total radiation emittance from July to August (Fig. 42). Similarly, at the estuary mouth the two main peaks of *Dinophysis* blooms correlate with increased levels of solar radiation in the first half of the summer along with the third peak bloom in the second half (Fig. 43).

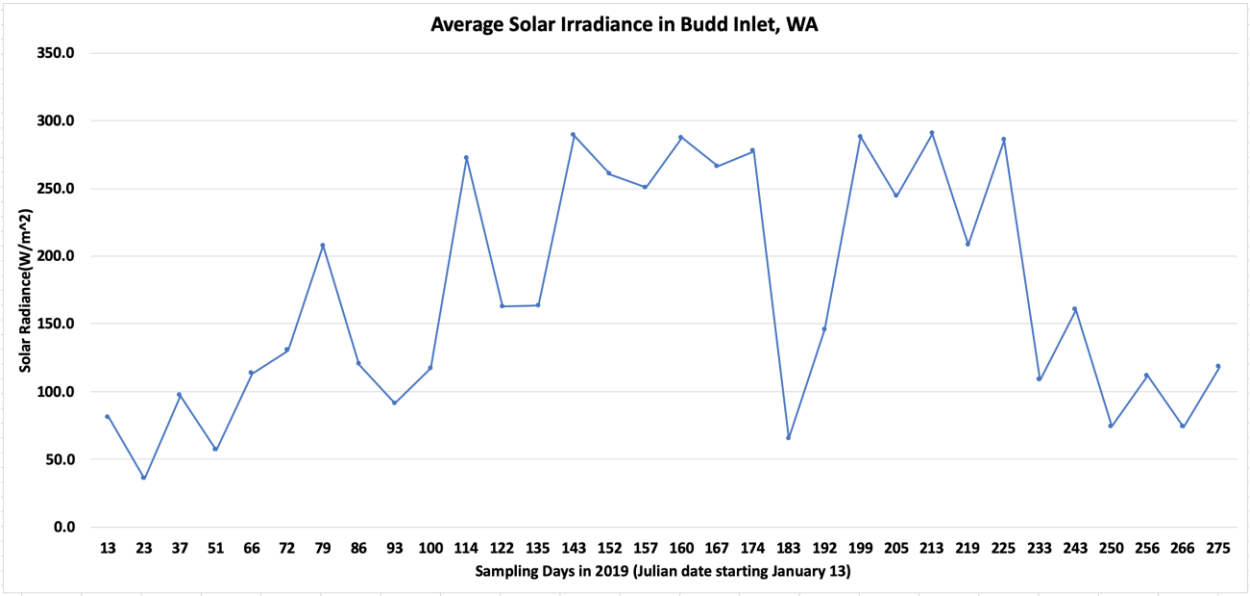

Figure 41: Time series of solar radiation in Budd Inlet during the seasonal cycle of winter to fall of 2019.

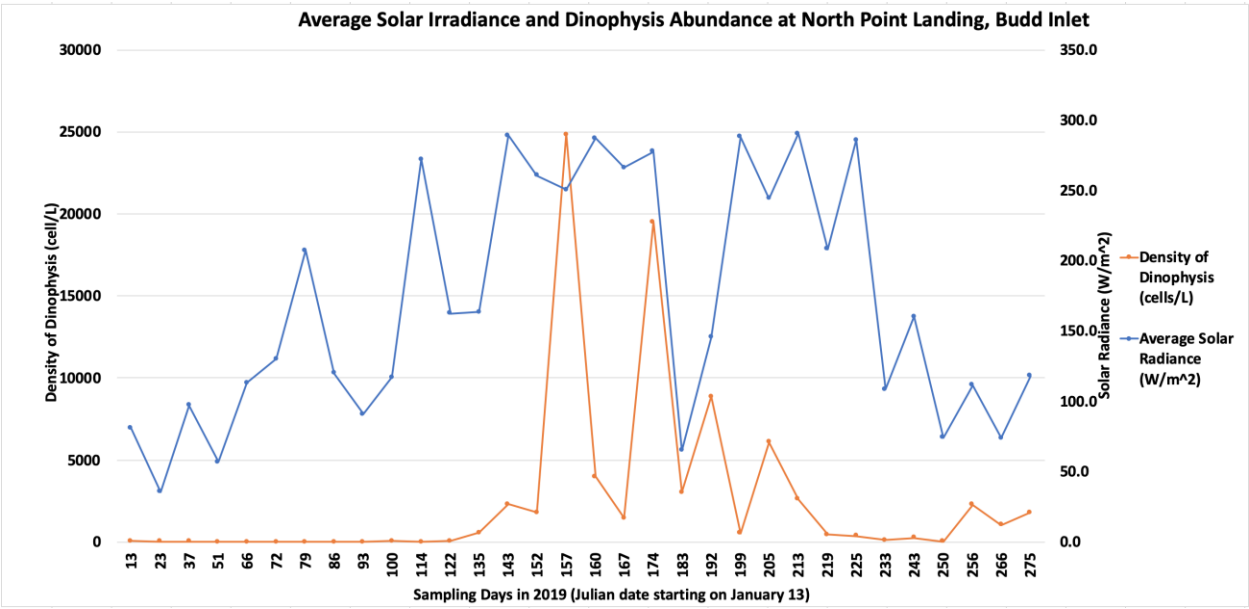

Figure 42: Time series of *Dinophysis* abundance versus solar radiation at the estuary head (NPL) in Budd Inlet.

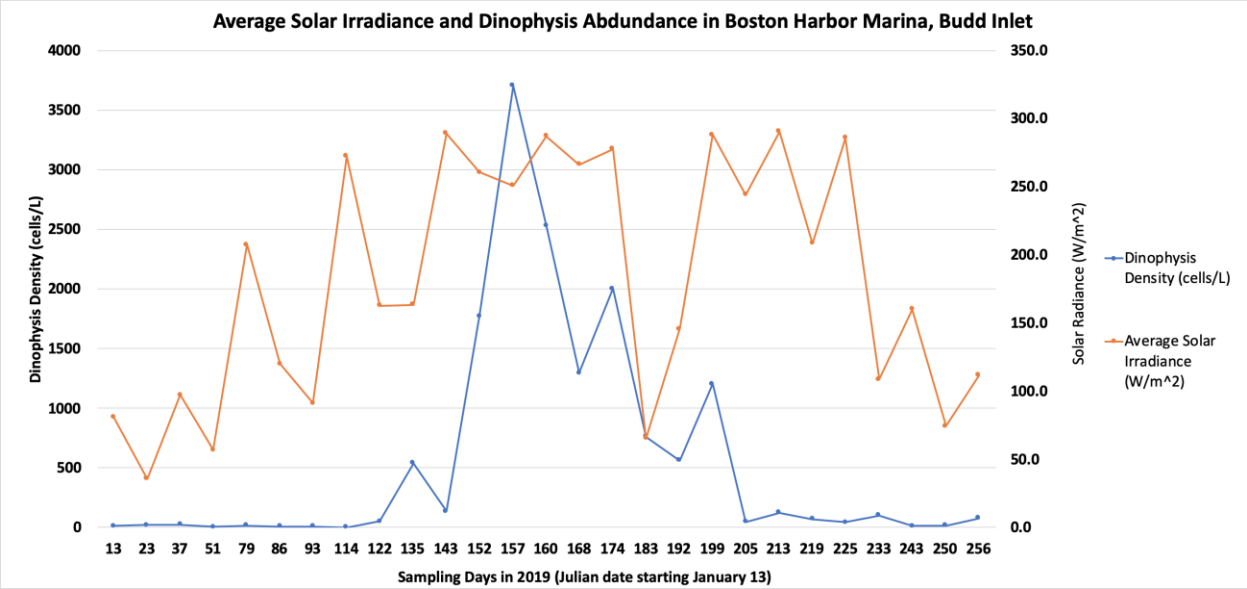

Figure 43: Time series of *Dinophysis* abundance versus solar radiation at the estuary mouth (BHM) in Budd Inlet.

Water transparency was measured via Secchi depth to understand the depth to which the light penetrates the water. Light penetration is an important component to phytoplankton growth because it is necessary for activities of photosynthesis. Water transparency (Secchi depth at 1m) ranged from 1.8 m to 5.8 m at the estuary mouth. While the head of the estuary ranged from 2.9 m to 5.6 m, water transparency was not qualitatively nor statistically related to *Dinophysis* abundance.

Time series between *Dinophysis* abundance and rainfall were analyzed with respect to the possible lag time between the input of the rain and the response time from *Dinophysis*. Rainfall events are potential important contributors to inputs of dissolved inorganic nutrients in the estuaries that can support phytoplankton growth and activity. Rainfall showed maximal values in the winter (0.04 m) and fall (0.02 m) (Fig. 44). While the early spring season exhibited moderate levels of rainfall reaching up to 0.42 in, lowest levels of rainfall occurred during late spring into the end of the summer season. High

levels of rainfall coincided with low densities of *Dinophysis* at both stations (Fig. 45). At both the estuary head and mouth, blooms developed in the summer months after a period of low precipitation. There was a peak of 0.13 inches of rainfall on 7/2/19 between the two initial *Dinophysis* blooms and the remaining blooms at both stations. In addition, rainfall also displayed potential influences on ammonium concentrations throughout the seasonal cycle. At the estuary head, concentrations of ammonium remained at low levels during the winter and considerably increased during the summer (Fig. 46). The estuary mouth showed increasing levels of ammonium during the summer (Fig. 47). The concentrations were considerably lower than the estuary head after the rainfall periods occurred.

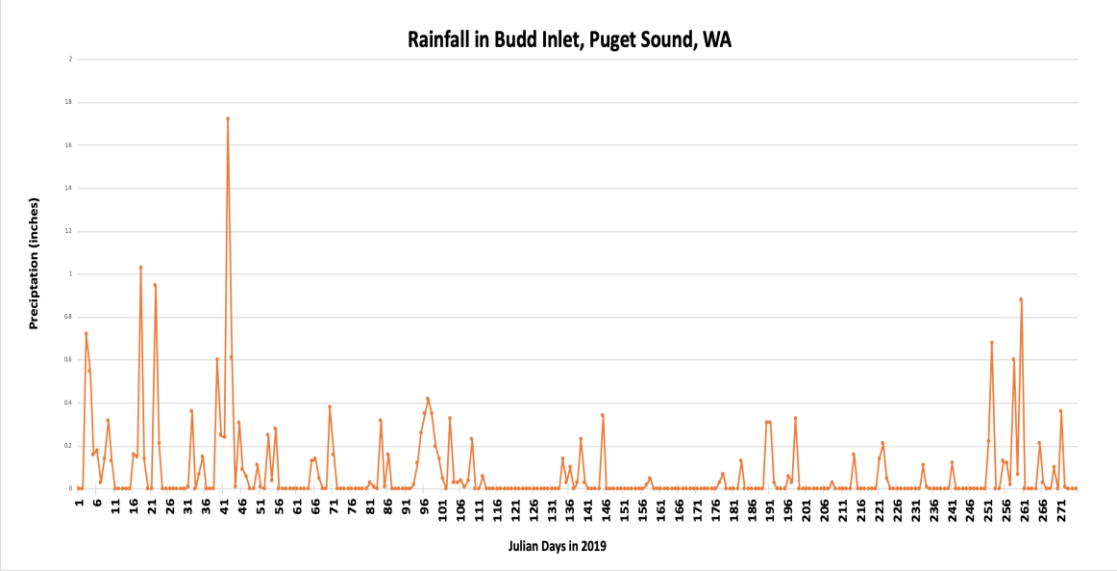

Figure 44: Time series of solar radiation in Budd Inlet during the seasonal cycle of winter to fall in 2019.

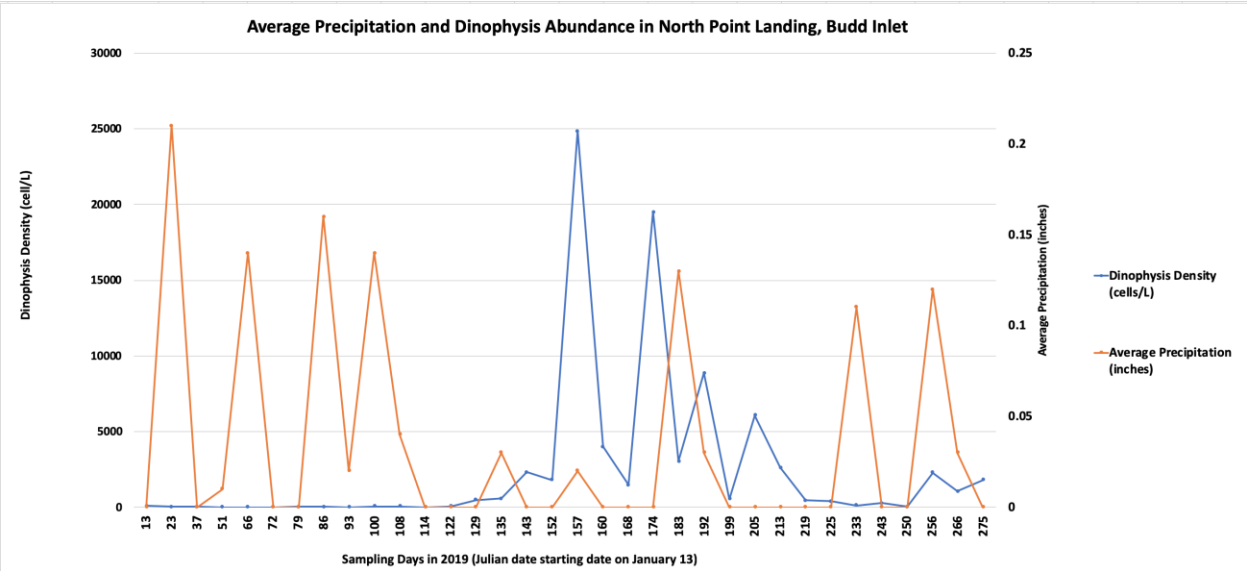

Figure 45: Time series of *Dinophysis* abundance versus average rainfall at the estuary head (NPL) in Budd Inlet.

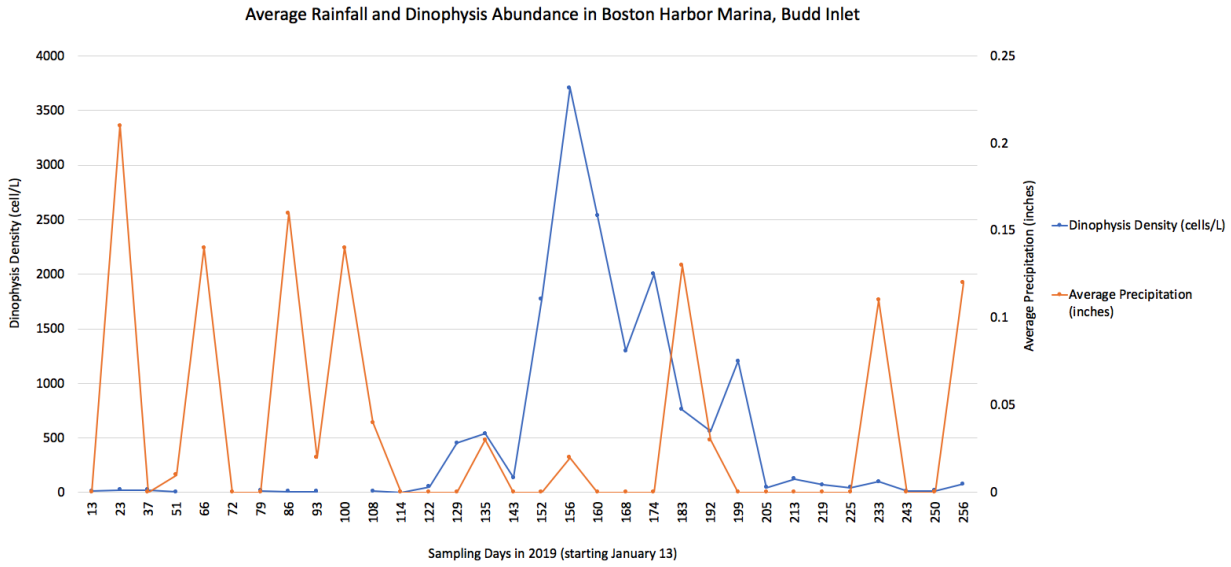

Figure 46: Time series of *Dinophysis* abundance versus average rainfall at the estuary mouth (BHM) in Budd Inlet.

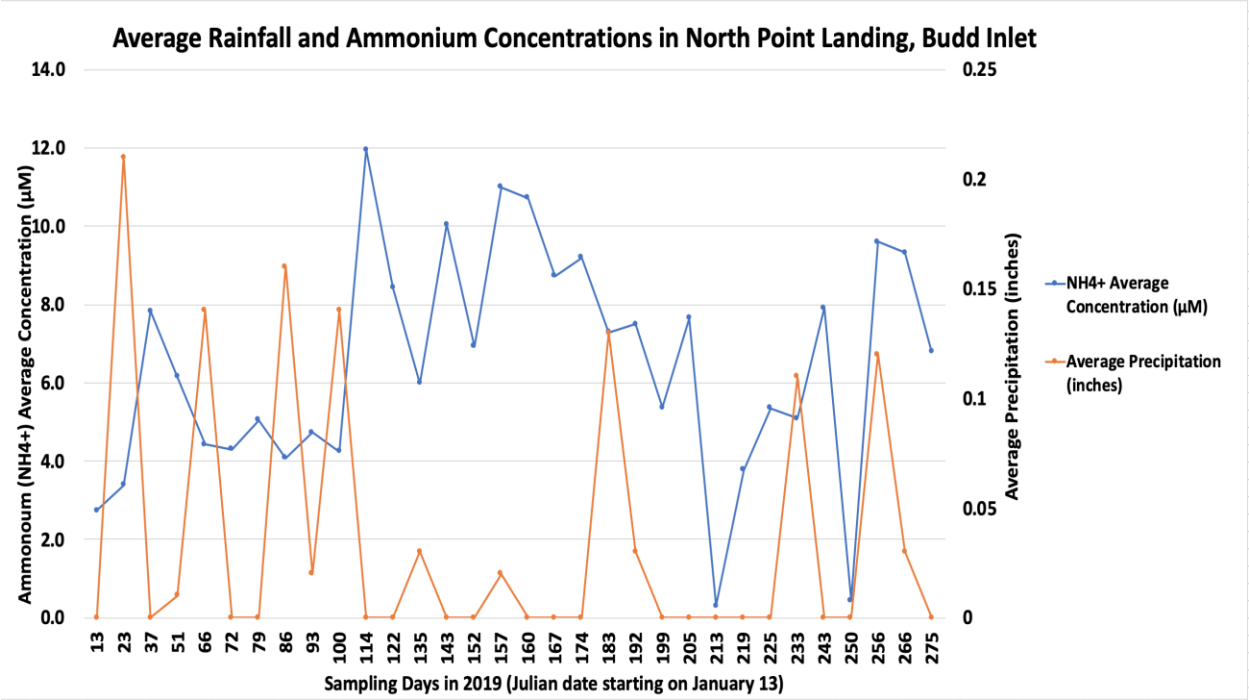

Figure 47: Time series of average rainfall and ammonium levels at the estuary head (NPL) during the seasonal cycle of winter to fall in 2019.

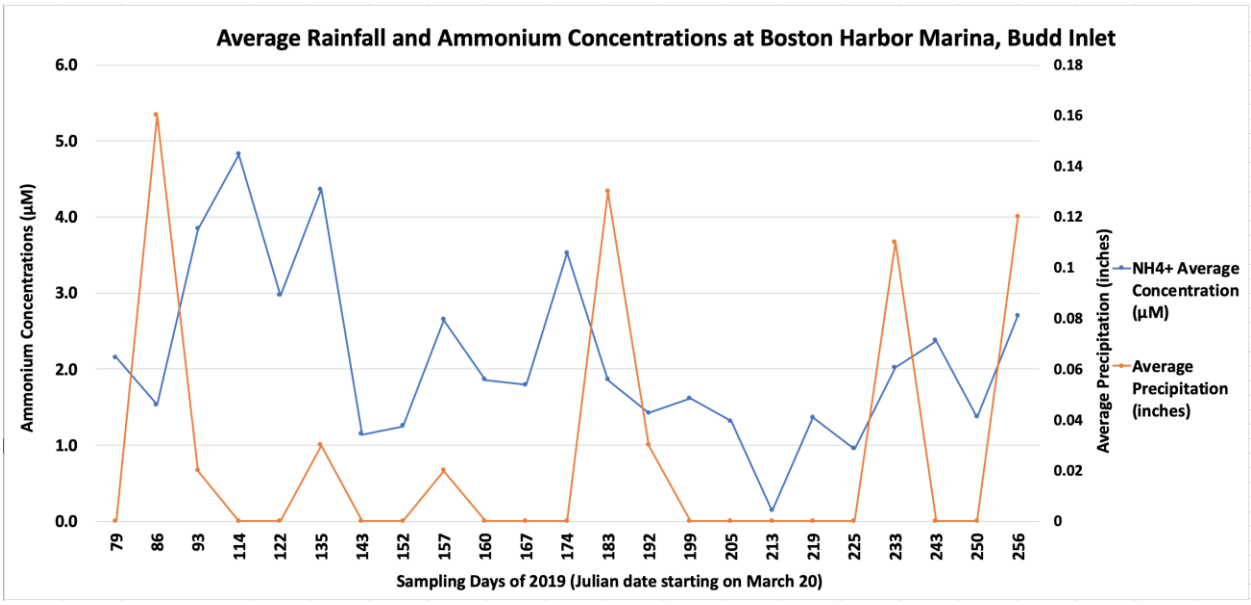

Figure 48: Time series of average rainfall and ammonium levels at the estuary mouth (BHM) during the seasonal cycle of winter to fall in 2019.

4.6 Shellfish Toxicity

A way to monitor for biotoxins is to measure diarrhetic shellfish poisoning (DSP) toxins in mussel tissues. Mussels filter a tremendous amount of water, thus concentrating the algal toxins. WDOH routinely collects mussels (sentinel mussels) and analyzes their tissues for algal toxins. WDOH collected, processed, and analyzed blue mussel tissue samples for okadaic acid, dinophysistoxin-1 (DTX-1), and dinophysistoxin-2 (DTX-2) at both stations. *Dinophysis* enumeration was completed within $\pm$48 hours (majority of samples) of the time the DSP toxin sampling was completed. This generates data that allows the WDOH to manage the closures of shellfish beds for harvesting when toxin levels pass given minimum concentrations. Total diarrhetic shellfish toxins were statistically and quantitively analyzed.

While DSP toxins are generated by *Dinophysis,* its abundance and DSP in toxins may not coincide in time. This is because the concentration of toxin by mussels occurs over an unknown period of time. The same toxin level, for example, could be achieved by filtering small concentrations of cells over a long period of time, or by consuming a large concentration of cells over a short period of time. Furthermore, mussels can get rid of the toxin following continued filtration (depuration) of non-toxic cells. If a *Dinophysis* bloom occurs following depuration, there will not be a relationship between abundance and toxins in mussels (Svensson, 2003). In the context of this study and an additional complication is that the WDOH data was collected at much longer time intervals than the abundance data. Given that WDOH provided the DSP data and in spite of these issues described, I ran linear regression analysis to evaluate if there is a relationship between *Dinophysis* abundance and DSP.

There were 20 samples from January to the end of September at NPL with DSP concentrations ranging from 0.50 to 9 μg/100g (Fig. 49). There were 11 samples collected at BHM from mid-May to end of September with DSP concentrations ranging from 0.24 to 1.16 μg/100g (Fig. 50). Three samples were taken around the time of *Dinophysis* blooms. The highest DSP levels were located at NPL, occurring on March 20. These high DSP levels occurred in the mid-spring before the summer bloom period. During the bloom period, there was also another minor peak in the month of June reaching a maximal DSP level of 3.52 μg/100g.

Levels of DSP toxins were very low over the seasons at both stations—not reaching the USDA action level of 16 µg/100g. The majority of the DSP toxin present was DTX-1, and minimal levels of okadaic acid were present throughout the study. *Dinophysis* abundance and DSP toxin concentrations from WDOH (Table 8) were not significantly related.

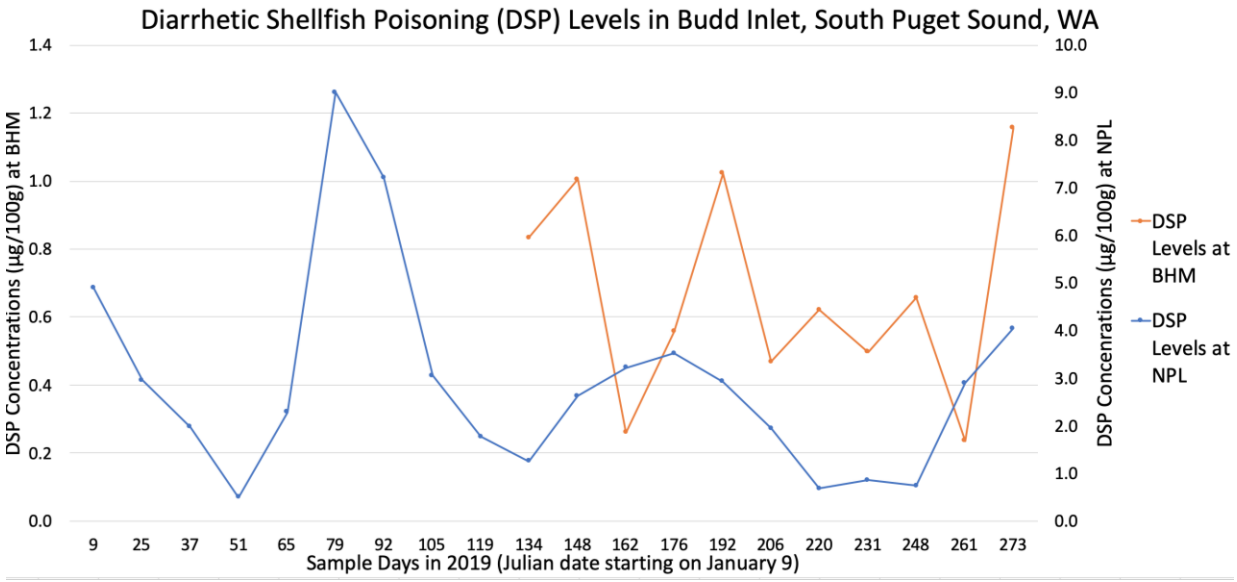

Figure 49: Time series of *Dinophysis* abundance versus the total DSP toxin levels at the estuary head (NPL) during the seasonal cycle of winter to fall in 2019.

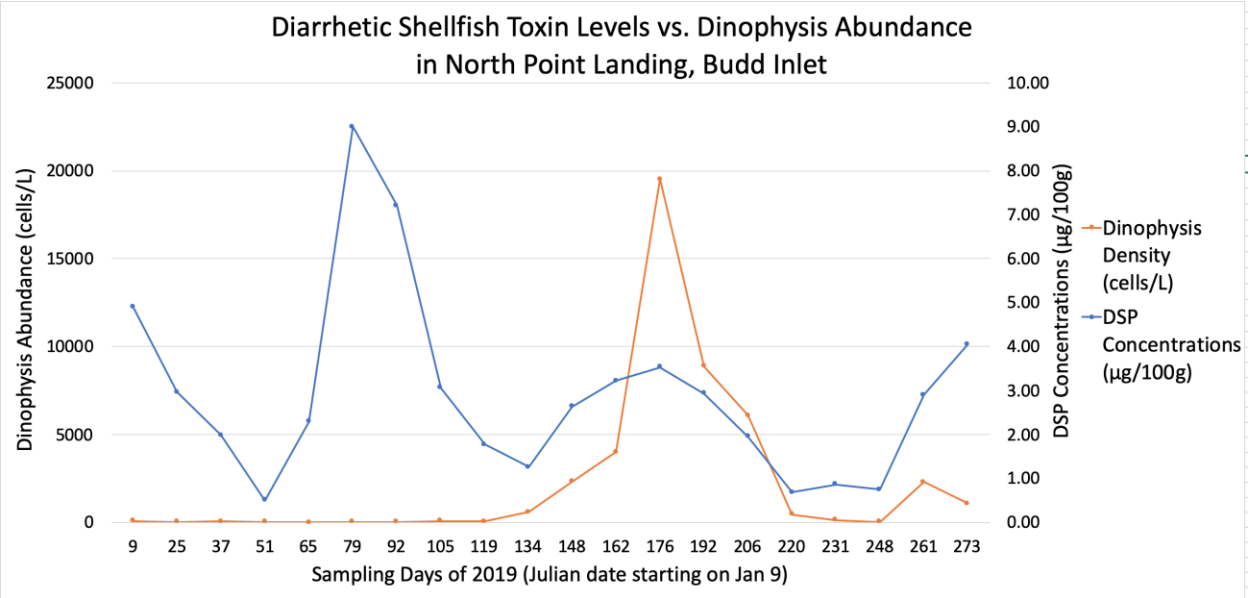

Figure 50: Time series of *Dinophysis* abundance versus the total DSP toxin levels at the estuary mouth (BHM) during the seasonal cycle of winter to fall in 2019.

Table 8: Regression analysis between *Dinophysis* abundance versus DSP toxins at the estuary head and mouth in Budd Inlet (significant p-values are boldfaced).

Dinophysis Density vs. Diarrhetic Shellfish Toxin Levels			
Parameters	**Statistics**	**Estuary Head (NPL)**	**Estuary Mouth (BHM)**
Diarretic Shellfish Toxins	R-squared	0.00	0.02
	P-value	0.83	0.83

CHAPTER 5: DISCUSSION

5.1: Overview of Research Questions & Hypotheses

This is this the first study to characterize *Dinophysis* bloom activity with high frequency sampling of biological and environmental parameters over a 10-month period in Budd Inlet, Puget Sound, Washington. The high concentration method was developed because *Dinophysis* was reported to be rare in this area particularly in winter. This method was critical to determining the changes in the abundance and distribution over space and time of six toxic *Dinophysis* species. My research questions were: What is the spatiotemporal distribution of *Dinophysis* between the estuary head (near Deschutes River) and the mouth (near south sound basin) over the seasonal cycle from winter to fall of 2019 in Budd Inlet? What environmental factors control the abundance of *Dinophysis* during the study period?

I hypothesize that the station near the head of the estuary would have greater phytoplankton abundance relative to the mouth. The station adjacent to the Deschutes river may be more heavily influenced by the river discharge which might support the notion of elevated nutrient loading and high density stratification that promote an increase dinoflagellate bloom activity.

The hypothesis also recognizes several meteorological and water quality factors that were related to *Dinophysis* abundance and timing of blooms. Availability of nitrogen, ammonium, and phosphorous were considered to be major factors controlling abundance of *Dinophysis* or of its prey (Hattenrath-Lehmann et al., 2015; Gao et al, 2011). *Dinophysis* cells are mixotrophic usually predating on *Myrionecta rubra* but can be autotrophic when starved. River discharge was hypothesized to be another factor

contributing to *Dinophysis* blooms because in addition to being a source of nutrients, the freshwater contributes to creating a stratified water column, which tends to benefit dinoflagellates (Sellner et al., 2011; Gentien et al., 2015).

Now, I will discuss how my findings provide answers to the research questions. In this discussion, I will provide an overview of the phytoplankton species composition and biomass. Then, I will discuss what I found regarding the distribution of *Dinophysis* both spatially and temporally and the environmental factors that may explain these trends. In closing, suggestions for future *Dinophysis* research are mentioned.

5.2: Phytoplankton Species Composition and Biomass

Diatom species dominated in winter and dinoflagellates species dominated in spring to summer. This is consistent with the general concept of a shift from diatom to dinoflagellates when transitioning from cooler to warmer seasons of the year in other temperate estuaries similar to Budd Inlet. Although the species richness was similar at both sites, each station species' evenness varied with higher cell abundance of dinoflagellates species at the head of the estuary. Dinoflagellate (including *Dinophysis* spp.) domination occurs because they benefit from the stratified conditions that are more common at the head of the estuary due to its proximity to the river (Mackenzie, 2018; Mena et al., 2019).

Phytoplankton biomass as estimated by chlorophyll-a was only related to *Dinophysis* abundance at the head of the estuary. This was most likely due to diatoms which have more chlorophyll-a content per cell, are generally larger, and more abundant at the mouth of the estuary.

5.3: Spatiotemporal Distribution of *Dinophysis* spp.

The results show 4 out of 13 toxic species of *Dinophysis* are commonly found in Budd Inlet, Puget Sound. Using a high concentration method, *Dinophysis* was detected throughout the four seasons at both stations. In the winter, *Dinophysis* mainly comprised *D. norvegica, D. acuminata,* and *D. fortii*, while the late spring throughout the summer was dominated by *D. norvegica*. *D. norvegica* was the most common *Dinophysis* species found at both locations in all but one week. The density of *Dinophysis norvegica* blooms increased during the summer months. This indicates that summer has optimal conditions for *D. norvegica* growth, allowing it to outcompete other species. When *Dinophysis* bloomed, few other phytoplankton genera were observed. These results are consistent with *D. norvegica* blooms on the Pacific Coast of Canada that reached cell densities exceeding $5x10^5$ cells/L (Hattenrath-Lehmann et al., 2013).

The densities of *Dinophysis* did not support my hypothesis because the dominance of *D.* norvegica was unexpected and *D. acuminata* has been the most prevalent species of *Dinophysis* in Puget Sound and United States, responsible for DSP outbreaks (Trainer et al., 2013). *Dinophysis norvegica* has been associated with DSP outbreaks but these are not as extensive as DSP events associated *Dinophysis acuminata* blooms. To date, *D. norvegica* is not known to be a major contributor to DSP outbreaks in cold-temperate waters and the DSP events it causes have been mild.

Dense cell abundances of *D. norvegica* were found at the estuary head relative to the mouth. At the head, *D. norvegica* co-occurred more frequently with *D. acuminata* and *D. fortii.* These two species have been known to produce diarrhetic shellfish toxins

(DSTs) that cause extensive DSP outbreaks. Their abundance at the head may result from hydrographic conditions of strong thermal water-column stratification during late spring and early summer which seem to favor cell densities of *Dinophysis* (Delmas et al., 1992; Reguera et al., 1995; Godhe et al., 2002; Hattenrath-Lehmann et al., 2015).

5.4 *Dinophysis* Abundances and Environmental Factors

In this study, several environmental factors were examined to understand the bottom-up control of *Dinophysis* abundance. These included water quality and meteorological variables.

The question of whether nutrient loading contributes to *Dinophysis* blooms has not been addressed extensively in the literature because *Dinophysis* is mixotrophic. Nutrients, however, can be important because they are needed by *Dinophysis* prey and also by *D. acuminata and D. fortii* when starved. I considered the nutrients needed for phytoplankton growth and computed various nutrient ratios to explore if variations in nutrient composition are important (Kim et al., 2015; Tong et al., 2015). Simple linear regressions and time series graphs were used to test for the relationship between *Dinophysis* abundances and nutrients concentration and composition (ratios). During the initiation of bloom observed in late spring to late summer, nitrate, phosphate, and ammonium levels appeared to enhance the bloom. Prior to the blooms where *Dinophysis* reached their maximal abundance, ammonium and phosphate were high. Other studies have shown that groundwater which is enriched with nitrogen and benthic levels of ammonium during the late spring to early summer may be contributors to *Dinophysis* blooms (Steenhuis et al., 1985; Gobler et al., 2001; Young et al., 2013).

The role of nutrient composition in determining phytoplankton occurrence and distribution was examined by computing nutrient ratios (DIN:DIP, DIN:DSi, DSi:DIP) and comparing them to the fixed Redfield Ratios, which represents the fixed ratio of selected elements in phytoplankton cells. Deviations of the available nutrient ratios relative to the needed Redfield Ratio can reveal the times when nutrient limitation can affect occurrence and distribution of specific plankton species.

The nutrient ratios of DIN:DIP varied substantially and appeared to be related to *Dinophysis* abundances at the head of the estuary ($r^2 = 0.19$). During the winter and early spring, when the nutrient ratio of DIN:DIP was higher than the Redfield ratio of 16:1, represents the proportion at which inorganic nitrogen is an excess and phosphorus is limited. The ratios in the winter directly before the bloom activity were high at 20.4, showing a significant deviation potentially indicating a period of increased phosphorous limitation during mid-spring, while during late spring, ratios declined to 2.8 before the onset of the first bloom in late spring. The shift from high to low proportions of DIN:DIP occurring in late spring/early summer is indicative of nitrogen limitations for growth (Danish EPA, 2011). The ratios remained low as the bloom progressed over the summer. This data supported DIN:DIP ratios which deviated from the optimal ratios for phytoplankton growth at the start of the *Dinophysis* blooms to the end of the study period. This evidence supports the conclusion that *Dinophysis norvegica* blooms occur under nitrogen-limited conditions. Thus, the low DIN:DIP ratios may be a result of high prey and *Dinophysis* growth which used up the available inorganic nitrogen.

These data suggest a strong nitrogen demand at the onset of the largest bloom (occurring on 6/6/19) while phosphorous limitations are also present. This is consistent

with other findings of lower DIN:DIP ratios throughout all stages of a *Dinophysis* bloom (Hattenrath et al., 2015). Excess nitrogen and limitation of phosphate have both shown strong relationships to high *Dinophysis* abundances (Hattenrath-Lehmann & Gobler, 2015). Anthropogenic nitrogen inputs from fertilizer use and fossil fuel emissions to estuarine and coastal systems has changed ecosystem functioning of (Galloway, 2004). The eutrophic conditions due to anthropogenic pressures of nitrogen loading from river runoff and wastewater treatment plant result in high nitrogen levels for sustaining *Dinophysis* blooms such as those in Budd Inlet (Glibert & Burkholder, 2011; Hattenrath-Lehmann & Gobler, 2015). Variable elemental composition from nutrient loading—such as elevated nitrogen levels from effluent discharge—may induce a response factor from cells exposed to rapidly changing environments. These high turnover responses may suggest *Dinophysis* spp. exhibit a high degree of cellular plasticity to nutrient loading (Falkowski, 2000). In turn, these nutrient loads can influence the prey populations, therefore indirectly stimulating *Dinophysis* blooms (Gao et al., 2018).

Of several physicochemical parameters considered in this study, river flow discharge was the most significant factor ($r^2 = 0.51$ at head; $r^2 = 0.32$ at mouth) related to *Dinophysis* abundance at both stations. The time series graph also provided evidence of the blooms closely coinciding with seasonal changes in the biogeochemical cycling of nutrients in estuaries, which are in turn influenced by riverine inputs. The data provided evidence to support the conclusion that river flow discharge is one of the main contributing factors enhancing bloom activity in Budd Inlet. River inputs greatly influence phytoplankton blooms because they enhance water-column stratification, and provides a source of nutrients needed to sustain *Dinophysis* growth and/or their prey.

This evidence supports the conclusion that levels of phosphate and nitrogen river discharge into the estuary were elevated. Riverine runoff can produce large salinity gradients where vertical stratification occurs as the marine waters from the ocean mix with river water (Szymczycha et al., 2019).

Solar radiation, surface water temperatures (1m depth), and air temperature were also noteworthy factors influencing *Dinophysis* populations at both stations. There was significant variation in the water temperature throughout the study period ranging from 12.6 to 17.3℃ at the head and 14.2 to 14.9 ℃ at the mouth. The head exhibited more variation in water temperatures relative to the mouth. *Dinophysis* blooms occurred during high intensity of solar radiation. When solar radiation decreased, the bloom activity followed the same pattern. These trends are also consistent with other studies that reported *Dinophysis* being associated with warmer waters (Caroppo, 2001; Hattenrath-Lehmann et al., 2015).

The large accumulations of *Dinophysis* occurred during the summer months when water was warm. Others have also showed that *Dinophysis*—and dinoflagellates in general—aggregate at the surface of the water-column during warmer water conditions and high light intensities from solar radiation (Nielsen et al., 2012). High productivity of *D. norvegica* during increased radiation, water temperature, and air temperature showcases possible characteristics of a highly adaptable species to spring-summer changes within its environment (Basti et al., 2018).

Another contributing factor explaining the distribution of *Dinophysis* species may involve variations in dissolved oxygen. Dissolved oxygen levels were stable in the winter yet decreased as the seasons progressed into summer

which suggests that temperature may influence these trends. Warmer waters may be influencing this trend. Warmer conditions after the peak blooms occurred during early summer displayed levels of dissolved oxygen which decreased from 8.32 mg/L to 3.92 mg/L.

Other studies have also shown *Dinophysis* to thrive in water saturated with oxygen (Caroppo, 2001). High cell accumulations of *Dinophysis* occurring in early summer showed a corresponding decrease in oxygen levels during the cessation of blooms from 6/6/19 to 8/21/19. When surface waters are more stable in the winter, dissolved oxygen concentrations are elevated. However, dissolved oxygen decreases when due to increases in photosynthesis driven by heterotrophic activities of grazing and decomposition. Dinoflagellate bloom activities can decrease the oxygen to very low levels causing hypoxic conditions within the water-column or can increase if in autotrophic mode. These conditions have been closely correlated with blooms of *Dinophysis* spp. and *Ceratium fusus* (Pitcher & Probyn, 2011).

Wind was another significant factor explaining *Dinophysis* abundance at the mouth. During the three main peaks at BHM, wind speed ranged from 6.9 to 8.8 mph and the wind direction varied from 230° to 240° indicating that *Dinophysis* blooms are associated with southwesterly winds. The same evidence was found by Hattenrath-Lehmann (2015), showing the same associations to SW winds over several years. *Dinophysis* abundances may be influenced by the advection processes and relaxation of upwelling related to winds. The speed and directionality may influence the growth, dispersal, and spreading of the blooms (Anjani et al., 2016; Moita et al., 2016). This data

supports the conclusion that winds are related to *Dinophysis* abundances. During another long-term study, the onset of *Dinophysis* blooms occurred two months after the maximal wind differences were noticed (Hattenrath-Lehmann et al., 2015). Low velocity winds from the south and north have been associated with maximum counts of several *Dinophysis* species in the Greek coastal waters (Vlamis & Katikou, 2014).

The DSP levels were not significantly related to *Dinophysis* abundance. At the head, in spring high DSP levels were measured when cell abundances were low. In summer, when *Dinophysis* abundance was highest, DSP levels did not increase. In late summer variations in abundance appeared to be related to changes in DSP but the relationship was weak. Possible reasons for the lack of a relationship include: toxicity of toxins may be species-specific and cells may be stressed.

D. norvegica dominated during summer blooms when DSP levels were low. These data are consistent with other studies showing *D. norvegica* is mildy toxic compared to other highly toxic species, *D. acuminata* and *D. fortii* (Hattenrath et al., 2015). *D. acuminata* and *D. fortii* exhibited were present but in low cell densities during the winter and spring which may explain why there was an increased levels of DSP toxins during the winter to spring period. The presence of highly toxic species of *D. acuminata* and *D. fortii* may be a contributing factor to increased levels of toxins. Also, the winter could have yielded conditions to increase the toxicity of *D. acuminata* and *D. fortii* because these species have been linked to cellular stress from low nutrient and prey concentrations (Alves-de-Souza et al., 2014).

As mentioned in the previous chapters, the comparison between DSP levels in mussels and *Dinophysis* abundances is complex because mussels represent both

concentration and depuration over an unknown period of time. Also, the DSP sampling occurred at longer time frequency that of *Dinophysis* monitoring which could affect the timing of concentration and depuration of the cells.

5.5: Suggestions for Future Research

More research on *Dinophysis* is needed to understand the dynamics between the physiological processes of the cells and how they interact with the local environmental conditions. Suggestions for the future would involve more intensive analysis of spatiotemporal distribution by increasing the time resolution to capture all seasons over a long-term (>2 years) period as well as focusing on toxicity of the cells by addressing the relationships between DSP and *Dinophysis* abundances of individual species.

Other factors may potentially be stimulating and driving blooms in late spring to summer. Organic nitrogen loading might also have an effect on the *Dinophysis* blooms and toxicity; therefore, providing a more robust nutrient assay and ratio of nutrient compositions by adding organic nitrogen and carbon to a study might give more insight into other contributing nutrients. Also, the inclusion of nutrient molecular tracers in experimental studies could showcase the physiological processes and preferences for different forms of nutrients, organic versus inorganic.

Other work could also develop modeling and analysis of both bottom-up and top-down controls. This study was limited in noting any top-down controls that could potentially influence *Dinophysis* abundances. Addressing grazing from predators (i.e. zooplankton, planktivorous fish) could affect the abundance, assemblage structure, and species composition of phytoplankton in a local body of water. This study was limited in addressing how *Dinophysis* blooms are related to its prey. Quantification of prey, such as

Myrionecta rubra, would also be able to provide information about possible grazing pressures.

Another limitation in this study corresponded with performing statistical analyses on individual environmental factors by solely investigating if responses of *Dinophysis* were related to environmental variables independently of each other. To understand the interactions between various environmental parameters, deterministic modeling should be applied. Modelling will assist in determining the dynamic relationship of *Dinophysis* abundances and species-specific toxicity to various environmental parameters in order to capture the complexity of the ecophysiological response of *Dinophysis.* There could be several variables at play instead and using multiple linear regression and other modeling tools, such as canonical correspondence analysis (CCA), can represent multiple variables potentially stimulating the *Dinophysis* blooms (Smida et al., 2014; Tibirica et al., 2015).

BIBLIOGRAPHY

Accoroni, S., Ceci, M., Tartaglione, L., Romagnoli, T., Campanelli, A., Marini, M., … Totti, C. (2018). Role of temperature and nutrients on the growth and toxin production of Prorocentrum hoffmannianum (Dinophyceae) from the Florida Keys. *Harmful Algae*, *80*, 140–148. https://doi.org/10.1016/j.hal.2018.11.005

Ahmed, A., Figueroa-Kaminsky, C., Mohamedali, J., Pelletier, G., & McCarty, S. (2019). Puget Sound Nutrient Source Reduction Project. Volume 1: Model Updates and Bounding Scenarios. Retrieved December 19, 2019, from https://fortress.wa.gov/ecy/publications/SummaryPages/1903001.html

Ajani, P. A., Larsson, M. E., Woodcock, S., Rubio, A., Farrell, H., Brett, S., & Murray, S. A. (2018). Bloom drivers of the potentially harmful dinoflagellate Prorocentrum minimum (Pavillard) Schiller in a south eastern temperate Australian estuary. *Estuarine, Coastal and Shelf Science*, *215*, 161–171. https://doi.org/10.1016/j.ecss.2018.09.029

Ajani, P., Larsson, M. E., Rubio, A., Bush, S., Brett, S., & Farrell, H. (2016). Modelling bloom formation of the toxic dinoflagellates Dinophysis acuminata and Dinophysis caudata in a highly modified estuary, south eastern Australia. *Estuarine, Coastal and Shelf Science*, *183*, 95–106. https://doi.org/10.1016/j.ecss.2016.10.020

Alves-de-Souza, C., Varela, D., Contreras, C., de La Iglesia, P., Fernández, P., Hipp, B., … Lagos, N. (2014). Seasonal variability of Dinophysis spp. And Protoceratium reticulatum associated to lipophilic shellfish toxins in a strongly stratified Chilean

fjord. *Deep Sea Research Part II: Topical Studies in Oceanography*, *101*, 152–162. https://doi.org/10.1016/j.dsr2.2013.01.014

Anderson, D. M., Cembella, A. D., & Hallegraeff, G. M. (2012). Progress in understanding harmful algal blooms: Paradigm shifts and new technologies for research, monitoring, and management. *Annual Review of Marine Science*, *4*, 143–176. https://doi.org/10.1146/annurev-marine-120308-081121

Anderson, D. M., Glibert, P. M., & Burkholder, J. M. (2002). Harmful algal blooms and eutrophication: Nutrient sources, composition, and consequences. *Estuaries*, *25*(4), 704–726. https://doi.org/10.1007/BF02804901

Anderson, D. M., Alpermann, T. J., Cembella, A. D., Collos, Y., Masseret, E., & Montresor, M. (2012). The globally distributed genus Alexandrium: multifaceted roles in marine ecosystems and impacts on human health. *Harmful Algae*, *14*, 10–35. https://doi.org/10.1016/j.hal.2011.10.012

Basti, L., Suzuki, T., Uchida, H., Kamiyama, T., & Nagai, S. (2018). Thermal acclimation affects growth and lipophilic toxin production in a strain of cosmopolitan harmful alga Dinophysis acuminata. *Harmful Algae*, *73*, 119–128. https://doi.org/10.1016/j.hal.2018.02.004

Berg, G. M., Glibert, P. M., Lomas, M. W., & Burford, M. A. (1997). Organic nitrogen uptake and growth by the chrysophyte Aureococcus anophagefferens during a brown tide event. *Marine Biology*, *129*(2), 377–387. https://doi.org/10.1007/s002270050178

Bockstahler, K. R., & Coats, D. W. (1993). Spatial and Temporal Aspects of Mixotrophy In Chesapeake Bay Dinoflagellates. *Journal of Eukaryotic Microbiology*, *40*(1), 49–60. https://doi.org/10.1111/j.1550-7408.1993.tb04881.x

Borchert. J. (2019, April 1). Personal interview.

Bouwman, A. F., Beusen, A. H. W., & Billen, G. (2009). Human alteration of the global nitrogen and phosphorus soil balances for the period 1970–2050. *Global Biogeochemical Cycles*, *23*(4). https://doi.org/10.1029/2009GB003576

Burkholder, J. M., Glibert, P. M., & Skelton, H. M. (2008). Mixotrophy, a major mode of nutrition for harmful algal species in eutrophic waters. *Harmful Algae*, *8*(1), 77–93. https://doi.org/10.1016/j.hal.2008.08.010

Campos, M. J., Fraga, S., Mariño, J., & Sanchez, F. J. (1982). Red Tide Monitoring Programme in NW Spain: Report of 1977–1981. *International Council for the Exploration of the Sea: Copenhagen, Denmark*

Carlsson, P., Granéli, E., Finenko, G., & Maestrini, S. Y. (1995). Copepod grazing on a phytoplankton community containing the toxic dinoflagellate Dinophysis acuminata. *Journal of Plankton Research*, *17*(10), 1925–1938. https://doi.org/10.1093/plankt/17.10.1925

Caroppo, C., Congestri, R., & Bruno, M. (2001). Dynamics of Dinophysis sensu lato species (Dinophyceae) in a coastal Mediterranean environment (Adriatic Sea). *Continental Shelf Research*, *21*(16), 1839–1854. https://doi.org/10.1016/S0278-4343(01)00028-0

Chin-Leo, G. (2018, July 15). Personal interview.

Cloern, James E. (2001). Our evolving conceptual model of the coastal eutrophication problem. *Marine Ecology Progress Series*, *210*, 223253. https://doi.org/10.3354/meps210223

Cloern, J.E., & Dufford, R. (2005). Phytoplankton community ecology: Principles applied in San Francisco Bay. *Marine Ecology Progress Series*, *285*, 1128. https://doi.org/10.3354/meps285011

Cohen, P., Holmes, C. F., & Tsukitani, Y. (1990). Okadaic acid: a new probe for the study of cellular regulation. *Trends in Biochemical Sciences*, *15*(3), 98–102. https://doi.org/10.1016/0968-0004(90)90192-e

Conley, D., Paerl, H., Howarth, R., Boesch, D., Seitzinger, S., Havens, K., … Likens, G. (2009). Controlling Eutrophication: Nitrogen and Phosphorus. *Science*, *323*, 1014–1015.

Cordier, S., Monfort, C., Miossec, L., Richardson, S., & Belin, C. (2000). Ecological analysis of digestive cancer mortality related to contamination by diarrhetic shellfish poisoning toxins along the coasts of France. *Environmental Research*, *84*(2), 145–150. https://doi.org/10.1006/enrs.2000.4103

Crête-Lafrenière, A., Weir, L. K., & Bernatchez, L. (2012). Framing the Salmonidae Family Phylogenetic Portrait: A More Complete Picture from Increased Taxon Sampling. *PLOS ONE*, *7*(10), e46662. https://doi.org/10.1371/journal.pone.0046662

Danchenko, S., Fragoso, B., Guillebault, D., Icely, J., Berzano, M., & Newton, A. (2019). Harmful phytoplankton diversity and dynamics in an upwelling region (Sagres, SW Portugal) revealed by ribosomal RNA microarray combined with microscopy. *Harmful Algae*, *82*, 52–71. https://doi.org/10.1016/j.hal.2018.12.002

Davidson, K., Gowen, R. J., Tett, P., Bresnan, E., Harrison, P. J., McKinney, A., … Crooks, A.-M. (2012). Harmful algal blooms: How strong is the evidence that nutrient ratios and forms influence their occurrence? *Estuarine, Coastal and Shelf Science*, *115*, 399–413. https://doi.org/10.1016/j.ecss.2012.09.019

Delmas, D., Herbland, A., & Maestrini, S. (1992). Environmental conditions which lead to increase in cell density of the toxic dinoflagellates Dinophysis spp. In nutrient-rich and nutrient-poor waters of the French Atlantic coast. *Marine Ecology Progress Series*, *89*(1), 53–61. https://doi.org/10.3354/meps089053

Dhanji-Rapkova, M., O'Neill, A., Maskrey, B. H., Coates, L., Teixeira Alves, M., Kelly, R. J., … Turner, A. D. (2018). Variability and profiles of lipophilic toxins in bivalves from Great Britain during five and a half years of monitoring: Okadaic acid, dinophysis toxins and pectenotoxins. *Harmful Algae*, *77*, 66–80. https://doi.org/10.1016/j.hal.2018.05.011

Díaz, P. A., Reguera, B., Ruiz-Villarreal, M., Pazos, Y., Velo-Suárez, L., Berger, H., & Sourisseau, M. (2013). Climate Variability and Oceanographic Settings Associated with Interannual Variability in the Initiation of Dinophysis acuminata Blooms. *Marine Drugs*, *11*(8), 2964–2981. https://doi.org/10.3390/md11082964

Draisci, R., Lucentini, L., Giannetti, L., Boria, P., & Poletti, R. (1996). First report of pectenotoxin-2 (PTX-2) in algae (Dinophysis fortii) related to seafood poisoning in Europe. *Toxicon*, *34*(8), 923–935. https://doi.org/10.1016/0041-0101(96)00030-X

Eberhart, B.-T. L., Moore, L. K., Harrington, N., Adams, N. G., Borchert, J., & Trainer, V. L. (2013). Screening tests for the rapid detection of diarrhetic shellfish toxins in Washington State. *Marine Drugs*, *11*(10), 3718–3734. https://doi.org/10.3390/md11103718

Egmond, H., Aune, T., Patrick, L., Speijers, G. J. ., & Waldock, M. (1993). Paralytic and Diarrheic Shellfish Poisons : occurrence in Europe, toxicity analysis and regulation. *Journal of Natural Toxins*, *2*, 41–83.

Escalera, L., Reguera, B., Pazos, Y., Moroño, A., & Cabanas, J. M. (2006). Are different species of Dinophysis selected by climatological conditions? *African Journal of Marine Science*, *28*(2), 283–288. https://doi.org/10.2989/18142320609504163

Federal Drug Administration. (2011). Marine Biotoxins. Retrieved February 19, 2019, from https://www.accessdata.fda.gov/ORAU/ShellfishGrowingAreas/SGA_05_summary.htm

Fabro, E., Almandoz, G. O., Ferrario, M., Tillmann, U., Cembella, A., & Krock, B. (2016). Distribution of Dinophysis species and their association with lipophilic phycotoxins in plankton from the Argentine Sea. *Harmful Algae*, *59*, 31–41. https://doi.org/10.1016/j.hal.2016.09.001

Fernández, R., Mamán, L., Jaén, D., Fuentes, L. F., Ocaña, M. A., & Gordillo, M. M. (2019). Dinophysis Species and Diarrhetic Shellfish Toxins: 20 Years of Monitoring Program in Andalusia, South of Spain. *Toxins*, *11*(4). https://doi.org/10.3390/toxins11040189

Flynn, K. J. (2010). Ecological modelling in a sea of variable stoichiometry: Dysfunctionality and the legacy of Redfield and Monod. *Progress in Oceanography*, *84*, 52–65. https://doi.org/10.1016/j.pocean.2009.09.006

Food and Agriculture Organization of the United Nations (2004) Retrieved November 24, 2019, from http://www.fao.org/3/Y5160E/Y5160E00.htm

Food Safety Authority of Ireland. (2011). Retrieved November 24, 2019, from https://www.fsai.ie/legislation/food_legislation/food_hygiene/specific_hygiene_rules_for_food.html

Fu, F. X., Tatters, A. O., & Hutchins, D. A. (2012). Global change and the future of harmful algal blooms in the ocean. *Marine Ecology Progress Series*, *470*, 207–233. https://doi.org/10.3354/meps10047

Fujiki, H., & Suganuma, M. (1999). Unique features of the okadaic acid activity class of tumor promoters. *Journal of Cancer Research and Clinical Oncology*, *125*(3–4), 150–155. https://doi.org/10.1007/s004320050257

Fux, E., Smith, J. L., Tong, M., Guzmán, L., & Anderson, D. M. (2011). Toxin profiles of five geographical isolates of Dinophysis spp. From North and South America. *Toxicon: Official Journal of the International Society on Toxinology*, *57*(2), 275–287. https://doi.org/10.1016/j.toxicon.2010.12.002

Gentien, P., Donaghay, P., Yamazaki, H., Raine, R., Reguera, B., & Osborn, T. (2005). Harmful Algal Blooms in Stratified Environments. *Oceanography*, *18*(2), 172–183. https://doi.org/10.5670/oceanog.2005.52

Giacobbe, M., Oliva, F., La Ferla, R., Puglisi, A., Crisafi, E., & Maimone, G. (1995). Potentially toxic dinoflagellates in Mediterranean waters (Sicily) and related hydrobiological conditions. *Aquatic Microbial Ecology - AQUAT MICROB ECOL*, *9*, 63–68. https://doi.org/10.3354/ame009063

Glibert, P., Anderson, D., Gentien, P., Granéli, E., & Sellner, K. (2005). The Global, Complex Phenomena of Harmful Algal Blooms. *Oceanography*, *18*(2), 136–147. https://doi.org/10.5670/oceanog.2005.49

Glibert, P. M., Burkholder, J. M., & Kana, T. M. (2012). *Recent insights about relationships between nutrient availability, forms, and stoichiometry, and the distribution, ecophysiology, and food web effects of pelagic and benthic Prorocentrum species*. https://doi.org/10.1016/j.hal.2011.10.023

Glibert, P. M., Heil, C. A., Hollander, D., Revilla, M., Hoare, A., Alexander, J., & Murasko, S. (2004). Evidence for dissolved organic nitrogen and phosphorus uptake during a cyanobacterial bloom in Florida Bay. *Marine Ecology Progress Series*, *280*, 73–83. https://doi.org/10.3354/meps280073

Glibert, Patricia M., Magnien, R., Lomas, M. W., Alexander, J., Tan, C., Haramoto, E., … Kana, T. M. (2001). Harmful algal blooms in the Chesapeake and Coastal Bays of Maryland, USA: Comparison of 1997, 1998, and 1999 events. *Estuaries*, *24*(6), 875–883. https://doi.org/10.2307/1353178

Gobler, C. J., Renaghan, M. J., & Buck, N. J. (2002). Impacts of nutrients and grazing mortality on the abundance of Aureococcus anophagefferens during a New York brown tide bloom. *Limnology and Oceanography*, *47*(1), 129–141. https://doi.org/10.4319/lo.2002.47.1.0129

Glibert, P. M., & Burkholder, J. M. (2011). Harmful algal blooms and eutrophication: "Strategies" for nutrient uptake and growth outside the Redfield comfort zone. *Chinese Journal of Oceanology and Limnology*, *29*(4), 724–738. https://doi.org/10.1007/s00343-011-0502-z

González-Gil, S., Velo-Suárez, L., Gentien, P., Ramilo, I., & Reguera, B. (2010). Phytoplankton assemblages and characterization of a Dinophysis acuminata population during an upwelling–downwelling cycle. *Aquatic Microbial Ecology*, *58*(3), 273–286. https://doi.org/10.3354/ame01372

Granéli, E., & Flynn, K. (2006). Chemical and Physical Factors Influencing Toxin Content. In Edna Granéli & J. T. Turner (Eds.), *Ecology of Harmful Algae* (pp. 229–241). https://doi.org/10.1007/978-3-540-32210-8_18

Granéli, Edna, & Hansen, P. (2006). Allelopathy in Harmful Algae: A Mechanism to Compete for Resources? In *Ecology of Harmful Algae* (Vol. 189, pp. 189–202). https://doi.org/10.1007/978-3-540-32210-8_15

Granéli, Edna, Weberg, M., & Salomon, P. (2008). Harmful algal blooms of allelopathic microalgal species: The role of eutrophication. *Harmful Algae*, *8*, 94–102. https://doi.org/10.1016/j.hal.2008.08.011

Grattan, L. M., Holobaugh, S., & Morris, J. G. (2016). Harmful Algal Blooms and Public Health. *Harmful Algae*, *57*(B), 2–8. https://doi.org/10.1016/j.hal.2016.05.003

Gross, E. (2003). Allelopathy of Aquatic Autotrophs. *Crit. Rev. Plant Sci*, *22*.

Hackett, J. D., Tong, M., Kulis, D. M., Fux, E., Hess, P., Bire, R., & Anderson, D. M. (2009). DSP toxin production de novo in cultures of Dinophysis acuminata (Dinophyceae) from North America. *Harmful Algae*, *8*(6), 873–879. https://doi.org/10.1016/j.hal.2009.04.004

Hallegraeff, G. (1993). A Review of Harmful Algal Blooms and Their Apparent Global Increase. *Phycologia*, *32*. https://doi.org/10.2216/i0031-8884-32-2-79.1

Hansson, L.-A., Nicolle, A., Granéli, W., Hallgren, P., Kritzberg, E., Persson, A., … Brönmark, C. (2013). Food-chain length alters community responses to global change in aquatic systems. *Nature Climate Change*, *3*(3), 228–233. https://doi.org/10.1038/nclimate1689

Harred, L. B., & Campbell, L. (2014). Predicting harmful algal blooms: a case study with Dinophysis ovum in the Gulf of Mexico. *Journal of Plankton Research*, *36*(6), 1434–1445. https://doi.org/10.1093/plankt/fbu070

Harris, G. (2012). *Phytoplankton Ecology: Structure, Function and Fluctuation*. Springer Science & Business Media.

Hattenrath-Lehmann, T. K., Marcoval, M. A., Berry, D. L., Fire, S., Wang, Z., Morton, S. L., & Gobler, C. J. (2013). The emergence of Dinophysis acuminata blooms and DSP toxins in shellfish in New York waters. *Harmful Algae*, *26*, 33–44. https://doi.org/10.1016/j.hal.2013.03.005

Hattenrath-Lehmann, T., & Gobler, C. J. (2015). The contribution of inorganic and organic nutrients to the growth of a North American isolate of the mixotrophic dinoflagellate, Dinophysis acuminata. *Limnology and Oceanography*, *60*(5), 1588–1603. https://doi.org/10.1002/lno.10119

Heisler, J., Glibert, P., Burkholder, J., Anderson, D., Cochlan, W., Dennison, W., … Suddleson, M. (2008). Eutrophication and Harmful Algal Blooms: A Scientific Consensus. *Harmful Algae*, *8*(1), 3–13. https://doi.org/10.1016/j.hal.2008.08.006

Howarth, R. W., Sharpley, A., & Walker, D. (2002). Sources of nutrient pollution to coastal waters in the United States: Implications for achieving coastal water quality goals. *Estuaries*, *25*(4), 656–676. https://doi.org/10.1007/BF02804898

Howarth, R. W., & Marino, R. (2006). Nitrogen as the limiting nutrient for eutrophication in coastal marine ecosystems: Evolving views over three decades. *Limnology and Oceanography*, *51*(1part2), 364–376. https://doi.org/10.4319/lo.2006.51.1_part_2.0364

Jickells, T. D. (1998). Nutrient Biogeochemistry of the Coastal Zone. *Science*, *281*(5374), 217–222. https://doi.org/10.1126/science.281.5374.217

Jephson, T., & Carlsson, P. (2009). Species- and stratification-dependent diel vertical migration behaviour of three dinoflagellate species in a laboratory study. *Journal of Plankton Research*, *31*(11), 1353–1362. https://doi.org/10.1093/plankt/fbp078

Kat, M. (1979). The occurrence of Prorocentrum species and coincidental gastrointestinal illness of mussel consumers. *Toxic Dinoflagellate Blooms*, 215–220.

Kelly, V., Heil, C., Seitzinger, S. P., Glibert, P. M., Codispoti, L. A., Parrow, M. W., & Burkholder, J. (2005). The Role of Eutrophication in the Global Proliferation of Harmful Algal Blooms. *Oceanography*. https://doi.org/10.5670/oceanog.2005.54

Kim, S., Kang, Y. G., Kim, H. S., Yih, W., Coats, D. W., & Park, M. G. (2008). Growth and grazing responses of the mixotrophic dinoflagellate Dinophysis acuminata as functions of light intensity and prey concentration. *Aquatic Microbial Ecology*, *51*(3), 301–310. https://doi.org/10.3354/ame01203

Kim, M., Nam, S. W., Shin, W., Coats, D. W., & Park, M. G. (2012). Dinophysis caudata (dinophyceae) sequesters and retains plastids from the mixotrophic ciliate prey mesodinium rubrum. *Journal of Phycology*, *48*(3), 569–579. https://doi.org/10.1111/j.1529-8817.2012.01150.x

Klöpper, S., Scharek, R., & Gerdts, G. (2003). Diarrhetic shellfish toxicity in relation to the abundance of Dinophysis spp. Ehrenberg 1839 in the German Bight near Helgoland. *Marine Ecology-Progress Series*, *259:*93–102.

Koike, K., Otobe, H., Takagi, M., Yoshida, T., Ogata, T., & Ishimaru, T. (2001). Recent Occurrences of Dinophysis fortii (Dinophyceae) in the Okkirai Bay, Sanriku, Northern Japan, and Related Environmental Factors. *Journal of Oceanography*, *57*, 165–175. https://doi.org/10.1023/A:1011191124025

Koukaras, K., & Nikolaidis, G. (2004). Dinophysis blooms in Greek coastal waters (Thermaikos Gulf, NW Aegean Sea). *Journal of Plankton Research*, *26*(4), 445–457. https://doi.org/10.1093/plankt/fbh042

Krogh, P., Edler, L., Granéli, E., & Nyman, U. (1985). *Outbreak of diarrheic shellfish poisoning on the west coast of Sweden*.

Krom, M. D., Herut, B., & Mantoura, R. F. C. (2004). Nutrient budget for the Eastern Mediterranean: Implications for phosphorus limitation. *Limnology and Oceanography*, *49*(5), 1582–1592. https://doi.org/10.4319/lo.2004.49.5.1582

Larsson, M. E., Ajani, P. A., Rubio, A. M., Guise, K., McPherson, R. G., Brett, S. J., … Doblin, M. A. (2017). Long-term perspective on the relationship between phytoplankton and nutrient concentrations in a southeastern Australian estuary. *Marine Pollution Bulletin*, *114*(1), 227–238. https://doi.org/10.1016/j.marpolbul.2016.09.011

Lelong, A., Hégaret, H., Soudant, P., & Bates, S. (2012). Pseudo-nitzschia (Bacillariophyceae) Species, Domoic Acid and Amnesic Shellfish Poisoning: Revisiting Previous Paradigms. *Phycologia*, *51*, 168–216. https://doi.org/10.2216/11-37.1

Lembeye, G. (1993). DSP outbreak in Chilean fjords. Toxic Phytoplankton blooms in the sea, 952: 525-529.

Manerio, E., Rodas, V. L., Costas, E., & Hernandez, J. M. (2008). Shellfish consumption: a major risk factor for colorectal cancer. *Medical Hypotheses*, *70*(2), 409–412. https://doi.org/10.1016/j.mehy.2007.03.041

McCarthy, S., Mohamedali, T., & Cracknell, P. (2018). Nitrogen in Puget Sound: A story map. *Salish Sea Ecosystem Conference*. Retrieved from https://cedar.wwu.edu/ssec/2018ssec/allsessions/431

Miles, C. O., Wilkins, A. L., Munday, R., Dines, M. H., Hawkes, A. D., Briggs, L. R., … Towers, N. R. (2004). Isolation of pectenotoxin-2 from Dinophysis acuta and its conversion to pectenotoxin-2 seco acid, and preliminary assessment of their acute toxicities. *Toxicon: Official Journal of the International Society on Toxinology*, *43*(1), 1–9. https://doi.org/10.1016/j.toxicon.2003.10.003

Moita, M. T., Pazos, Y., Rocha, C., Nolasco, R., & Oliveira, P. B. (2016). Toward predicting Dinophysis blooms off NW Iberia: A decade of events. *Harmful Algae*, *53*, 17–32. https://doi.org/10.1016/j.hal.2015.12.002

Murata, M., Shimatani, M., Sugitani, H., Oshima, Y., & Yasumoto, T. (1982). Isolation and Structural Elucidation of the Causative Toxin of the Diarrhetic Shellfish Poisoning. *Nippon Suisan Gakkaishi*, *48*(4), 549–552. https://doi.org/10.2331/suisan.48.549

Nagai, H., Satake, M., & Yasumoto, T. (1990). Antimicrobial activities of polyether compounds of dinoflagellate origins. *Journal of Applied Phycology*, *2*(4), 305–308. https://doi.org/10.1007/BF02180919

Nagai, S., Nitshitani, G., Tomaru, Y., Sakiyama, S., & Kamiyama, T. (2008). PREDATION BY THE TOXIC DINOFLAGELLATE DINOPHYSIS FORTII ON THE CILIATE MYRIONECTA RUBRA AND OBSERVATION OF SEQUESTRATION OF CILIATE CHLOROPLASTS(1). *Journal of Phycology*, *44*(4), 909–922. https://doi.org/10.1111/j.1529-8817.2008.00544.x

Nagai, S., Suzuki, T., Nishikawa, T., & Kamiyama, T. (2011). Differences in the Production and Excretion Kinetics of Okadaic Acid, Dinophysistoxin-1, and

Pectenotoxin-2 Between Cultures of Dinophysis Acuminata and Dinophysis Fortii Isolated from Western Japan1. *Journal of Phycology*, *47*(6), 1326–1337. https://doi.org/10.1111/j.1529-8817.2011.01076.x

Naustvoll, L.-J., Gustad, E., & Dahl, E. (2012). Monitoring of Dinophysis species and diarrhetic shellfish toxins in Flødevigen Bay, Norway: inter-annual variability over a 25-year time-series. *Food Additives & Contaminants. Part A, Chemistry, Analysis, Control, Exposure & Risk Assessment*, *29*(10), 1605–1615. https://doi.org/10.1080/19440049.2012.714908

Nielsen, L., Krock, B., & Hansen, P. (2012). Effects of light and food availability on toxin production, growth and photosynthesis in Dinophysis acuminata. *Marine Ecology-Progress Series, 471*. https://doi.org/10.3354/meps10027

Nielsen, L. T., Hansen, P. J., Krock, B., & Vismann, B. (2016). Accumulation, transformation and breakdown of DSP toxins from the toxic dinoflagellate Dinophysis acuta in blue mussels, Mytilus edulis. *Toxicon: Official Journal of the International Society on Toxinology*, *117*, 84–93. https://doi.org/10.1016/j.toxicon.2016.03.021

Nishitani, G., Nagai, S., Sakiyama, S., & Kamiyama, T. (2008). Successful cultivation of the toxic dinoflagellate Dinophysis caudata (Dinophyceae). *Plankton and Benthos Research*, *3*, 78–85. https://doi.org/10.3800/pbr.3.78

Officer, C., & Ryther, J. (1980). *The Possible Importance of Silicon in Marine Eutrophication*. https://doi.org/10.3354/meps003083

Pan, Y., Cembella, A. D., & Quilliam, M. A. (1999). Cell cycle and toxin production in the benthic dinoflagellate Prorocentrum lima. *Marine Biology*, *134*(3), 541–549. https://doi.org/10.1007/s002270050569

Park, M.G., Park, J. S., Kim, M., & Yih, W. (2007). Plastid retention and functionality in the dinoflagellates Dinophysis acuminata and Dinophysis caudata. *Journal of Phycology*, *43*, 7–8.

Park, Myung Gil, Kim, S., Kim, H. S., Myung, G., Kang, Y. G., & Yih, W. (2006). First successful culture of the marine dinoflagellate Dinophysis acuminata. *Aquatic Microbial Ecology*, *45*(2), 101–106. https://doi.org/10.3354/ame045101

Parson, T. (1984). *A Manual of Chemical & Biological Methods for Seawater Analysis*. https://doi.org/10.1016/C2009-0-07774-5

Pizarro, G., Paz, B., González-Gil, S., Franco, J. M., & Reguera, B. (2009). Seasonal variability of lipophilic toxins during a Dinophysis acuta bloom in Western Iberia: Differences between picked cells and plankton concentrates. *Harmful Algae*, *8*(6), 926–937. https://doi.org/10.1016/j.hal.2009.05.004

Prego-Faraldo, M. V., Valdiglesias, V., Méndez, J., & Eirín-López, J. M. (2013). Okadaic Acid Meet and Greet: An Insight into Detection Methods, Response Strategies and Genotoxic Effects in Marine Invertebrates. *Marine Drugs*, *11*(8), 2829–2845. https://doi.org/10.3390/md11082829

Rau, B. (2015). *Washington's Water Quality Management Plan to Control Nonpoint Sources of Pollution: Response to Comments*. 206.

Redfield, A. C. (1934). *On the Proportions of Organic Derivatives in Sea Water and Their Relation to the Composition of Plankton*. University Press of Liverpool.

Reguera, B., Riobó, P., Rodríguez, F., Díaz, P. A., Pizarro, G., Paz, B., … Blanco, J. (2014a). Dinophysis Toxins: Causative Organisms, Distribution and Fate in Shellfish. *Marine Drugs*, *12*(1), 394–461. https://doi.org/10.3390/md12010394

Reguera, B., Riobó, P., Rodríguez, F., Díaz, P. A., Pizarro, G., Paz, B., … Blanco, J. (2014b). Dinophysis Toxins: Causative Organisms, Distribution and Fate in Shellfish. *Marine Drugs*, *12*(1), 394–461. https://doi.org/10.3390/md12010394

Reguera, B., Velo-Suárez, L., Raine, R., & Park, M. G. (2012). Harmful Dinophysis species: A review. *Harmful Algae*, *14*, 87–106. https://doi.org/10.1016/j.hal.2011.10.016

Riisgaard, K., & Hansen, P. J. (2009). Role of food uptake for photosynthesis, growth and survival of the mixotrophic dinoflagellate Dinophysis acuminata. *Marine Ecology Progress Series*, *381*, 51–62. https://doi.org/10.3354/meps07953

Roberts, Pelletier, & Ahmed. (2015). *Deschutes River, Capitol Lake, and Budd Inlet Total Maximum Daily Load Study: Supplemental Modeling Scenarios*. Retrieved from https://fortress.wa.gov/ecy/publications/SummaryPages/1503002.html

Rossini. (2016, April 19). Harmful Algae and their Toxins: Progress, Paradoxes and. https://doi.org/10.1201/b16569-6

Sanders, R. W., Porter, K. G., & Caron, D. A. (1990). Relationship between Phototrophy and Phagotrophy in the Mixotrophic Chrysophyte Poterioochromonas malhamensis. *Microbial Ecology*, *19*(1), 97–109. Retrieved from JSTOR.

Seeyave, S., Probyn, T. A., Pitcher, G. C., Lucas, M. I., & Purdie, D. A. (2009). Nitrogen nutrition in assemblages dominated by Pseudo-nitzschia spp., Alexandrium catenella and Dinophysis acuminata off the west coast of South Africa. *Marine Ecology Progress Series*, *379*, 91–107. https://doi.org/10.3354/meps07898

Seitzinger, S., Harrison, J., Dumont, E. L., Beusen, A., & Bouwman, A. (2005). Sources and Delivery of Carbon, Nitrogen, and Phosphorus to the Coastal Zone: An Overview of Global Nutrient Export from Watersheds (NEWS) Models and Their Application. *Global Biogeochemical Cycles 19 (2005) GB4S01*, *19*. https://doi.org/10.1029/2005GB002606

Shumway, S. E., Burkholder, J. M., & Morton, S. L. (2018). *Harmful Algal Blooms: A Compendium Desk Reference*. John Wiley & Sons.

Simões, E., Vieira, R. C., Schramm, M. A., Mello, D. F., Pontinha, V. D. A., Silva, P. M. da, & Barracco, M. A. (2015). Impact of harmful algal blooms (Dinophysis acuminata) on the immune system of oysters and mussels from Santa Catarina, Brazil. *Journal of the Marine Biological Association of the United Kingdom*, *95*(4), 773–781. https://doi.org/10.1017/S0025315414001702

Singh, A., Hårding, K., Reddy, H. R. V., & Godhe, A. (2014). An assessment of Dinophysis blooms in the coastal Arabian Sea. *Harmful Algae*, *34*, 29–35. https://doi.org/10.1016/j.hal.2014.02.006

Skarlato, S., Filatova, N., Knyazev, N., Berdieva, M., & Telesh, I. (2018). Salinity stress response of the invasive dinoflagellate Prorocentrum minimum. *Estuarine, Coastal and Shelf Science*, *211*, 199–207. https://doi.org/10.1016/j.ecss.2017.07.007

Smayda, T. (1997). Harmful Algal Blooms: Their Ecophysiology and General Relevance to Phytoplankton Blooms in the Sea. *Limnology and Oceanography*, *42*. https://doi.org/10.4319/lo.1997.42.5_part_2.1137

Smith, J. L., Tong, M., Kulis, D., & Anderson, D. M. (2018). Effect of ciliate strain, size, and nutritional content on the growth and toxicity of mixotrophic Dinophysis acuminata. *Harmful Algae*, *78*, 95–105. https://doi.org/10.1016/j.hal.2018.08.001

SoundToxins. (2018). Harmful Algal Bloom Monitoring Data for Puget Sound—SoundToxins: Partnership for Enhanced Monitoring and Emergency Response to Harmful Algal Blooms in Puget Sound—Data.gov. Retrieved December 19, 2019, from https://catalog.data.gov/dataset/harmful-algal-bloom-monitoring-data-for-puget-sound-soundtoxins-partnership-for-enhanced-monitor

Swanson, K. M., Flewelling, L. J., Byrd, M., Nunez, A., & Villareal, T. A. (2010). The 2008 Texas Dinophysis ovum bloom: Distribution and toxicity. *Harmful Algae*, *9*(2), 190–199. https://doi.org/10.1016/j.hal.2009.10.001

Tachibana, K., Scheuer, P. J., Tsukitani, Y., Kikuchi, H., Van Engen, D., Clardy, J., … Schmitz, F. J. (1981). Okadaic acid, a cytotoxic polyether from two marine sponges of the genus Halichondria. *Journal of the American Chemical Society*, *103*(9), 2469–2471. https://doi.org/10.1021/ja00399a082

Terao, K., Ito, E., Yanagi, T., & Yasumoto, T. (1986). Histopathological studies on experimental marine toxin poisoning. I. Ultrastructural changes in the small intestine and liver of suckling mice induced by dinophysistoxin-1 and pectenotoxin-1. *Toxicon: Official*

Journal of the International Society on Toxinology, *24*(11–12), 1141–1151. https://doi.org/10.1016/0041-0101(86)90140-6

Tilman, D. (1977a). Resource Competition between Plankton Algae: An Experimental and Theoretical Approach. *Ecology*, *58*(2), 338–348. https://doi.org/10.2307/1935608

Tilman, D. (1977b). Resource Competition between Plankton Algae: An Experimental and Theoretical Approach. *Ecology*, *58*(2), 338–348. https://doi.org/10.2307/1935608

Tong, M., Kulis, D. M., Fux, E., Smith, J. L., Hess, P., Zhou, Q., & Anderson, D. M. (2011). The effects of growth phase and light intensity on toxin production by Dinophysis acuminata from the northeastern United States. *Harmful Algae, 10*(3), 254–264. https://doi.org/10.1016/j.hal.2010.10.005

Tong, M., Smith, J. L., Kulis, D. M., & Anderson, D. M. (2015). Role of dissolved nitrate and phosphate in isolates of Mesodinium rubrum and toxin-producing Dinophysis acuminata. *Aquatic Microbial Ecology : International Journal*, *75*(2), 169–185. https://doi.org/10.3354/ame01757

Tong, M., Smith, J. L., Richlen, M., Steidinger, K. A., Kulis, D. M., Fux, E., & Anderson, D. M. (2015). Characterization and comparison of toxin-producing isolates of Dinophysis acuminate from New England and Canada1. *Journal of Phycology*, *51*(1), 66–81. https://doi.org/10.1111/jpy.12251

Torgersen, T., Aasen, J., & Aune, T. (2005). Diarrhetic shellfish poisoning by okadaic acid esters from Brown crabs (Cancer pagurus) in Norway. *Toxicon: Official*

Journal of the International Society on Toxinology, *46*(5), 572–578. https://doi.org/10.1016/j.toxicon.2005.06.024

Trainer, V. L., Eberhart, B.-T. L., Wekell, J. C., Adams, N. G., Hanson, L., Cox, F., & Dowell, J. (2003). Paralytic shellfish toxins in Puget Sound, Washington State. *Journal of Shellfish Research*, *22*, 213–223.

Trainer, V. L., Moore, L., Bill, B. D., Adams, N. G., Harrington, N., Borchert, J., … Eberhart, B.-T. L. (2013). Diarrhetic Shellfish Toxins and Other Lipophilic Toxins of Human Health Concern in Washington State. *Marine Drugs*, *11*(6), 1815–1835. https://doi.org/10.3390/md11061815

Trainer, V. (2019, March 15). Personal interview.

Underdal, B., Yndestad, M., & Aune, T. (1985). *DSP intoxication in Norway and Sweden, autumn 1984-spring 1985*. Presented at the 3. International Conference on Toxic Dinoflagellates, St. Andrews, New Brunswick (Canada), 8-12 Jun 1985. Retrieved from http://agris.fao.org/agris-search/search.do?recordID=US8644422

Vale, P., & Sampayo, M. A. de M. (2003). Seasonality of diarrhetic shellfish poisoning at a coastal lagoon in Portugal: Rainfall patterns and folk wisdom. *Toxicon*, *41*(2), 187–197. https://doi.org/10.1016/S0041-0101(02)00276-3

Vanucci, S., Guerrini, F., Milandri, A., & Pistocchi, R. (2010). Effects of different levels of N- and P-deficiency on cell yield, okadaic acid, DTX-1, protein and carbohydrate dynamics in the benthic dinoflagellate Prorocentrum lima. *Harmful Algae*, *9*(6), 590–599. https://doi.org/10.1016/j.hal.2010.04.009

Vardi, A., Formiggini, F., Casotti, R., Martino, A. D., Ribalet, F., Miralto, A., & Bowler, C. (2006). A Stress Surveillance System Based on Calcium and Nitric Oxide in Marine Diatoms. *PLOS Biology*, *4*(3), e60. https://doi.org/10.1371/journal.pbio.0040060

Velo-Suárez, L., González-Gil, S., Pazos, Y., & Reguera, B. (2014). The growth season of Dinophysis acuminata in an upwelling system embayment: A conceptual model based on in situ measurements. *Deep Sea Research Part II: Topical Studies in Oceanography*, *101*, 141–151. https://doi.org/10.1016/j.dsr2.2013.03.033

Vlamis, Aristeidis, & Katikou, P. (2014). Climate influence on Dinophysis spp. Spatial and temporal distributions in Greek coastal water. *Plankton and Benthos Research*, *9*, 15–31. https://doi.org/10.3800/pbr.9.15

Vlamis, Aristidis, & Katikou, P. (2014). *Climate influence on Dinophysis spp. Spatial and temporal distributions in Greek coastal water*. https://doi.org/10.3800/pbr.9.15

Wells, M. L., Trainer, V. L., Smayda, T. J., Karlson, B. S. O., Trick, C. G., Kudela, R. M., … Cochlan, W. P. (2015). Harmful algal blooms and climate change: Learning from the past and present to forecast the future. *Harmful Algae*, *49*, 68–93. https://doi.org/10.1016/j.hal.2015.07.009

Wisecaver, J. H., & Hackett, J. D. (2010). Transcriptome analysis reveals nuclear-encoded proteins for the maintenance of temporary plastids in the dinoflagellate Dinophysis acuminata. *BMC Genomics*, *11*, 366. https://doi.org/10.1186/1471-2164-11-366

Xu, J., Ho, A. Y. T., Yin, K., Yuan, X., Anderson, D. M., Lee, J. H. W., & Harrison, P. J. (2008). Temporal and spatial variations in nutrient stoichiometry and regulation of phytoplankton biomass in Hong Kong waters: Influence of the Pearl River outflow and sewage inputs. *Marine Pollution Bulletin*, *57*(6–12), 335–348. https://doi.org/10.1016/j.marpolbul.2008.01.020

Yasumoto, T., Oshima, Y., Sugawara, W., Fukuyo, Y., Oguri, H., Igarashi, T., & Fujita, N. (1980). Identification of *Dinophysis fortii* as the Causative Organism of Diarrhetic Shellfish Poisoning. *Nippon Suisan Gakkaishi*, *46*(11), 1405–1411. https://doi.org/10.2331/suisan.46.1405

Yasumoto, T., Oshima, Y., & Yamaguchi, M. (1978). Occurrence of a New Type of Shellfish Poisoning in the Tohoku District. *Nippon Suisan Gakkaishi*, *44*(11), 1249–1255. https://doi.org/10.2331/suisan.44.1249

Yasumoto, T., Oshima, Y., & Yamaguchi, M. (1979). Occurrence of new type of toxic shellfish in Japan and chemical properties of the toxin. *Developments in Marine Biology*. Presented at the International Conference on Toxic Dinoflagellate Blooms. Key Biscayne, Florida, 1978. Retrieved from http://agris.fao.org/agris-search/search.do?recordID=US201301338051

Yin, K., Qian, P.-Y., Wu, M. C. S., Chen, J. C., Huang, L., Song, X., & Jian, W. (2001). Shift from P to N limitation of phytoplankton growth across the Pearl River estuarine plume during summer. *Marine Ecology Progress Series*, *221*, 17–28. https://doi.org/10.3354/meps221017

APPENDICES

Appendix A: Species Composition Supporting Data

LEGEND	
Abbreviations	**Relative abduance and Community Structure**
"+++"	Abundant
"++"	Common
"+"	Rare
"X"	Present
"Diatom Dom"	Diatom Dominant Community
"Mixed Assemblage"	Mixed Assemblage of Diatoms & Dinoflagellates
"Dinoflagellate Dom"	Dinoflagellate Dominant Community

North Point Landing (estuary head)

Season	Winter			
Month	January		February	
Sampling Dates	1/13/19	1/23/19	2/6/19	2/20/19
Assemblage (Diatom dom, Dinoflagellate dom, or Mixed)	Mixed	Diatom Dom	Diatom Dom	Diatom Dom
Dominant Genus or Species	*Thalassiosira rotula*	*Skeletonema costatum*	*Skeletonema costatum*	*Thalassiosira rotula*
Dinophysis norvegica	X+	X+	X+	
Dinophysis fortii	X+	X+	X+	X+
Dinophysis acuminata		X+		
Akashiwo sanguinea	X+++	X+		
Pseudo-nitzschia spp.	X++	X+	X+	X+
Chaetoceros decipens	X++	X++	X++	
Chaetoceros debilis	X++	X++	X++	X++
Ditylum brightwellii	X+	X+	X+	X+
Coscinodiscus curvatulus	X+++		X+	X++
Thalassiosira rotula	X+++			X+++
Protoperidinium conicum	X+++	X+	X+	
Asteromphalus heptactis	X+			
Thalassionema nitzschiodes	X+	X+	X+	X+
Navicula spp.	X+		X+	X+
Skeletonema costatum	X++	X+++	X+++	
Ceratium fusus	X+			X++
Oxyphysis oxytoxoides	X+		X+	
Pleurosigma spp.	X+			
Chaetoceros danicus		X+++	X++	
Coscinodiscus centralis		X++		
Thalassiosira punctigera		X+		
Gyrosigma sp.		X+		
Cylindrotheca closterium		X+	X+	
Asterionella formosa		X+		
Leptocylindrus danicus		X+		
Lauderia annulata		X+		
Bacterstatium sp.		X+		
Heterosigma heterocapsa		X+		
Chaetoceros didymus			X++	
Stephanopyxis palmeriana				
Thalassiosira anguste-lineata				
Asterionella formosa			X+	
Dictoycha fibula			X+	
Eucampia zodiacus			X+	
Detonula pumila			X+	
Protoperidinium stenii				
Chaetoceros similis				
Corymbellus aurens				
Thalassiosira pacifica/nordenskioeldii				
Nitzschia acicularis				
Protoperidinium leonis				
Alexandrium catenalla				
Scripsiella trochoidea				
Protoperidinium c.f. brevipes				
Leptocylindrus minimus				
Actinoptychus senarius				
Protoperidinium excentricum				
Chaetoceros teres				
Polykrikos shwartzii				
Odontella longicruis				
Chaetoceros diadema				
Rhizosolenia setigera				
Protoperidinium oblongum				
Pyrophaus horologinium				
Heterocapsa c.f. triquetra				
Protoperidinium depressum				
Melosira monolopsis				
Licomorpha spp.				
Unk 1-highly scilaceous transparent, solitary or stacked (2+ cells)				
Dinophysis rotundata				
Fragilaria striatula				
Noctiluca scintillans				
Thalassiosira eccentrica				
Odontella aurita				
Protoceratium reticulatum				
Alexandrium c.f. tamarense				
Dinophysis odiosa				
Chaetoceros lorenzianus				

Season				
Month	March			
Sampling Dates	3/6/19	3/13/19	3/20/19	3/27/19
Assemblage (Diatom dom, Dinoflagellate dom, or Mixed)	Diatom Dom	Diatom Dom	Diatom Dom	Diatom Dom
Dominant Genus or Species	*Thalassiosira rotula*	*Thalassiosira rotula*	*Thalassiosira spp.*	*Chaetoceros debilis (bloom)*
Dinophysis norvegica				
Dinophysis fortii				
Dinophysis acuminata				
Akashiwo sanguinea				
Pseudo-nitzschia spp.	X+	X++		
Chaetoceros decipens	X++			X++
Chaetoceros debilis	X++	X++	X++	X+++
Ditylum brightwellii	X+			X+
Coscinodiscus curvatulus				
Thalassiosira rotula	X+++	X+++	X++	X++
Protoperidinium conicum				
Asteromphalus heptactis			X++	
Thalassionema nitzschiodes	X++	X+		X+
Navicula spp.	X+			
Skeletonema costatum	X++		X++	X+++
Ceratium fusus				
Oxyphysis oxytoxoides				
Pleurosigma spp.				
Chaetoceros danicus		X+		
Coscinodiscus centralis				
Thalassiosira punctigera	X+			
Gyrosigma sp.	X+			
Cylindrotheca closterium			X+	
Asterionella formosa				
Leptocylindrus danicus				
Lauderia annulata				
Bacterstatium sp.				
Heterosigma heterocapsa				
Chaetoceros didymus				X+
Stephanopyxis palmeriana			X++	X+
Thalassiosira anguste-lineata		X+	X+	
Asterionella formosa	X+			X+
Dictoycha fibula				
Eucampia zodiacus				
Detonula pumila	X+	X+	X++	
Protoperidinium stenii		X+		
Chaetoceros similis		X++		
Corymbellus aurens		X+		
Thalassiosira pacifica/nordenskioeldii		X++		
Nitzschia acicularis			X+	X+
Protoperidinium leonis				X+
Alexandrium catenalla				X+
Scripsiella trochoidea				X+
Protoperidinium c.f. brevipes				
Leptocylindrus minimus				
Actinoptychus senarius				
Protoperidium excentricum				
Chaetoceros teres				
Polykrikos shwartzii				
Odontella longicruis				
Chaetoceros diadema				
Rhizosolenia setigera				
Protoperidinium oblongum				
Pyrophaus horologinium				
Heterocapsa c.f. triquetra				
Protoperidinium depressum				
Melosira monolopsis				
Licomorpha spp.				
Unk 1-highly scilaceous transparent, solitary or stacked (2+ cells)				
Dinophysis rotundata				
Fragilaria striatula				
Noctiluca scintillans				
Thalassiosira eccentrica				
Odontella aurita				
Protoceratium reticulatum				
Alexandrium c.f. tamarense				
Dinophysis odiosa				
Chaetoceros lorenzianus				

Season	Spring			
Month	April			
Sampling Dates	4/3/19	4/10/19	4/18/19	4/24/19
Assemblage (Diatom dom, Dinoflagellate dom, or Mixed)	Diatom dom	Diatom dom	Diatom dom	Diatom dom
Dominant Genus or Species	*Chaetoceros debilis (bloom)*	*Chaetoceros debilis (bloom)*	*Chaetoceros debilis (bloom)*	*Thalassiosira rotula*
Dinophysis norvegica				
Dinophysis fortii				
Dinophysis acuminata				
Akashiwo sanguinea				
Pseudo-nitzschia spp.				
Chaetoceros decipens			X+++	
Chaetoceros debilis	X+++	X+++	X+++	
Ditylum brightwellii				
Coscinodiscus curvatulus				
Thalassiosira rotula	X++	X++	X++	X++
Protoperidinium conicum				
Asteromphalus heptactis				
Thalassionema nitzschiodes			X+	
Navicula spp.				
Skeletonema costatum	X++			
Ceratium fusus				
Oxyphysis oxytoxoides				
Pleurosigma spp.	X+	X+	X+	
Chaetoceros danicus	X+			
Coscinodiscus centralis				
Thalassiosira punctigera				
Gyrosigma sp.				
Cylindrotheca closterium				
Asterionella formosa				
Leptocylindrus danicus				
Lauderia annulata				
Bacterstatium sp.				
Heterosigma heterocapsa				
Chaetoceros didymus	X+			
Stephanopyxis palmeriana	X++	X+		
Thalassiosira anguste-lineata				
Asterionella formosa				
Dictyocha fibula				
Eucampia zodiacus				
Detonula pumila				
Protoperidinium stenii				
Chaetoceros similis				
Corymbellus aurens				
Thalassiosira pacifica/nordenskioeldii				
Nitzschia acicularis				
Protoperidinium leonis				
Alexandrium catenalla				
Scripsiella trochoidea				
Protoperidinium c.f. brevipes				
Leptocylindrus minimus	X++	X+		
Actinoptychus senarius	X+			
Protoperidium excentricum				
Chaetoceros teres			X+	
Polykrikos shwartzii			X+	
Odontella longicruis				
Chaetoceros diadema				
Rhizosolenia setigera				
Protoperidinium oblongum				
Pyrophaus horologinium				
Heterocapsa c.f. triquetra				
Protoperidinium depressum				
Melosira monolopsis				
Licomorpha spp.				
Unk 1-highly scilaceous transparent, solitary or stacked (2+ cells)				
Dinophysis rotundata				
Fragilaria striatula				
Noctiluca scintillans				
Thalassiosira eccentrica				
Odontella aurita				
Protoceratium reticulatum				
Alexandrium c.f. tamarense				
Dinophysis odiosa				
Chaetoceros lorenzianus				

Season				
Month	May			
Sampling Dates	5/2/19	5/9/19	5/15/19	5/23/19
Assemblage (Diatom dom, Dinoflagellate dom, or Mixed)	Diatom dom	Diatom dom	Diatom dom	Mixed
Dominant Genus or Species	*Psuedo-nitzschia spp (bloom)*	*Psuedo-nitzschia spp (bloom)*	*Rhizosolenia setigeta (bloom)*	*Dinophysis and Rhizolenia spp (bloom)*
Dinophysis norvegica		X+	X+	X+++
Dinophysis fortii				
Dinophysis acuminata				
Akashiwo sanguinea				
Pseudo-nitzschia spp.	X+++	X+++		X++
Chaetoceros decipens			X++	
Chaetoceros debilis				
Ditylum brightwellii				
Coscinodiscus curvatulus				
Thalassiosira rotula				
Protoperidinium conicum				
Asteromphalus heptactis				
Thalassionema nitzschiodes				
Navicula spp.				
Skeletonema costatum		X+	X+	
Ceratium fusus				X+
Oxyphysis oxytoxoides				
Pleurosigma spp.	X+			
Chaetoceros danicus	X+			X+
Coscinodiscus centralis				
Thalassiosira punctigera				
Gyrosigma sp.				
Cylindrotheca closterium				
Asterionella formosa				
Leptocylindrus danicus	X+		X+	
Lauderia annulata				
Bacterstatium sp.				
Heterosigma heterocapsa				
Chaetoceros didymus				
Stephanopyxis palmeriana	X+			
Thalassiosira anguste-lineata				
Asterionella formosa				
Dictoycha fibula				
Eucampia zodiacus				
Detonula pumila				
Protoperidinium stenii				
Chaetoceros similis				
Corymbellus aurens			X+	X+
Thalassiosira pacifica/nordenskioeldii				
Nitzschia acicularis				
Protoperidinium leonis		X+		
Alexandrium catenalla				
Scripsiella trochoidea				X+
Protoperidinium c.f. brevipes				
Leptocylindrus minimus				
Actinoptychus senarius	X++	X++	X++	X++
Protoperidium excentricum				
Chaetoceros teres				
Polykrikos shwartzii				
Odontella longicruis	X++			
Chaetoceros diadema	X+			
Rhizosolenia setigera			X+++	X+++
Protoperidinium oblongum			X+	
Pyrophaus horologinium				
Heterocapsa c.f. triquetra				X+
Protoperidinium depressum				
Melosira monolopsis				
Licomorpha spp.				
Unk 1-highly scilaceous transparent, solitary or stacked (2+ cells)				
Dinophysis rotundata				
Fragilaria striatula				
Noctiluca scintillans				
Thalassiosira eccentrica				
Odontella aurita				
Protoceratium reticulatum				
Alexandrium c.f. tamarense				
Dinophysis odiosa				
Chaetoceros lorenzianus				

Season				
Month	June			
Sampling Dates	6/1/19	6/6/19	6/9/19	6/17/19
Assemblage (Diatom dom, Dinoflagellate dom, or Mixed)	Diatom dom	Dinoflagellate dom	Dinoflagellate dom	Dinoflagellate dom
Dominant Genus or Species	*Psuedo-nitzschia spp (bloom)*	*Dinophysis norvegica (bloom)*	*Dinophysis norvegica (bloom)*	*Dinophysis norvegica (bloom)*
Dinophysis norvegica		X+++	X+++	X+++
Dinophysis fortii			X+	X+
Dinophysis acuminata				X+
Akashiwo sanguinea				X++
Pseudo-nitzschia spp.	X+++	X++	X++	
Chaetoceros decipens				
Chaetoceros debilis				
Ditylum brightwellii			X+	
Coscinodiscus curvatulus				
Thalassiosira rotula			X++	X++
Protoperidinium conicum		X+		
Asteromphalus heptactis				
Thalassionema nitzschiodes				
Navicula spp.				
Skeletonema costatum				
Ceratium fusus		X+	X+	
Oxyphysis oxytoxoides				
Pleurosigma spp.				X+
Chaetoceros danicus				
Coscinodiscus centralis				
Thalassiosira punctigera				
Gyrosigma sp.				
Cylindrotheca closterium				
Asterionella formosa				X+
Leptocylindrus danicus				
Lauderia annulata				
Bacterstatium sp.				
Heterosigma heterocapsa				
Chaetoceros didymus				
Stephanopyxis palmeriana				
Thalassiosira anguste-lineata				
Asterionella formosa				
Dictoycha fibula				
Eucampia zodiacus				
Detonula pumila				
Protoperidinium stenii				
Chaetoceros similis				
Corymbellus aurens				
Thalassiosira pacifica/nordenskioeldii				
Nitzschia acicularis				
Protoperidinium leonis	X+		X+	
Alexandrium catenalla				
Scripsiella trochoidea	X++	X+	X+	
Protoperidinium c.f. brevipes				
Leptocylindrus minimus				
Actinoptychus senarius				X+
Protoperidium excentricum		X+	X++	
Chaetoceros teres				
Polykrikos shwartzii				
Odontella longicruis				
Chaetoceros diadema				
Rhizosolenia setigera	X+			
Protoperidinium oblongum	X+	X+	X+	
Pyrophaus horologinium			X+	
Heterocapsa c.f. triquetra				
Protoperidinium depressum			X+	X+
Melosira monolopsis			X+	
Licomorpha spp.			X+	
Unk 1-highly scilaceous transparent, solitary or stacked (2+ cells)			X+	X+
Dinophysis rotundata				
Fragilaria striatula				
Noctiluca scintillans				
Thalassiosira eccentrica				
Odontella aurita				
Protoceratium reticulatum				
Alexandrium c.f. tamarense				
Dinophysis odiosa				
Chaetoceros lorenzianus				

Season	Summer			
Month		July		
Sampling Dates	6/23/19	7/2/19	7/11/19	7/18/19
Assemblage (Diatom dom, Dinoflagellate dom, or Mixed)	Dinoflagellate dom	Dinoflagellate dom	Mixed assemblage	Dinoflagellate dom
Dominant Genus or Species	*Dinophysis norvegica (bloom)*	*Ceratium fusus (bloom)*	*Ceratium & Thalassiosira*	*Ceratium fusus (bloom)*
Dinophysis norvegica	X+++	X++	X+	X+
Dinophysis fortii	X+	X+		
Dinophysis acuminata	X+			
Akashiwo sanguinea				
Pseudo-nitzschia spp.				
Chaetoceros decipens				
Chaetoceros debilis				X+++
Ditylum brightwellii	X+	X+	X+	
Coscinodiscus curvatulus				
Thalassiosira rotula				
Protoperidinium conicum		X+		
Asteromphalus heptactis		X+	X+	
Thalassionema nitzschiodes				
Navicula spp.				
Skeletonema costatum			X+	
Ceratium fusus	X++	X+++	X+++	X+++
Oxyphysis oxytoxoides				
Pleurosigma spp.				X+
Chaetoceros danicus		X++		X+
Coscinodiscus centralis				
Thalassiosira punctigera		X+		
Gyrosigma sp.				
Cylindrotheca closterium				
Asterionella formosa				
Leptocylindrus danicus				
Lauderia annulata				
Bacterstatium sp.				
Heterosigma heterocapsa				
Chaetoceros didymus				
Stephanopyxis palmeriana				
Thalassiosira anguste-lineata				
Asterionella formosa				
Dictoycha fibula				
Eucampia zodiacus				
Detonula pumila				
Protoperidinium stenii		X+	X+	X+
Chaetoceros similis				
Corymbellus aurens				
Thalassiosira pacifica/nordenskioeldii				
Nitzschia acicularis				
Protoperidinium leonis				
Alexandrium catenalla		X+		
Scripsiella trochoidea		X+		X+
Protoperidinium c.f. brevipes				
Leptocylindrus minimus				
Actinoptychus senarius				
Protoperidium excentricum	X+			
Chaetoceros teres				
Polykrikos shwartzii				
Odontella longicruis				
Chaetoceros diadema				
Rhizosolenia setigera				
Protoperidinium oblongum				
Pyrophaus horologinium				
Heterocapsa c.f. triquetra				
Protoperidinium depressum				
Melosira monolopsis			X+	
Licomorpha spp.	X+	X+	X+	
Unk 1-highly scilaceous transparent, solitary or stacked (2+ cells)	X+			
Dinophysis rotundata				X+
Fragilaria striatula	X+			X+
Noctiluca scintillans	X+		X+	
Thalassiosira eccentrica	X+++			
Odontella aurita			X+	
Protoceratium reticulatum				X++
Alexandrium c.f. tamarense				
Dinophysis odiosa				
Chaetoceros lorenzianus				

Season				
Month		August		
Sampling Dates	7/24/19	8/1/19	8/7/19	8/13/19
Assemblage (Diatom dom, Dinoflagellate dom, or Mixed)	Dinoflagellate dom	Dinoflagellate dom	Dinoflagellate dom	Dinoflagellate dom
Dominant Genus or Species	*Ceratium fusus (bloom)*	*Ceratium fusus (bloom)*	*Ceratium fusus (bloom)*	*Ceratium fusus (bloom)*
Dinophysis norvegica	X++	X+	X+	X+
Dinophysis fortii		X+		X+
Dinophysis acuminata				X+
Akashiwo sanguinea			X+	X+
Pseudo-nitzschia spp.				
Chaetoceros decipens				
Chaetoceros debilis	X++		X++	
Ditylum brightwellii	X+		X+	X+
Coscinodiscus curvatulus				
Thalassiosira rotula				
Protoperidinium conicum	X+	X+	X+	
Asteromphalus heptactis		X+		
Thalassionema nitzschiodes				
Navicula spp.				
Skeletonema costatum		X+	X+	
Ceratium fusus	X+++	X+++	X+++	X+++
Oxyphysis oxytoxoides				
Pleurosigma spp.			X+	
Chaetoceros danicus				
Coscinodiscus centralis	X+			X+
Thalassiosira punctigera				
Gyrosigma sp.				
Cylindrotheca closterium				
Asterionella formosa				
Leptocylindrus danicus				
Lauderia annulata				
Bacterstatium sp.				
Heterosigma heterocapsa				
Chaetoceros didymus				
Stephanopyxis palmeriana				
Thalassiosira anguste-lineata				
Asterionella formosa				
Dictoycha fibula				
Eucampia zodiacus				
Detonula pumila				
Protoperidinium stenii				
Chaetoceros similis			X+	
Corymbellus aurens				
Thalassiosira pacifica/nordenskioeldii				
Nitzschia acicularis				
Protoperidinium leonis				X+
Alexandrium catenalla				
Scripsiella trochoidea				X+
Protoperidinium c.f. brevipes				
Leptocylindrus minimus				
Actinoptychus senarius				
Protoperidium excentricum				
Chaetoceros teres				
Polykrikos shwartzii				
Odontella longicruis				
Chaetoceros diadema				
Rhizosolenia setigera				
Protoperidinium oblongum				
Pyrophaus horologinium				
Heterocapsa c.f. triquetra				
Protoperidinium depressum				
Melosira monolopsis				
Licomorpha spp.		X+		X+
Unk 1-highly scilaceous transparent, solitary or stacked (2+ cells)				
Dinophysis rotundata				
Fragilaria striatula				
Noctiluca scintillans	X+	X+	X+	X+
Thalassiosira eccentrica	X++	X+	X+	
Odontella aurita				
Protoceratium reticulatum	X+	X+	X+	X++
Alexandrium c.f. tamarense			X+	
Dinophysis odiosa		X+		
Chaetoceros lorenzianus				

Season		
Month		
Sampling Dates	8/21/19	8/31/19
Assemblage (Diatom dom, Dinoflagellate dom, or Mixed)	Dinoflagellate dom	Mixed assemblage
Dominant Genus or Species	*Ceratium fusus (bloom)*	*Ceratium fusus*
Dinophysis norvegica		X+
Dinophysis fortii		X+
Dinophysis acuminata		
Akashiwo sanguinea		
Pseudo-nitzschia spp.		
Chaetoceros decipens		
Chaetoceros debilis		X++
Ditylum brightwellii		
Coscinodiscus curvatulus		
Thalassiosira rotula		X++
Protoperidinium conicum	X+	X+
Asteromphalus heptactis		
Thalassionema nitzschiodes		X+
Navicula spp.		
Skeletonema costatum		X++
Ceratium fusus	X+++	X+++
Oxyphysis oxytoxoides		
Pleurosigma spp.	X+	X+
Chaetoceros danicus		
Coscinodiscus centralis		X+
Thalassiosira punctigera		
Gyrosigma sp.		
Cylindrotheca closterium		
Asterionella formosa		
Leptocylindrus danicus		
Lauderia annulata		
Bacterstatium sp.		
Heterosigma heterocapsa		
Chaetoceros didymus		
Stephanopyxis palmeriana	X+	
Thalassiosira anguste-lineata		X++
Asterionella formosa		
Dictoycha fibula		
Eucampia zodiacus		
Detonula pumila		
Protoperidinium stenii	X+	
Chaetoceros similis		
Corymbellus aurens		
Thalassiosira pacifica/nordenskioeldii		
Nitzschia acicularis		
Protoperidinium leonis		X+
Alexandrium catenalla		
Scripsiella trochoidea		X++
Protoperidinium c.f. brevipes		
Leptocylindrus minimus		
Actinoptychus senarius		
Protoperidium excentricum		X+
Chaetoceros teres		
Polykrikos shwartzii		
Odontella longicruis		
Chaetoceros diadema		
Rhizosolenia setigera		
Protoperidinium oblongum		
Pyrophaus horologinium		
Heterocapsa c.f. triquetra		
Protoperidinium depressum		
Melosira monolopsis		X+
Licomorpha spp.		
Unk 1-highly scilaceous transparent, solitary or stacked (2+ cells)		
Dinophysis rotundata		
Fragilaria striatula		
Noctiluca scintillans	X+	X+
Thalassiosira eccentrica		X++
Odontella aurita		
Protoceratium reticulatum	X+	
Alexandrium c.f. tamarense		X+
Dinophysis odiosa		
Chaetoceros lorenzianus		

Season	Fall			
Month	September			October
Sampling Dates	9/7/19	9/13/19	9/23/19	10/2/19
Assemblage (Diatom dom, Dinoflagellate dom, or Mixed)	Dinoflagellate dom	Dinoflagellate dom	Dinoflagellate dom	Dinoflagellate dom
Dominant Genus or Species	*Akashiwo sanguinea(bloom)*	*Ceratium fusus*	*Ceratium fusus (bloom)*	*Ceratium fusus*
Dinophysis norvegica			X+	X+
Dinophysis fortii		X++	X+	
Dinophysis acuminata			X+	
Akashiwo sanguinea	X+++	X+	X+	X+
Pseudo-nitzschia spp.				
Chaetoceros decipens				
Chaetoceros debilis	X++	X++	X++	X++
Ditylum brightwellii	X+	X+		X+
Coscinodiscus curvatulus				
Thalassiosira rotula			X++	
Protoperidinium conicum	X+	X+	X+	X+
Asteromphalus heptactis				
Thalassionema nitzschiodes				
Navicula spp.				
Skeletonema costatum	X+	X+	X+	
Ceratium fusus	X++	X+++	X+++	X+++
Oxyphysis oxytoxoides			X+	
Pleurosigma spp.			X+	
Chaetoceros danicus			X+	
Coscinodiscus centralis		X+		
Thalassiosira punctigera		X+	X+	
Gyrosigma sp.				
Cylindrotheca closterium				
Asterionella formosa				
Leptocylindrus danicus				
Lauderia annulata				
Bacterstatium sp.				
Heterosigma heterocapsa				
Chaetoceros didymus				
Stephanopyxis palmeriana				
Thalassiosira anguste-lineata	X+	X+		
Asterionella formosa				
Dictoycha fibula				
Eucampia zodiacus	X+			
Detonula pumila				X+
Protoperidinium stenii		X+	X+	X+
Chaetoceros similis				
Corymbellus aurens				
Thalassiosira pacifica/nordenskioeldii				
Nitzschia acicularis				X+
Protoperidinium leonis				
Alexandrium catenalla	X+			
Scripsiella trochoidea				
Protoperidinium c.f. brevipes				
Leptocylindrus minimus				X+
Actinoptychus senarius				X+
Protoperidium excentricum				
Chaetoceros teres				
Polykrikos shwartzii				
Odontella longicruis				
Chaetoceros diadema				
Rhizosolenia setigera				
Protoperidinium oblongum				
Pyrophaus horologinium				
Heterocapsa c.f. triquetra				X+
Protoperidinium depressum	X+			
Melosira monolopsis			X+	
Licomorpha spp.				
Unk 1-highly scilaceous transparent, solitary or stacked (2+ cells)				
Dinophysis rotundata				
Fragilaria striatula				
Noctiluca scintillans	X+			X+
Thalassiosira eccentrica	X+			X+
Odontella aurita				
Protoceratium reticulatum				
Alexandrium c.f. tamarense				X++
Dinophysis odiosa				
Chaetoceros lorenzianus				X+

Boston Harbor Marin (estuary mouth)

Season	Winter		
Month	January		February
Sampling Dates	1/13/19	1/23/19	2/6/19
Assemblage (Diatom dom, Dinoflagellate dom, or mixed)	Diatom Dom	Diatom Dom	Diatom Dom
Dominant Genus or Species	*Chaetoceros debilis*	*Chaetoceros debilis*	*Skeletonema costatum*
Dinophysis norvegica			
Dinophysis fortii	X+	X+	X+
Dinophysis acuminata	X+	X+	X+
Akashiwo sanguinea	X+	X+	
Thalassiosira anguste-lineata	X+	X+	
Chaetoceros decipens	X+		X++
Chaetoceros debilis	X+++	X+++	X++
Ditylum brightwellii	X+++		
Coscinodiscus c.f. curvatulus	X+		
Thalassiosira rotula	X++	X+	
Protoperidinium conicum	X++	X+	
Asteromphalus heptactis	X+	X+	
Thalassionema nitzschiodes	X+	X++	
Navicula spp.	X++	X+	X+
Skeletonema costatum	X++	X++	X+++
Dictyocha fibula	X+	X+	X+
Protocentrum micans	X+	X+++	
Chaetoceros danicus	X+	X++	
Pseudo-nitzschia spp.		X++	X++
Thalassoisira punctigera		X+	X++
Coscinodiscus centralis		X+	
Ceratium fusus		X+	
Gyrosigma spp.		X+	
Detonula pumila		X+	
Oxyphysis oxytoxoides		X+	
Cylindrotheca closterium		X+	
Chaetoceros laciniosus		X+	
Pleurosigma sp.		X+	X+
Protoperidinium depressum			X+
Leptocylindrus danicus			X+
Chaetoceros socialis			X++
Pleurosigma sp.			
Licmorpha abbreviata			
Nitzschia acicularis			
Scripsiella trochoidea			
Stephanopyxis palmeriana			
Chaetoceros didymus			
Leptocylindrus minimus			
Striatella unipunctata			
Actinoptychus senarius			
Chaetoceros lorenzianus			
Actinoptychus splendens			
Thalassiosira eccentrica			
Odontella longicuris			
Chaetoceros diadema			
Stephanopyxis turris			
Melosira monoliformis			
Rhizosolenia setigera			
Protoperidinium leonis			
Protoperidinium excentricum			
Fragilaria striatula			
Gonyaulax c.f. verior			
Chaetoceros vanheurckii			
Alexandrium c.f. tamarense			
Protoperidinium c.f. oblongum			
Bacillaria paxillifera			
Thalassiosira pacifica			
Chaetoceros c.f. teres			
Pyrophacus horologium			
Thalassiosira nordenskioeldii			
Protoperidinium steinii			
Alexandrium cf. fundyense			
Protocentrum gracile			
Noctiluca scintillans			
Odontella aurita			
Chaetoceros similis			
Alexandrium cantella			
Protoceratium reticulatum			
Eucampia zodiacus			
Hemiaulus hauckii			
Protocentrum lima			
Dinophysis parva			
Dinophysis odiosa			
Dactyliosolen fragilissimus			
Corymbellus aurens			

Season			
Month	March	April	
Sampling Dates	3/27/19	4/3/19	4/18/19
Assemblage (Diatom dom, Dinoflagellate dom, or mixed)	Diatom Dom	Diatom Dom	Diatom Dom
Dominant Genus or Species	*Skeletonema costatum*	*Chaetoceros debilis*	*Chaetoceros debilis (bloom)*
Dinophysis norvegica			
Dinophysis fortii			
Dinophysis acuminata			
Akashiwo sanguinea			
Thalassiosira anguste-lineata	X+		
Chaetoceros decipens			X+
Chaetoceros debilis	X++	X+++	X+++
Ditylum brightwellii	X++		
Coscinodiscus c.f. curvatulus			
Thalassiosira rotula	X++		X+
Protoperidinium conicum			
Asteromphalus heptactis			
Thalassionema nitzschiodes	X+	X++	
Navicula spp.			
Skeletonema costatum	X+++	X++	
Dictyocha fibula	X++		
Protocentrum micans			
Chaetoceros danicus	X+	X+	
Pseudo-nitzschia spp.	X+		X+
Thalassoisira punctigera			
Coscinodiscus centralis			
Ceratium fusus			
Gyrosigma spp.			
Detonula pumila	X++		
Oxyphysis oxytoxoides			
Cylindrotheca closterium	X+		
Chaetoceros laciniosus			
Pleurosigma sp.			X+
Protoperidinium depressum	X+		
Leptocylindrus danicus			
Chaetoceros socialis			
Pleurosigma sp.	X++		
Licmorpha abbreviata	X+		
Nitzschia acicularis		X+	
Scripsiella trochoidea			
Stephanopyxis palmeriana		X+	X+
Chaetoceros didymus		X++	
Leptocylindrus minimus		X++	
Striatella unipunctata		X+	
Actinoptychus senarius			X++
Chaetoceros lorenzianus			
Actinoptychus splendens			
Thalassiosira eccentrica			
Odontella longicuris			
Chaetoceros diadema			
Stephanopyxis turris			
Melosira monoliformis			
Rhizosolenia setigera			
Protoperidinium leonis			
Protoperidinium excentricum			
Fragilaria striatula			
Gonyaulax c.f. verior			
Chaetoceros vanheurckii			
Alexandrium c.f. tamarense			
Protoperidimium c.f. oblongum			
Bacillaria paxillifera			
Thalassiosira pacifica			
Chaetoceros c.f. teres			
Pyrophacus horologium			
Thalassiosira nordenskioeldii			
Protoperidinium steinii			
Alexandrium cf. fundyense			
Protocentrum gracile			
Noctiluca scintillans			
Odontella aurita			
Chaetoceros similis			
Alexandrium cantella			
Protoceratium reticulatum			
Eucampia zodiacus			
Hemiaulus hauckii			
Protocentrum lima			
Dinophysis parva			
Dinophysis odiosa			
Dactyliosolen fragilissimus			
Corymbellus aurens			

Season	Spring		
Month			
Sampling Dates	4/24/19	5/2/19	5/9/19
Assemblage (Diatom dom, Dinoflagellate dom, or mixed)	Diatom Dom	Diatom Dom	Diatom Dom
Dominant Genus or Species	*Chaetoceros debilis (bloom)*	*Psuedo-nitzschia spp.*	*Pseudo-nitzschia spp.*
Dinophysis norvegica		X+	
Dinophysis fortii			
Dinophysis acuminata			
Akashiwo sanguinea			
Thalassiosira anguste-lineata		X+	
Chaetoceros decipens	X++		
Chaetoceros debilis	X++		
Ditylum brightwellii		X+	
Cosinodiscus c.f. curvatulus			
Thalassiosira rotula	X+		
Protoperidinium conicum		X+	
Asteromphalus heptactis			
Thalassionema nitzschiodes			
Navicula spp.			
Skeletonema costatum	X++	X++	X++
Dictyocha fibula			
Protocentrum micans			
Chaetoceros danicus		X++	
Pseudo-nitzschia spp.		X+++	X+++
Thalassoisira punctigera			
Cosinodiscus centralis			
Ceratium fusus		X+	
Gyrosigma spp.			
Detonula pumila			
Oxyphysis oxytoxoides			
Cylindrotheca closterium			
Chaetoceros laciniosus			
Pleurosigma sp.		X+	
Protoperidinium depressum			
Leptocylindrus danicus		X++	
Chaetoceros socialis		X++	
Pleurosigma sp.			
Licmorpha abbreviata		X+	X+
Nitzschia acicularis			
Scripsiella trochoidea			
Stephanopyxis palmeriana	X+	X+	
Chaetoceros didymus	X+	X+	
Leptocylindrus minimus			
Striatella unipunctata			
Actinoptychus senarius		X+	X++
Chaetoceros lorenzianus		X++	
Actinoptychus splendens		X+	
Thalassiosira eccentrica		X+++	
Odontella longicuris		X+	
Chaetoceros diadema		X+	
Stephanopyxis turris		X+	
Melosira monoliformis			X+
Rhizosolenia setigera			X+
Protoperidinium leonis			
Protoperidinium excentricum			
Fragilaria striatula			
Gonyaulax c.f. verior			
Chaetoceros vanheurckii			
Alexandrium c.f. tamarense			
Protoperidimium c.f. oblongum			
Bacillaria paxillifera			
Thalassiosira pacifica			
Chaetoceros c.f. teres			
Pyrophacus horologium			
Thalassiosira nordenskioeldii			
Protoperidinium steni			
Alexandrium cf. fundyense			
Protocentrum gracile			
Noctiluca scintillans			
Odontella aurita			
Chaetoceros similis			
Alexandrium cantella			
Protoceratium reticulatum			
Eucampia zodiacus			
Hemiaulus hauckii			
Protocentrum lima			
Dinophysis parva			
Dinophysis odiosa			
Dactyliosolen fragilissimus			
Corymbellus aurens			

Season			
Month	May		
Sampling Dates	5/15/19	5/23/19	6/1/19
Assemblage (Diatom dom, Dinoflagellate dom, or mixed)	Diatom Dom	Mixed	Diatom Dom
Dominant Genus or Species	*Rhizosolenia setigera*	*Rhizosolenia setigera/Dinophysis norvegica*	*Pseudo-nitzschia spp.*
Dinophysis norvegica	X+	X+++	X+
Dinophysis fortii			
Dinophysis acuminata			X+
Akashiwo sanguinea			
Thalassiosira anguste-lineata			
Chaetoceros decipens			
Chaetoceros debilis	X++		X++
Ditylum brightwellii	X+	X+	X+
Coscinodiscus c.f. curvatulus			
Thalassiosira rotula			X+
Protoperidinium conicum		X+	X+
Asteromphalus heptactis	X+		X++
Thalassionema nitzschiodes		X+	X+
Navicula spp.			
Skeletonema costatum	X++	X++	
Dictyocha fibula			
Protocentrum micans			
Chaetoceros danicus			
Pseudo-nitzschia spp.		X+++	X+++
Thalassoisira punctigera			
Coscinodiscus centralis	X+		
Ceratium fusus			
Gyrosigma spp.			
Detonula pumila			
Oxyphysis oxytoxoides			
Cylindrotheca closterium			
Chaetoceros laciniosus			
Pleurosigma sp.			
Protoperidinium depressum	X+		
Leptocylindrus danicus			
Chaetoceros socialis			
Pleurosigma sp.			X+
Liamorpha abbreviata			
Nitzschia acicularis			
Scrippsiella trochoidea		X+	X++
Stephanopyxis palmeriana			
Chaetoceros didymus			
Leptocylindrus minimus			
Striatella unipunctata			
Actinoptychus senarius	X+++	X+	
Chaetoceros lorenzianus			
Actinoptychus splendens			
Thalassiosira eccentrica			
Odontella longicuris	X+		
Chaetoceros diadema			
Stephanopyxis turris			
Melosira monoliformis			
Rhizosolenia setigera	X+++	X+++	X++
Protoperidinium leonis	X+		X++
Protoperidinium excentricum	X+		X++
Fragilaria striatula	X+	X+	
Gonyaulax c.f. verior			
Chaetoceros vanheurckii		X++	
Alexandrium c.f. tamarense			X+
Protoperidimium c.f. oblongum			X+
Bacillaria paxillifera			X+
Thalassiosira pacifica			
Chaetoceros c.f. teres			
Pyrophacus horologium			
Thalassiosira nordenskioeldii			
Protoperidinium steinii			
Alexandrium cf. fundyense			
Protocentrum gracile			
Noctiluca scintillans			
Odontella aurita			
Chaetoceros similis			
Alexandrium cantella			
Protoceratium reticulatum			
Eucampia zodiacus			
Hemiaulus hauckii			
Protocentrum lima			
Dinophysis parva			
Dinophysis odiosa			
Dactyliosolen fragilissimus			
Corymbellus aureus			

Season			
Month	June		
Sampling Dates	6/1/19	6/6/19	6/9/19
Assemblage (Diatom dom, Dinoflagellate dom, or mixed)	Diatom Dom	Dinoflagellate dom	Diatom dom
Dominant Genus or Species	*Pseudo-nitzschia spp.*	*Dinophysis norvegica (bloom)*	*Thalassiosira spp.*
Dinophysis norvegica	X+	X+++	X++
Dinophysis fortii			
Dinophysis acuminata	X+		
Akashiwo sanguinea			
Thalassiosira anguste-lineata		X+	
Chaetoceros decipens			
Chaetoceros debilis	X++		
Ditylum brightwellii	X+	X+	X+
Coscinodiscus c.f. curvatulus			
Thalassiosira rotula	X+		X+++
Protoperidinium conicum	X+	X+	X++
Asteromphalus heptactis	X++		
Thalassionema nitzschiodes	X+	X+	
Navicula spp.			
Skeletonema costatum		X++	
Dictyocha fibula			
Protocentrum micans			
Chaetoceros danicus			
Pseudo-nitzschia spp.	X+++	X+	X+
Thalassoisira punctigera		X++	
Coscinodiscus centralis		X+	
Ceratium fusus			
Gyrosigma spp.			
Detonula pumila		X+	
Oxyphysis oxytoxoides			
Cylindrotheca closterium			
Chaetoceros laciniosus			
Pleurosigma sp.			
Protoperidinium depressum			
Leptocylindrus danicus			
Chaetoceros socialis			
Pleurosigma sp.	X+		
Licmorpha abbreviata		X+	
Nitzschia acicularis			X+
Scripsiella trochoidea	X++		
Stephanopyxis palmeriana			
Chaetoceros didymus			
Leptocylindrus minimus			
Striatella unipunctata			
Actinoptychus senarius			X++
Chaetoceros lorenzianus			
Actinoptychus splendens			
Thalassiosira eccentrica			
Odontella longicuris			
Chaetoceros diadema			
Stephanopyxis turris			
Melosira monoliformis			
Rhizosolenia setigera	X++	X+	
Protoperidinium leonis	X++		
Protoperidinium excentricum	X++	X+	
Fragilaria striatula			
Gonyaulax c.f. verior			
Chaetoceros vanheurckii			
Alexandrium c.f. tamarense	X+		
Protoperidimium c.f. oblongum	X+		X+
Bacillaria paxillifera	X+		
Thalassiosira pacifica		X++	X+
Chaetoceros c.f. teres		X++	
Pyrophacus horologium			X+
Thalassiosira nordenskioeldii			X++
Protoperidinium steinii			
Alexandrium cf. fundyense			
Protocentrum gracile			
Noctiluca scintillans			
Odontella aurita			
Chaetoceros similis			
Alexandrium cantella			
Protoceratium reticulatum			
Eucampia zodiacus			
Hemiaulus hauckii			
Protocentrum lima			
Dinophysis parva			
Dinophysis odiosa			
Dactyliosolen fragilissimus			
Corymbellus aurens			

Season			
Month			
Sampling Dates	6/16/19	7/2/19	7/11/19
Assemblage (Diatom dom, Dinoflagellate dom, or mixed)	Dinoflagellate dom	Mixed	Diatom dom
Dominant Genus or Species	*Dinophysis norveigca (bloom)*	*Thalassiosira spp.*	*Odontella aurita*
Dinophysis norvegica	X+++	X++	X+
Dinophysis fortii		X+	
Dinophysis acuminata		X+	X+
Akashiwo sanguinea	X++		
Thalassiosira anguste-lineata			
Chaetoceros decipens			
Chaetoceros debilis			
Ditylum brightwellii	X+	X+	X+
Coscinodiscus c.f. curvatulus			
Thalassiosira rotula	X++		
Protoperidinium conicum		X+	X+
Asteromphalus heptactis			
Thalassionema nitzschiodes	X+		
Navicula spp.			X+
Skeletonema costatum			X++
Dictyocha fibula			
Protocentrum micans			
Chaetoceros danicus		X++	
Pseudo-nitzschia spp.	X+		
Thalassoisira punctigera			
Coscinodiscus centralis			X+
Ceratium fusus	X+	X+	X+
Gyrosigma spp.			
Detonula pumila	X++	X+	
Oxyphysis oxytoxoides			
Cylindrotheca closterium			X+
Chaetoceros laciniosus			
Pleurosigma sp.	X+		
Protoperidinium depressum			
Leptocylindrus danicus		X+	
Chaetoceros socialis			
Pleurosigma sp.		X+	
Liamorpha abbreviata		X+	
Nitzschia acicularis	X+		
Scripsiella trochoidea		X+	X+
Stephanopyxis palmeriana			
Chaetoceros didymus			
Leptocylindrus minimus			
Striatella unipunctata			
Actinoptychus senarius			
Chaetoceros lorenzianus			
Actinoptychus splendens			
Thalassiosira eccentrica		X+++	X++
Odontella longicuris			
Chaetoceros diadema			
Stephanopyxis turris			
Melosira moniliformis		X+	X+
Rhizosolenia setigera			
Protoperidinium leonis			X+
Protoperidinium excentricum	X+	X+	X+
Fragilaria striatula		X+	
Gonyaulax c.f. verior		X+	
Chaetoceros vanheurckii			
Alexandrium c.f. tamarense			
Protoperidimium c.f. oblongum		X+	
Bacillaria paxillifera		X+	
Thalassiosira pacifica			
Chaetoceros c.f. teres		X+	
Pyrophacus horologium			
Thalassiosira nordenskioeldii			
Protoperidinium stenii	X+	X+	
Alexandrium cf. fundyense		X+	
Protocentrum gracile		X+	
Noctiluca scintillans		X+	
Odontella aurita			X+++
Chaetoceros similis			X+
Alexandrium cantella			X+
Protoceratium reticulatum			
Eucampia zodiacus			
Hemiaulus hauckii			
Protocentrum lima			
Dinophysis parva			
Dinophysis odiosa			
Dactyliosolen fragillissimus			
Corymbellus aurens			

Season	Summer		
Month	July		
Sampling Dates	7/18/19	7/24/19	8/1/19
Assemblage (Diatom dom, Dinoflagellate dom, or mixed)	Dinoflagellate dom	Dinoflagellate dom	Diatom dom
Dominant Genus or Species	*Ceratium fusus (bloom)*	*Protoceratrium reticulatum*	*Thalassiosira eccentrica (bloom)*
Dinophysis norvegica			X+
Dinophysis fortii	X+		
Dinophysis acuminata			
Akashiwo sanguinea			
Thalassiosira anguste-lineata			
Chaetoceros decipens			
Chaetoceros debilis		X++	
Ditylum brightwellii			X+
Coscinodiscus c.f. curvatulus			
Thalassiosira rotula		X+++	
Protoperidinium conicum	X+		
Asteromphalus heptactis			
Thalassionema nitzschiodes			X+
Navicula spp.			
Skeletonema costatum	X++	X+++	X++
Dictyocha fibula			
Protocentrum micans			
Chaetoceros danicus			
Pseudo-nitzschia spp.			
Thalassoisira punctigera			X+
Coscinodiscus centralis			
Ceratium fusus	X+++	X++	
Gyrosigma spp.			
Detonula pumila			
Oxyphysis oxytoxoides			
Cylindrotheca closterium			
Chaetoceros laciniosus			
Pleurosigma sp.			
Protoperidinium depressum			
Leptocylindrus danicus			
Chaetoceros socialis			
Pleurosigma sp.			
Liamorpha abbreviata			
Nitzschia acicularis			
Scripsiella trochoidea	X+	X+	
Stephanopyxis palmeriana			
Chaetoceros didymus			
Leptocylindrus minimus			X+
Striatella unipunctata			
Actinoptychus senarius			
Chaetoceros lorenzianus			
Actinoptychus splendens			
Thalassiosira eccentrica	X++	X+++	X+++
Odontella longicuris			
Chaetoceros diadema			
Stephanopyxis turris			
Melosira moniliformis			
Rhizosolenia setigera			
Protoperidinium leonis			
Protoperidinium excentricum			
Fragilaria striatula			
Gonyaulax c.f. verior			
Chaetoceros vanheurckii			
Alexandrium c.f. tamarense			
Protoperidimium c.f. oblongum			
Bacillaria paxillifera	X+		X+
Thalassiosira pacifica			X++
Chaetoceros c.f. teres			
Pyrophacus horologium			
Thalassiosira nordenskioeldii			
Protoperidinium steinii		X+	
Alexandrium cf. fundyense			
Protocentrum gracile			
Noctiluca scintillans			
Odontella aurita			
Chaetoceros similis	X+		
Alexandrium cantella			
Protoceratium reticulatum	X++	X+++	X+
Eucampia zodiacus			X+
Hemiaulus hauckii			
Protocentrum lima			
Dinophysis parva			
Dinophysis odiosa			
Dactyliosolen fragilissimus			
Corymbellus aureus			

Season			
Month	August		
Sampling Dates	8/7/19	8/13/19	8/21/19
Assemblage (Diatom dom, Dinoflagellate dom, or mixed)	Mixed	Mixed	Mixed
Dominant Genus or Species	*Thalassiosira spp/Ceratium fusus*	*Thalassiosira spp/Ceratium fusus*	*Thalassiosira spp/Ceratium fusus*
Dinophysis norvegica			
Dinophysis fortii		X+	
Dinophysis acuminata			
Akashiwo sanguinea			
Thalassiosira anguste-lineata			
Chaetoceros decipens			
Chaetoceros debilis		X++	
Ditylum brightwellii	X+	X+	X++
Coscinodiscus c.f. curvatulus			
Thalassiosira rotula			
Protoperidinium conicum		X+	X+
Asteromphalus heptactis		X+	X+
Thalassionema nitzschiodes	X+	X+	X+
Navicula spp.	X+		
Skeletonema costatum		X++	
Dictyocha fibula			
Protocentrum micans			
Chaetoceros danicus			
Pseudo-nitzschia spp.			
Thalassoisira punctigera	X+		
Coscinodiscus centralis			
Ceratium fusus	X+++	X++	X++
Gyrosigma spp.			
Detonula pumila	X++	X+	X+
Oxyphysis oxytoxoides			
Cylindrotheca closterium			
Chaetoceros laciniosus			
Pleurosigma sp.			
Protoperidinium depressum			
Leptocylindrus danicus			
Chaetoceros socialis			
Pleurosigma sp.			
Licmorpha abbreviata			
Nitzschia acicularis			
Scripsiella trochoidea	X+		X+
Stephanopyxis palmeriana			
Chaetoceros didymus			
Leptocylindrus minimus	X+		X+
Striatella unipunctata			
Actinoptychus senarius			X+
Chaetoceros lorenzianus			
Actinoptychus splendens			
Thalassiosira eccentrica	X+++	X++	X++
Odontella longicuris			
Chaetoceros diadema			
Stephanopyxis turris			
Melosira monoliformis			
Rhizosolenia setigera	X+	X+	
Protoperidinium leonis	X+	X++	X+
Protoperidinium excentricum		X+	X+
Fragilaria striatula			X++
Gonyaulax c.f. verior			
Chaetoceros vanheurckii			
Alexandrium c.f. tamarense			
Protoperidimium c.f. oblongum			
Bacillaria paxillifera			
Thalassiosira pacifica	X+	X++	X++
Chaetoceros c.f. teres			
Pyrophacus horologium			
Thalassiosira nordenskioeldii			
Protoperidinium stenii	X+		X+
Alexandrium cf. fundyense			
Protocentrum gracile			
Noctiluca scintillans		X++	X+
Odontella aurita			
Chaetoceros similis			
Alexandrium cantella			
Protoceratium reticulatum	X+	X+	X+
Eucampia zodiacus	X+		
Hemiaulus hauckii	X+		
Protocentrum lima			X+
Dinophysis parva			
Dinophysis odiosa			
Dactyliosolen fragilissimus			
Corymbellus aureus			

Season		Fall	
Month		September	
Sampling Dates	8/31/19	9/7/19	9/13/19
Assemblage (Diatom dom, Dinoflagellate dom, or mixed)	Diatom dom	Diatom dom	Mixed
Dominant Genus or Species	*Thalassiosira spp (bloom)*	*Akashiwo sanguinea (bloom)*	*Ceratum fusus/Thalassiosira spp.*
Dinophysis norvegica			
Dinophysis fortii	X+		X+
Dinophysis acuminata		X+	X+
Akashiwo sanguinea			X+
Thalassiosira anguste-lineata			X+
Chaetoceros decipens			
Chaetoceros debilis			X++
Ditylum brightwellii	X+	X+	X+
Coscinodiscus c.f. curvatulus			
Thalassiosira rotula	X+++	X+	X+
Protoperidinium conicum		X+	X+
Asteromphalus heptactis			
Thalassionema nitzschiodes	X+		X+
Navicula spp.			
Skeletonema costatum	X++	X++	X++
Dictyocha fibula		X+	X+
Protocentrum micans	X+	X++	X+
Chaetoceros danicus	X+	X+	X+
Pseudo-nitzschia spp.			
Thalassoisira punctigera	X++		
Coscinodiscus centralis		X+	
Ceratium fusus	X++	X++	X+++
Gyrosigma spp.			
Detonula pumila	X+	X+	X+
Oxyphysis oxytoxoides			
Cylindrotheca closterium			
Chaetoceros laciniosus			
Pleurosigma sp.	X+		
Protoperidinium depressum			
Leptocylindrus danicus			
Chaetoceros socialis			
Pleurosigma sp.			
Licmorpha abbreviata	X+		X+
Nitzschia acicularis			
Scrippsiella trochoidea	X+	X+	
Stephanopyxis palmeriana			
Chaetoceros didymus			
Leptocylindrus minimus	X+	X+	X+
Striatella unipunctata			
Actinoptychus senarius			
Chaetoceros lorenzianus			
Actinoptychus splendens			
Thalassiosira eccentrica	X+++	X+	X+
Odontella longicuris			
Chaetoceros diadema			
Stephanopyxis turris			
Melosira monoliformis		X+	
Rhizosolenia setigera			
Protoperidinium leonis	X+		
Protoperidinium excentricum	X+		
Fragilaria striatula			X+
Gonyaulax c.f. verior			
Chaetoceros vanheurckii			
Alexandrium c.f. tamarense			
Protoperidimium c.f. oblongum	X+		
Bacillaria paxillifera			
Thalassiosira pacifica			
Chaetoceros c.f. teres			
Pyrophacus horologium			
Thalassiosira nordenskioeldii			
Protoperidinium steinii		X+	X+
Alexandrium cf. fundyense		X+	X+
Protocentrum gracile			
Noctiluca scintillans	X+		
Odontella aurita			
Chaetoceros similis	X+	X+	X+
Alexandrium cantella			
Protoceratium reticulatum		X+	
Eucampia zodiacus			
Hemiaulus hauckii			
Protocentrum lima			
Dinophysis parva	X+		
Dinophysis odiosa		X+	
Dactyliosolen fragillissimus		X+	
Corymbellus aureus			X+

Appendix B: Dinoflagellate Scanning Electron Microscopy Project

Sample Preparation of Athecate (Unarmored) Dinoflagellates for Scanning Electron Microscopy

Dinoflagellates—microalgae—play an important role in the primary production of marine ecosystems. There are three main groups of dinoflagellates: dinoflagellates that produce thecal plates, those lacking thecal plates, and an intermediate group recently identified as "thinned-walled" (Moestrup & Daugbjerg 2007). Athecate dinoflagellates are those without thecal plates, whereby they do not produce cellulose in their vesicles—the vesicles are completely empty (Orr et al. 2012). Thecate (armored) dinoflagellates have been identified to belong to a primary phylogeny. However, athecate (or unarmored) flagellates species have been known to be polyphyletic due to illustrating particular characteristics of more than one order (e.g. members of Gymnodiniales) (Daugjerg et al. 2000 and Orr et al. 2012). Assessment of the biodiversity of dinoflagellates is critical to evaluate species richness and provide accurate identification of these species, which are challenging to identify due to the subtle morphological differences.

Under various environmental conditions, certain dinoflagellates (i.e. *Akashiwo sanguinea, Alexandrium catenalla, Azadinium spp.*) are able to form harmful blooms with the potential to produce high concentrations of toxins released in ambient waters throughout coastal areas (Wang 2008; Anderson et al. 2012). These harmful algal blooms cause various consequences to the overall health of the marine ecosystem, human health, and can also impact the various aspects of the local economies (Anderson et al. 2012). Several species of athecate flagellates produce toxins, yet are very challenging to identify

due to being small in size and fragility in structural composition. Thereby, strict protocols have to be ensued for the specimens to be observed.

Identification of athecate dinoflagellates is based on the morphological features. It is dependent on its size and cellular shape, displacement of cingulum and correlated sizing (width), sizing (length) of sulcal intrusion, presence or absence of apical groove, presence of ventral pores, dorsal-ventral compression, and surface cellular structures (if present) (Truby 1997; Bergholtz et al. 2005; Haifeng et al. 2013). The scanning electron microscopy (SEM) is a primary method to observe the ultrastructure and explore the biodiversity of athecate dinoflagellates. The primary advantages of SEM includes: powerful magnification (maximum of 1,000,000x), high-resolution, and detection of fine details of the both the outside and inside of cells. This is necessary to measure and recognize features for species identification. The SEM enhances the topography of the cellular surface and assists in accentuating fine-details and structures of the cell. The SEM is a tool necessary to identify organisms to the species level, especially species that do not show strict structural shapes, exhibit similarities in color, and small in size.

A proper application of the preparation method is necessary to observe the ultrastructure of athecate dinoflagellates and obtain acceptable quality SEM micrographs. Most studies involving athecate dinoflagellates followed the similar process of SEM preparation involving: fixation, dehydration, critical point drying, and sputter coating with gold onto the specimens (Botes et al. 2002; Jung et al. 2010; Gomez et al. 2016; Haifeng et al. 2013). Dr. Chin-Leo's SEM preparation method (G. Chin-Leo, personal communication, December 1st, 2019) can be applicable for athecate dinoflagellates. The process of fixation with 2.5% gluteraldehyde, dehydration with ethanol via a gradient

process critical point drying, and a sputter coating of argon worked for the species isolate of *Akashiwo sanguinea*. Minute adjustments to the preparation method included: a longer dehydration process of 15-20 minutes for each ethanol solution of 25, 50, 75, 90, and 100% (repeated 3 times). Longer duration assisted in drawing out the water more slowly. Also, the chamber was filled and purged with CO_2 to remove ethanol about 15 times to ensure the complete removal. This slow process of gradually removing the ethanol from the cells and removing it with CO_2 allows the specimen to not distort the surface tension of the cells. If the whole sample preparation process is not done properly you will acquire cells that are distorted, damaged and considerable shrinkage of the cell can be found. The preparation method used for the SEM project should be slightly altered to attain better results of intact cells.

There are many factors influencing the sample preparation of specimens for the SEM including: the fixation process, temperature and duration of fixation, pH, and osmolarity (Murtey & Ramasamy 2016). The fixation process of the samples is the most critical phase of the SEM preparation. According to Montanaro et al. (2016), the buffer solution of preservation method is of great importance because the changes of pH and osmolarity cannot be changed after the fixation step has occurred. The study further explains the aldehydes in the fixation process, such as glutaraldehyde, should be applied with a buffer to maintain a specific pH for the specimen to limit the structural changes because seawater is known to have little buffering capacity (Montanaro et al. 2016). Osmium tetroxide is known to be an agent for post-fixation because it ensures the outer cellular membrane is preserved by acting as a buffer for the cells and enables stability of cell structure in a short period of time (Kownacki et al. 2015).

After the primary fixation of gluteraldehyde has occurred, post-fixation is recommended with osmium tetroxide—a very toxic chemical—of 2% to 4% solution for 20 minutes to an hour (Botes et al. 2002; Jung et al. 2010; Gomez et al. 2016; Haifeng et al. 2013). Gluteraldehyde act as a cross-linker for proteins, while osmium tetroxide is a cross-linker for the lipids of the cells (Murtey and Ramasamy 2016). Other buffers that are most widely used by research scientists are phosphate buffer and cacodyalte buffer. These buffers have considerable issues including: 1) phosphate buffer creates a precipitate that can damage delicate tissues or membranes of the cell, and 2) the cacodyalte buffer can be extremely toxic posing health problems to humans and can causes alteration to the cellular membrane and thus preservation of the cell (Dykstra & Reuss, 2003).

Due to this high toxicity of most post-fixatives, I have found a study that reported a different method of post-fixation that is non-toxic. This method has only been used for delicate marine invertebrates, such as ctenophores (Montanaro et al. 2016), but the application could potentially be applied to the athecate dinoflagellates due to similarities of complex lipid structures (Murtey & Ramasamy 2016). Schliwa & Van Blerkom (1981) first recommended the buffer and fixative formula known as the PHEM buffer. The PHEM buffer consists of four components: PIPES (1,4-Piperazinediethanesulfonic acid), HEPES (*4-(2-Hydroxyethyl)piperazine-1-ethanesulfonic acid)*, EGTA (Ethylene glycol-bis(2-aminoethylether)-*N,N,N′,N′*-tetraacetic acid) and $MgCl_2$ (Magnesium Chloride). The PHEM buffer is particularly useful because it properly preserves the specimen with minimal damage. The fixative formulation has been used for the stabilization of cytoskeleton of eukaryotes (Schliwa & Van Blerkom 1981), for embryos of amoebae's

(Schieber et al. 2010), detecting and localizing proteins in single-cell organisms or culture of cells (Griffith et al. 2008), and the preservation of fish gill tissue and deep-sea mussels tissue (Monantaro et al. 2016). The PHEM method is excellent for maintaining the lipid structures of the cells, thereby, also acting as an agent for maintaining osmolality and pH (2016). Montanaro et al. (2016) recognized PHEM buffered gluteraldehyde improved the quality of the specimen by enhancing the preservation of the outer cellular membrane tissue resulting in high-quality SEM micrographs relative to the other buffers used.

Athecate dinoflagellates are complex and challenging species to identify. Most studies illustrate routine fixation of specimens using gluteraldehyde and osmium tetroxide for SEM preparation protocol that can ensure specimens are well preserved to produce high-quality micrographs. The key for producing the best specimen is to involve a buffer technique. The buffer assists in the preservation of the sample due to the maintaining the correct pH and osmolarity to keep the cells intact without damage or shrinking. Although osmium tetroxide is widely used by researchers for preservation of fragile and delicate cells and tissues, there is limited research and studies exploring non-toxic SEM techniques. For future studies, the PHEM method would be a useful tool to try with athecate dinoflagellates because it is formulated with several reagents that are not harmful to the specimens or to human health.

Literature Cited

Anderson, D. M., Cembella, A. D., & Hallegraeff, G. M. (2012). Progress in Understanding Harmful Algal Blooms: Paradigm Shifts and New Technologies for Research, Monitoring, and Management. *Annual Review of Marine Science*, *4*(1), 143–176. https://doi.org/10.1146/annurev-marine-120308-081121

Bergholtz, T., Daugbjerg, N., Moestrup, Ø., & Fernández-Tejedor, M. (2006). On the Identity of Karlodinium Veneficum and Description of Karlodinium Armiger Sp. Nov. (dinophyceae), Based on Light and Electron Microscopy, Nuclear-Encoded Lsu Rdna, and Pigment Composition1. *Journal of Phycology*, *42*(1), 170–193. https://doi.org/10.1111/j.1529-8817.2006.00172.x

Botes, L., Price, B., Waldron, M., & Pitcher, G. C. (2002). A simple and rapid scanning electron microscope preparative technique for delicate "gymnodinioid" dinoflagellates. *Microscopy Research and Technique*, *59*(2), 128–130. https://doi.org/10.1002/jemt.10184

Daugbjerg, N., Hansen, G., Larsen, J., & Mosetrup, O. (2000). Phylogeny of someof the major genera of dinoflagellates based on ultrastructure and partial LSU rDNA sequence data, including the erection of three new genera of unarmoured dinoflagellates. *Phycologia, 39*(4), 302. https://doi.org/10.2216/i0031-8884-39-4-302.1

Escobar-Morales, S., & Hernández-Becerril, D. U. (2015). Free-living marine planktonic unarmoured dinoflagellates from the Gulf of Mexico and the Mexican Pacific. *Botanica Marina*, *58*(1). https://doi.org/10.1515/bot-2014-0049

Gómez, F., Takayama, H., Moreira, D., & López-García, P. (2016). Unarmoured dinoflagellates with a small hyposome: Torodinium and Lebouridinium gen. nov. for Katodinium glaucum (Gymnodiniales, Dinophyceae). *European Journal of Phycology*, *51*(2), 226–241. https://doi.org/10.1080/09670262.2015.1126767

Griffith, J., Mari, M., De Mazière, A., & Reggiori, F. (2008). A cryosectioning procedure for the ultrastructural analysis and the immunogold labelling of yeast Saccharomyces cerevisiae. *Traffic (Copenhagen, Denmark)*, *9*(7), 1060–1072. https://doi.org/10.1111/j.1600-0854.2008.00753.x

Haifeng, G., Zhaohe, L., Xiaodong, Z., Bin, X., & Qi, F. (2013). Morphology, ultrastructure and phylogeny of Takayama xiamenensis sp. nov. (Gymnodiniales, Dinophyceae) from the East China Sea | Article Information | J-GLOBAL. *Phycologia*, *52*(3), 256–265.

Jung, S. W., Joo, H. M., Park, J. S., & Lee, J. H. (2010). Development of a rapid and effective method for preparing delicate dinoflagellates for scanning electron microscopy. *Journal of Applied Phycology*, *22*(3), 313–317. https://doi.org/10.1007/s10811-009-9461-6

Kownacki, A., Szarek-Gwiazda, E., & Woźnicka, O. (2015). The importance of scanning electron microscopy (SEM) in taxonomy and morphology of Chironomidae (Diptera). *European Journal of Environmental Sciences*, *5*(1). https://doi.org/10.14712/23361964.2015.75

Moestrup, Ø. and N. Daugbjerg. 2007. On dinoflagellate phylogeny and classification. *In*: (J. Brodies and J. Lewis, eds). *Unraveling the algae, the past, present, and future*

of algal systematics. CRC Press, New York. pp. 215–230.

Murtey, M. D., & Ramasamy, P. (2016). Sample Preparations for Scanning Electron Microscopy – Life Sciences. *Modern Electron Microscopy in Physical and Life Sciences*. https://doi.org/10.5772/61720

Orr, R. J. S., Murray, S. A., Stüken, A., Rhodes, L., & Jakobsen, K. S. (2012). When Naked Became Armored: An Eight-Gene Phylogeny Reveals Monophyletic Origin of Theca in Dinoflagellates. *PLoS ONE*, *7*(11). https://doi.org/10.1371/journal.pone.0050004

Schieber, N. L., Nixon, S. J., Webb, R. I., Oorschot, V. M. J., & Parton, R. G. (2010). Modern approaches for ultrastructural analysis of the zebrafish embryo. *Methods in Cell Biology*, *96*, 425–442. https://doi.org/10.1016/S0091-679X(10)96018-4

Schliwa, M., & van Blerkom, J. (1981). Structural interaction of cytoskeletal components. *The Journal of Cell Biology*, *90*(1), 222–235.

Truby, E. W. (1997). Preparation of single-celled marine dinoflagellates for electron microscopy. *Microscopy Research and Technique*, *36*(4), 337–340. https://doi.org/10.1002/(SICI)1097-0029(19970215)36:4<337::AID-JEMT11>3.0.CO;2-Q

Wang, D.-Z. (2008). Neurotoxins from Marine Dinoflagellates: A Brief Review. *Marine Drugs*, *6*(2), 349–371. https://doi.org/10.3390/md20080016

Wergin, W. P. (1993). Biological electron microscopy: Theory, Techniques, and Troubleshooting by Michael J. Dykstra Plenum Press, New York (1992) ISBN 0-

306-442779; 360 pages, illustrated, $49.50. *Scanning*, *15*(4), 243–243. https://doi.org/10.1002/sca.4950150411